A PROTON NUCLEAR MAGNETIC RESONANCE STUDY OF MUSCLE GROWTH, DYSTROPHY, REPAIR AND DRUG TREATMENTS IN CONTROL AND *MDX* MICE

BY

LAURA M. MCINTOSH

A Thesis
Submitted to the Faculty of Graduate Studies
in Partial Fulfillment of the Requirements
for the Degree of

DOCTOR OF PHILOSOPHY (Ph.D.)

Department of Human Anatomy and Cell Science
University of Manitoba
Winnipeg, Manitoba

THE UNIVERSITY OF MANITOBA

FACULTY OF GRADUATE STUDIES

*****

COPYRIGHT PERMISSION PAGE

A PROTON NUCLEAR MAGNETIC RESONANCE STUDY OF MUSCLE GROWTH, DYSTROPHY, REPAIR AND DRUG TREATMENTS IN CONTROL AND MDX MICE

BY

LAURA M. MCINTOSH

A Thesis/Practicum submitted to the Faculty of Graduate Studies of The University of Manitoba in partial fulfillment of the requirements of the degree of

DOCTOR OF PHILOSOPHY

ABSTRACT

Proton nuclear magnetic resonance spectroscopy (1-H NMR) can be used to study skeletal muscle metabolism. The *mdx* mouse is a unique animal which allows study of muscle regeneration, and models the disease of Duchenne muscular dystrophy (DMD). The goals of these studies were to determine the potential of 1-H NMR spectroscopy as an alternative to conventional histology in monitoring: 1) the progression of *mdx* dystrophy, and 2) beneficial treatments (glucocorticoids) on *mdx* dystrophy. *In vitro* 1-H NMR spectra (*ex vivo* and perchloric acid extracts) of limb and diaphragm muscles were obtained from different ages of control and *mdx* mice, and from mice which were treated with prednisone or deflazacort. Peaks with contributions from creatine, taurine and lipids were examined in the *ex vivo* samples. Additionally, valine, lactate, alanine, glutamate, succinate, glutamine, carnitine, glycine and glucose peaks were examined in spectra from extracts. Decreased levels of taurine and carnitine characterized pre- and active dystrophy intervals in *mdx* muscle compared to control. Levels of taurine increased with stabilization of the disease with repair. Measures of accumulated muscle repair and many spectral peaks were highly and significantly correlated. Increased amounts of lipids were found in the diaphragm compared to limb spectra. Treatment, which improved muscle phenotype, resulted in increased levels of taurine. Also, glutamate, alanine and succinate were decreased in *mdx* diaphragm compared to control, and increased with deflazacort-treatment in *mdx* DIA. Therefore, 1-H NMR differentially discriminates: 1) control and *mdx* muscle, 2) the progression of *mdx* dystrophy and developmental stages in normal growth, 3) mild and severe dystrophic phenotypes (diaphragm vs. limb), and 4) changes associated with improved muscle phenotype and regeneration (due to treatment or injury). The results focus on monitoring muscle repair, not degeneration. Preliminary magnetic resonance imaging studies point to eventual application of the findings to non-invasive measurement of treatment effects by *in vivo* 1-H NMR spectroscopy. We conclude that 1-H NMR is a reliable tool in the objective investigation of muscle repair status during muscular dystrophy.

Acknowledgements

I would like to take this opportunity to thank the many special people who have encouraged me along the pathway to a Ph.D.

Dr. Judy Anderson, my mentor and friend, enabled me, not only to conduct experiments, but also to develop, critically analyze, and discuss ideas in a truly scientific and supportive environment. Her integrity, insights and dedication have been an inspiration, and it has been an honour to work under her guidance.

Dr's Greenberg, Kardami and Peeling, my committee members, were (and will continue to be) valuable resource people abundant with important suggestions and contributions about experiments and interpretation of results. Insightful questions and comments from Dr. Butler-Browne were also appreciated.

I would like to thank the staff and students of the Anatomy department for their encouragement and helpful comments. The Medical Research Council of Canada contributed financial support for the duration of my Ph.D. studies, while the Anatomy department contributed travel support, and I am sincerely grateful.

I would also like to acknowledge the expertise of some individuals. Cinthya Vargas helped in many ways, and the sectioning of endless tissues was performed without complaint. Maureen Donnelly, Kathleen Brière, Terry Wolowiec, Richard Buist and Tony Shaw all helped me to become literate (at least partially) in the world of NMR and analysis. Thanks also to Roberta VanAertselaer for keeping me organized, and to Roy Simpson for his photographic expertise.

I must thank the other people in the lab (Andrea Moor, Ross Baker, Cinthya Vargas, Rob Poettcker, Karl Granberg, Kerryn Garrett, Tina Hibbs and Annyue Wong), for their scientific contributions, friendship and encouragement. Scientific (and not so scientific) discussions with Andrea will be especially missed since we have been in the lab together since day one.

My mother will always be the guiding light in my life and I thank her for her faith that I would complete my Ph.D. I am the person I am because of her and my family. I am forever grateful to my Dad, sister Karen and Mom and Dad Sims, for their constant encouragement and faith in me. Also, thanks to Roxy and Dale, Brad and Donna, Sherry and Brett and Uncle Henry and Auntie Mary for their support and the interest they showed in my many years of school.

Finally, I would like to thank my family, Warren and Katie, for fulfilling my life and giving me perspective. Warren's quiet patience, endless support and curiousity kept me motivated, and I thank him for supporting me during 9 long years of university! Thanks to Katie for keeping me smiling with her hugs and giggles. Since Warren read this word for word, when you learn to read, I expect you to read this too Katie!

LIST OF ABBREVIATIONS

DMD	Duchenne muscular dystrophy
MRF	muscle regulatory factor
NMR	nuclear magnetic resonance
MRI	magnetic resonance imaging
TA	tibialis anterior
DIA	diaphragm
PABA	paraminobenzoic acid
LDA	linear discriminant analysis
PCA	perchloric acid
TSP	sodium 3-trimethysilylpropionate
LTA	left tibialis anterior - uncrushed
RTA	right tibialis anterior - crushed
RTA-2d	right tibialis anterior - 2 days recovery post crush
RTA-4d	right tibialis anterior - 4 days recovery post crush
LD	low dose deflazacort treatment (0.67mg/kg body weight)
HD	high dose deflazacort treatment (1.2mg/kg body weight)
PR	prednisone treatment (1.0mg/kg body weight)
PL	placebo

LIST OF FIGURES AND TABLES

TABLE OF CONTENTS

CHAPTER 1

INTRODUCTION

1. DUCHENNE MUSCULAR DYSTROPHY

Duchenne muscular dystrophy (DMD) is a serious X-linked recessive disease with a relatively high incidence (1 in 3500) (reviewed by Bieber & Hoffman, 1990; Partridge, 1993). It is a primary myopathy resulting from a lack of dystrophin (Hoffman et al., 1987) and a decrease in dystrophin-associated proteins in all cells of the body (Ohlendieck & Campbell, 1991; Matsumura & Campbell, 1994; Worton, 1995). Dystrophin is believed to stabilize the sarcolemma (Petrof et al., 1993a) and regulate intracellular calcium (Dunn & Radda, 1991; Turner et al., 1991).

1.1. Course of Duchenne dystrophy

DMD primarily affects skeletal muscle and is characterized by persistent cycles of degeneration followed at first by regeneration, and later failure to regenerate as myofibers gradually become replaced by adipose and fibrotic tissue. Each muscle is affected at a different time in DMD, with some muscles more susceptible to damage (Liu, Chino al., 1993).

At birth, serum creatine kinase (CK) levels are at least 40 times the upper normal limit, and in Manitoba this measure is used for screening virtually all newborn males (Greenberg et al., 1991). Upon a high CK measure, the disease is confirmed almost invariably by a muscle biopsy (Bieber & Hoffman, 1990; Greenberg et al., 1991). Clinically, the onset of muscle weakness occurs at about 3 years, with loss of ambulation at around 10 years, and death from respiratory or cardiac failure in the patient's mid-twenties (Brooke et al., 1989). There is no cure for DMD, but since diagnosis occurs very early in life, it is

important to study possible treatments that might be implemented early, and to monitor the progression of the disease. The development of treatments for DMD is aimed at: 1) replacing dystrophin in an attempt to create a normal muscle phenotype (cell and gene therapies), or 2) slowing the disease progression. Currently, assessment of rate of disease progression depends upon standardized clinical muscle testing or timed functional assessments of routine muscular activities such as walking, climbing stairs and sitting (Brooke et al., 1989).

1.2. Cell and gene therapy

DMD is a candidate for cell or gene therapies (reviewed by Hauser & Chamberlain, 1996) because the gene responsible has been identified, skeletal muscle cells are accessible targets, and they are multinucleated and post-mitotic. Myoblast (cell) transfer (Gussoni et al., 1992; Huard et al., 1992; Mendell et al., 1995), in which normal donor muscle cells are injected into the patient, is not efficient in restoring muscle force or preventing deterioration in its present state (Mendell et al., 1995). Therefore, recent studies have focused on developing alternate dystrophin delivery methods in the form of plasmids (Acsadi et al., 1991; Davis & Jasmin, 1993), liposomes (Trivedi & Dickson, 1995), retroviruses (Dunckley et al., 1993) and adenoviruses (Ragot et al., 1993; Vincent et al., 1993; Acsadi et al., 1996). The results of gene transfer studies on the animal model of DMD (the *mdx* mouse) are very encouraging, but at present, the efficiency is insufficient to justify human trials.

1.3. Glucocorticoid treatment

The glucocorticoids prednisone and deflazacort are the only known treatments that

alleviate the progression of DMD. Prednisone has been studied in clinical trials (for examples see Mendell et al., 1989; Fenichel et al., 1991; Griggs et al., 1991; Khan, 1993) using varying doses for varying amounts of time. All studies report an initial increase in muscle strength with treatment compared to placebo-treated DMD patients. Effects are observed as early as 10 days after the beginning of treatment (Griggs et al., 1991). Longer term studies (Fenichel et al., 1991) demonstrate that prednisone decreases loss of function and slows the progression of muscle weakness, but does not change aspects of the disease that were present at the beginning of treatment (i.e. the ability to walk does not return; Mendell et al., 1989). The occurrence of adverse side-effects (Cushingoid appearance, weight gain, increased hair growth, bone fractures, irritability) prevents the use of prednisone over extended periods of time. Deflazacort, an oxazoline derivative of prednisone, has been suggested as an alternate treatment and has been used in clinical trials (Mesa et al., 1991; Angelini et al., 1994). It significantly improves muscle strength and functional ability, with lower side-effects than prednisone (i.e. moderate weight gain and slight behavioral changes).

Glucocorticoids are generally considered to have catabolic effects on mature muscle (Mayer & Rosen, 1977; Kelly et al., 1986). Thus, mechanisms of prednisone- and deflazacort-induced decreases of DMD progression are unknown. Many theories have been proposed (reviewed by Khan, 1993) which implicate prednisone in: 1) upregulating dystrophin, dystrophin-related proteins (Passaquin et al., 1993) or an alternative protein to dystrophin (Mesa et al., 1991), 2) changing calcium handling by decreasing cellular Ca^{2+}

content (Metzinger et al., 1995), 3) anti-inflammation or alteration of the amount of necrosis (Kissel et al., 1991; 1993), 4) decreasing the rate of muscle protein breakdown (Rifai et al., 1992), and 5) enhancement of muscle regeneration (see section 2.4).

2. THE *MDX* MOUSE AND MUSCLE REGENERATION

Mdx mice suffer from an X-linked (Bulfield et al., 1984) lack of dystrophin (Sicinski et al., 1989) identical to DMD. Muscle fibers undergo segmental necrosis, but muscle regeneration is accentuated instead of muscles succumbing to fibrosis and adipose replacement. Therefore, the *mdx* mouse is a useful model for studying muscle regeneration, in addition to studying Duchenne dystrophy.

2.1. Course of *mdx* dystrophy

Histologically, skeletal muscle fibers of the *mdx* mouse undergo three distinct phases: pre-dystrophy, active dystrophy and stable dystrophy (McArdle et al., 1995). Pre-dystrophy occurs during the first 10-15 days of life when *mdx* fibers appear normal (Bulfield et al., 1984; Dangain & Vrbova, 1984). Degeneration becomes very active between 3 and 6 weeks of age (Bulfield et al., 1984; Dangain & Vrbova, 1984), and this stage is termed active dystrophy. Grouped necrosis of segments of fibers occurs, with subsequent successful regeneration (Anderson et al., 1987), probably due to maximal muscle cell replication at this time (McGeachie et al., 1993). Regenerated fibers are evident by their centrally located nuclei, and this often serves as an index of accumulated muscle repair (Anderson et al., 1987; 1988; Karpati et al., 1988). Slight contractile weakness accompanies active dystrophy

(*in vivo*-Muntoni et al., 1993; Pastoret & Sebille, 1993; *in vitro*-Anderson et al., 1988).

In the stable dystrophic phase (after 8 weeks of age), muscle necrosis decreases in intensity (Dangain & Vrbova, 1984; Zacharias & Anderson, 1991). Regeneration, albeit at lower intensity, occurs throughout the life of the *mdx* mouse (Anderson et al., 1987; Zacharias & Anderson, 1991; McGeachie et al., 1993; Penner, 1993; Lefaucheur et al., 1995). Adult *mdx* limb muscle exhibits very little adipose or connective tissue, and there is no apparent fiber loss (Tanabe et al., 1986; Anderson et al., 1987; 1988; Carnwath & Shotton, 1987). However, one study suggests that after 23 months of age, *mdx* mice suffer from muscle wasting and fibrosis and a progressive motor deficit (Lefaucheur et al., 1995), not withstanding apparent intra-strain differences between *mdx* colonies. Some muscles are preferentially affected by dystrophy (i.e. soleus more than extensor digitorum longus) (Anderson et al., 1987; Carnwath & Shotton, 1987), with a higher potential for regeneration in slow-twitch muscles (Anderson et al., 1988).

In contrast to limb muscles, the *mdx* diaphragm exhibits a more severe pattern of degeneration, fibrosis and functional deficit (Stedman et al., 1991; Dupont-Versteegden & McCarter, 1992; Louboutin et al., 1993; Penner, 1993; Petrof et al., 1993b). However, adult *mdx* mice show no overt respiratory impairment. The differences between DMD and *mdx* disease progression and outcomes have lead some investigators to question the use of *mdx* mice to model DMD or its treatments. Others interpret *mdx* results in view of the differences and with caution.

2.2. Muscle regeneration

Skeletal muscle has the remarkable capacity to form essentially normal tissue after an insult (reviewed by Carlson & Faulkner, 1983; Grounds, 1991; Hurme et al., 1991; Grounds & Yablonka-Reuveni, 1993). The basic process of regeneration is similar regardless of the cause (i.e. dystrophy, mechanical insult), but the outcome and time course may vary.

After an insult to skeletal muscle, membrane damage, disruption of sarcomeres, mitochondrial swelling and nuclear pyknosis occur which lead to necrosis of myofibers. Phagocytic polymorphonuclear leukocytes and macrophages (Robertson et al., 1993a) are primarily responsible for cell-mediated fragmentation of damaged myofibers. Revascularization occurs under the stimulation of many factors (reviewed Grounds, 1991), and if revascularization does not occur, minimal regeneration results. Once the removal of necrotic myofibers is underway, a population of activated spindle-shaped muscle precursor cells appear beneath the external lamina. These are generally considered to originate from satellite cells (Moss & Leblond, 1971; Schmalbruch, 1976; Snow, 1981; Yablonka-Reuveni & Rivera, 1994), which are mononucleated, spindle-shaped cells located between the external lamina and the sarcolemma of adult muscle tissue. Upon activation, satellite cells are thought to migrate to the damaged area (Schultz et al., 1988; Allen & Rankin, 1990) and re-enter the cell cycle to serve as the pool of precursor cells for regenerating muscle (see Grounds, 1991). Growth factors and hormones (reviewed by Grounds, 1991), such as basic fibroblast growth factor (DiMario et al., 1989; Anderson et al., 1991; 1993) and thyroid

hormone (McIntosh et al., 1994; Pernitsky et al., 1996; Pernitsky & Anderson, 1996) have roles in proliferation and/or differentiation.

Upon withdrawal from the cell cycle, some muscle precursor cells, now known as myoblasts, fuse to form centrally-nucleated myotubes. Others fuse to the ends and sides of remaining myofibers. The damaged area is thereby spanned by new muscle (Robertson et al., 1993b; McIntosh et al., 1994; Pernitsky et al., 1996). Myotubes increase in diameter, myofibrils become completely organized, muscle proteins change from embryonic or juvenile isoforms to adult forms, and muscle generally appears normal. The persistence of centrally-nucleated fibers is common. The crush injury (McGeachie & Grounds, 1987; Mitchell et al., 1992; McIntosh et al., 1994; McIntosh & Anderson, 1995; Pernitsky et al., 1996) is the method of choice for studying synchronous regeneration in the experiments reported in this thesis, although other investigators use freeze or marcaine-induced injury to study repair *in vivo*.

2.3. Myogenic regulatory factors

The myogenic regulatory factors (MRFs; MyoD, myf-5, myogenin, myf-6) play roles in determination and differentiation of skeletal muscle (reviewed in Olson, 1990; Weintraub, 1993; Rudnicki & Jaenisch, 1995), and are the most reliable markers of early myogenic committed cells. They show a distinct temporal and spatial expression pattern in muscle development (see Bober et al., 1991; Hannon et al., 1992). Each member expressed alone can convert a variety of cell lines into muscle cells (Tapscott et al., 1988). Gene knockout experiments have and continue to elucidate the many roles of the MRFs during

embryogenesis (Braun et al., 1992; Rudnicki et al., 1992; 1993; Venuti et al., 1995; Zhang et al., 1995). These experiments show that MyoD and myf-5 play crucial roles in the early events of myoblast formation. On the other hand, myogenin and myf-6 are reportedly expressed only in postmitotic muscle cells, although cells positive for myogenin and myf-6 can be found in the S phase of mitosis. These 2 MRFs respectively have functions in the late events of myotube formation, differentiation, and the final events leading to a fully differentiated myofiber (Weintraub, 1993). Functional redundancy is a feature of MRF expression, at least during development (Rudnicki et al., 1992; 1993; reviewed by Weintraub, 1993).

Convincing evidence exists for a role of MRFs in muscle regeneration. However, the pattern of expression and redundancy of the MRFs in regenerating skeletal muscle differs from developing muscle (Bhagwati et al., 1996). MyoD and myogenin mRNA levels parallel the most active phases of muscle precursor cell replication after a crush-injury and in *mdx* mice (Beilharz et al., 1992). Studies show that MyoD is widely expressed in satellite cells and small regenerating myotubes in *mdx* mice (Garrett & Anderson, 1995; Bhagwati et al., 1996). In addition, mice which lack MyoD have poor repair, and there is a shift to proliferation by uncommitted stem cells (Megeney et al., 1996). *Mdx* mutant mice which also lack MyoD exhibit a worsened disease phenotype, a severe deficit in regenerative ability and a decrease in proliferation of myogenic cells during regeneration compared to that in *mdx* mice (Anderson et al., 1996a). It is concluded that MyoD acts at the level of satellite cells in regeneration (Anderson et al., 1996a; Megeney et al., 1996) and plays a critical role

in the induction of muscle regeneration (Bhagwati et al., 1996) for which myf-5 cannot substitute (Anderson et al., 1996a; Megeney et al., 1996).

2.4. Effects of glucocorticoids on the *mdx* mouse and muscle regeneration

Prednisone probably does not increase strength by suppressing immunologically mediated muscle damage alone (Kissel et al., 1993). At present the most convincing evidence suggests that glucocorticoids affect muscle regeneration. In *mdx* and control mouse myoblast cultures (Metzinger et al., 1993; Passaquin et al., 1993) and in primary cultures of control human myoblasts (Hardiman et al., 1992), treatment with prednisone enhances myogenesis by accelerating myoblast proliferation and myotube formation. Prednisone improves myogenesis in mixed cultures from young DMD muscle, but has no effect on cultures from older DMD patients (Hardiman et al., 1992). Evidence from experiments on cloned human myoblast cultures indicates that the increased number of myotubes with prednisone treatment may be due to a mechanism that prevents myotube death (Sklar & Brown, 1991) or death of cycling cells (Sklar et al., 1991).

A recent *in vivo* morphological study (Anderson et al., 1996b) reports that deflazacort promotes myogenesis (proliferation and/or fusion of muscle precursor cells) early in the repair response to injury in *mdx* mice. It also has long-term beneficial effects on myotube growth. In addition, deflazacort partially spares the *mdx* diaphragm (Anderson et al., 1996b) and cardiac muscle (unpublished data) from inflammation. Prednisone promotes only the longer-term effects of myofiber growth (i.e. increased diameter of total pool of fibers) (Anderson et al., 1996b). One study reports that prednisone has no effect on *mdx* muscle

(Weller et al., 1991). However, prednisone elicits a significant increase in whole body strength in *mdx* mice (Hudecki et al., 1993). Therefore, prednisone and deflazacort are very promising treatments for DMD and many DMD boys are now receiving one or the other drug.

3. NUCLEAR MAGNETIC RESONANCE

Fourier-transform nuclear magnetic resonance spectroscopy (NMR) has been used widely in basic chemistry research for compound identification and structure determination. Recently, NMR has been applied to the study of normal and diseased tissues in the hope of eventually elucidating biochemical information in a non-invasive manner. In this section, a brief summary of nuclear magnetic resonance principles will be presented (from Petersen et al., 1985; Derome, 1987; Garlick & Maisey, 1992; Andrew, 1994), followed by the rationale and methods for using NMR in the study of medical problems. A brief discussion of magnetic resonance imaging (MRI) will conclude the section.

3.1. NMR Spectroscopy

Some nuclei have an inherent spin associated with them and all nuclei have a positive charge. A magnetic moment accompanies the spin and charge combination. When in a magnetic field, a magnetic nucleus will precess around the field. After applying a brief pulse of a magnetic field oscillating at radiofrequency at a right angle to the fixed magnetic field, an exchange of energy between the nuclei and the applied electromagnetic field occurs. This is nuclear magnetic resonance (Andrew, 1994). The weak radiofrequency

signal induced from the nuclei can be measured by placing a coil around the sample which is attached to a radio receiver. Then the detected NMR signal (free induction decay; FID) is amplified, displayed (amplitude vs. time) and Fourier transformed into a spectrum showing amplitude vs. frequency.

Different NMR-active nuclei (see Andrew, 1994 for a complete listing) resonate at different frequencies. Therefore, a particular nucleus can be selectively excited by choosing the proper radiofrequency pulse. In addition, for a given nucleus, various chemical constituents resonate at slightly different frequencies (the chemical shift) depending on the physical and chemical environment of the molecules and the field strength. NMR spectroscopy is thus able to identify the molecular constituents of a biological sample based on the differences in the observed frequencies between constituents. To be detectable by NMR, molecular constituents must have a high enough concentration and be fairly mobile.

Phosphorus 31 (31-P) and the proton (1-H) are two NMR nuclei of particular and practical interest in physiology and biomedicine. 31-P is universally present and is present in many tissues, and as such, is an effective NMR nucleus for monitoring tissue energetics and pH. The low and interpretable background of the 31-P NMR signal is of benefit in studying energetics, but it is limited in terms of cellular biochemical processes (Sze & Jardetzky, 1990). 1-H NMR is very sensitive with a larger number of metabolites being observable compared to 31-P NMR, but is not adequate to study tissue energetics. The proton has an isotopic abundance of almost 100%, a high magnetic moment and high physiological concentrations. Sequences (algorithms in collecting NMR spectra) exist by

which to suppress the strong water 1-H NMR signal. However, a severe overlap of the resonances of interest is often a problem, owing to the small chemical-shift range of 1-H NMR (Andrew, 1994). High resolution NMR of extracts (Sze & Jardetzky, 1990; 1994), selective solvent suppression techniques (Rothman et al., 1984) and the use of two-dimensional (2D) NMR help overcome these problems. 2D NMR separates NMR information in 2 dimensions on a surface so that each peak has a pair of coordinates instead of the single coordinate in a 1D spectrum.

3.2. NMR applied to studying medical problems

The level of some endogenous metabolites is affected by disease (Andrew, 1994). Therefore, it is rationalized that high-field, high-resolution NMR spectroscopy can monitor subtle biochemical differences which correlate with different disease states. Several methods for examining tissue have been used to study diseases, and exemplify the discriminating power of NMR for diagnosis (Mountford et al., 1986; Peeling & Sutherland, 1992; Kuesel et al., 1994; Rutter et al., 1995).

Investigation of tissue extracts by NMR can be performed in a variety of manners (Bell et al., 1994), with the usual purpose of isolating precisely-localized cells, removing the extracellular background and extracting the remaining substances. Perchloric acid extraction is the method of choice for water soluble metabolites of low molecular weight, resulting in high reliable yields of substances of interest (Sze & Jardetzky, 1990; 1994). Studying biological compartments in isolation and under optimal conditions aids in the understanding of complex data from complex tissues (Sze & Jardetzky, 1994), and often

assists and complements *in vivo* NMR studies. Spectra of extracts have higher resolution than *in vivo* spectra because they are homogeneous samples which can be studied at a higher, uniform magnetic field, giving greater spectral dispersion (Peeling & Sutherland, 1992). Therefore, quantification of metabolites can be readily carried out (Bell et al., 1994). Despite the above-mentioned advantages of tissue extractions, rapid postmortem changes in tissue metabolites occur, necessitating speedy removal of samples and preparation. As well, perchloric acid extractions preclude estimation of a cell's redox state, degradation of RNA occurs, and hydrolytic products from the extraction are often observed in the spectra (Sze & Jardetzky, 1994).

The use of pieces of excised tissue *(ex vivo)* for NMR analysis is intermediate between extract and *in vivo* analyses for advantages and limitations. The heterogeneity of the sample results in lower resolution than that of extracts, but this method has been successfully used to study various tissues, such as brain (Kuesel et al., 1994; Rutter et al., 1995), colon (Brière et al., 1995) and the cervix (Mountford et al., 1990) in various pathological states. Very small sample sizes may cause problems in positioning and shimming. The coaxial tube method proposed by Kuesel et al. (1992) is quite reliable and the position of the tissue in the coil is stable. The main advantage of the *ex vivo* NMR method is that it allows precisely-defined pieces of tissue to be studied with high-field NMR which subsequently can be followed by histological examination of the same sample (albeit partly degraded by freeze, thaw and signal collection prior to fixation).

The development of NMR spectroscopy for clinical practice has been relatively slow.

Most human whole-body magnets have low magnetic-field strengths (1.5-2T) and patient examination time is limited. Therefore, the heterogeneity of living tissue results in broad and often overlapping peaks, decreased resolution and low sensitivity (Burt et al., 1986; Andrew, 1994). Peak assignment and metabolite quantification become problematic (Heinriksen, 1994). However, with special editing techniques and pulse sequences, studies of living animal models in high-field magnets can yield high-resolution spectra. Since contamination from neighboring regions is unwanted, several methods have been used for spatial localization of *in vivo* NMR spectra (Howe et al., 1993; Alger, 1994; Andrew, 1994).

A surface coil, a flat receiver coil which is laid on or over the region of interest, is commonly used for regions on or just below the surface that need not be accurately localized. Signals from tissue deep to the coil and tissues close to the coil cannot be discriminated. Other localization techniques, used in conjunction with the gradients of magnetic resonance imaging, include single and multivoxel methods. In the single voxel method, a spectrum is acquired from one volume of interest, which is usually cuboid. In the multivoxel (spectroscopic imaging) method, a series of NMR spectra are acquired from multiple slices or voxels from a magnetic resonance image. In this way, metabolite maps which indicate the spatial distribution of particular metabolites are acquired.

3.3. Magnetic resonance imaging (MRI)

Since the technical and interpretational demands of *in vivo* spectroscopy are as yet so high, magnetic resonance imaging has been the method of choice for most *in vivo* studies. MRI is primarily an anatomic and pathologic imaging modality and does not provide

the biochemical information that NMR spectroscopy does. However, the basic NMR phenomena of spectroscopy and imaging are the same (see Karczmar, 1994). Medical MRI uses the nucleus of the body's water protons to obtain an image (Garlick & Maisey, 1992).

In MRI, a heterogeneous sample (the body) is placed in a non-uniform magnetic field in which different parts of the sample experience different field strengths. As a result, the water protons in different areas respond at recognizably different NMR frequencies, and images of sections of the body are obtained (reviewed by Andrew, 1994). In other words, an MRI is a two-dimensional representation of the NMR signal from the protons in a thin slice of the body.

In order to obtain a good image, good contrast is required. MRI generally provides better contrast for soft tissues than other imaging methods due to the variation in nuclear spin relaxation properties in normal and diseased tissues. This has an effect on image intensity. There are two measures of relaxation (the time it takes for nuclei to return to equilibrium after an applied pulse): T1 and T2. Images can either be T1-weighted or T2-weighted. A T1-weighted image is one in which T1 is an important factor in controlling image intensity. T1, or longitudinal relaxation, refers to the realignment of magnetic moments along the applied field after excitation. Tissues with a short T1 (they realign rapidly) appear brighter in T1-weighted images than tissues with a long T1. For example, fat appears bright and edema appears dark. A T2-weighted image is one in which T2 is an important factor in controlling image intensity. T2, or transverse relaxation, refers to the decrease in signal and loss of phase coherence due to magnetic moments not precessing

at exactly the same frequency after excitation. Tissues with a long T2 are bright (fat), while tissues with a short T2 are dark (liver). Both T1- and T2-weighted images are used clinically to interpret imagery of body anatomy in health and disease.

4. NMR SPECTROSCOPY AND SKELETAL MUSCLE

An enormous range of magnetic resonance studies using a number of NMR-active nuclei have been performed on various tissues (for example see Lundberg et al., 1990; Henriksen, 1994). Skeletal muscle is an ideal candidate for study by NMR spectroscopy since it is relatively easy to position a surface coil accurately *in vivo*, and studies can be performed either at rest or during exercise. In this section, a brief review of some important NMR-visible metabolites will occur followed by a review of 31-P and 1-H NMR spectroscopy studies of skeletal muscle. MRI studies of skeletal muscle will also be discussed.

4.1. Important NMR-visible metabolites (see Appendix A for the structures)

Muscle fibers get energy (see McComas, 1996) by splitting ATP (adenosine triphosphate). As ATP is expended, it is replenished from phosphocreatine (PCr). PCr is an thus an energy reserve for skeletal muscle. Creatine (Cr) results from the production of ATP from ADP and PCr. A fall in PCr directly correlates to a rise in Cr. These two metabolites cannot be distinguished from one another by 1-H NMR spectroscopy (Styles et al., 1995), and levels are measured in terms of total creatine (Crs).

Eventually during work the production of ATP from PCr is inadequate, and fibers become dependent upon the oxidation of fat and glucose (mostly derived from glycogen).

Glycolysis (the breakdown of glucose) occurs under both aerobic and anaerobic conditions in the myofiber's cytosol, and produces ATP. In anaerobic conditions, the pyruvate produced from glycolysis is converted to lactate. Therefore, high lactate levels are probably a result of high glucose consumption and increased glucose uptake (Moreno & Arús, 1996). Glucose breakdown is completed by the citric acid cycle in the mitochondrion to produce further ATP. Succinate is a citric acid cycle intermediate, while glutamate and glutamine are formed by pathways originating from another intermediate, α-ketoglutarate. In normal muscle, glutamine has anabolic effects and may stimulate glycogen resynthesis (Rennie et al., 1996). Glucose and the above amino acids are visible in 1-H NMR spectra of skeletal muscle (for example see Venkatasubramanian et al., 1986).

In prolonged exercise, glycogen is consumed and continued force production depends on lipid metabolism. In addition, lipid breakdown supplies energy requirements of resting muscle and in low intensity exercise. Fat is available to muscle as fatty acids from blood or from lipid droplets in the cytosol of myofibers. Soluble phospholipids and fatty acids can be studied by NMR (see Yoshizaki et al., 1981). Studying them in membranes requires special techniques.

Carnitine, another skeletal muscle NMR-visible metabolite (Nakajima et al., 1994), is utilized in transport of long chain fatty acids into the mitochondrion for metabolic processing, while medium and short-chain fatty acids pass directly into mitochondria. Carnitine is essential for the normal oxidation of fats by the mitochondria and is involved in the transesterification and excretion of acyl-CoA esters, the oxidation of branched chain

alpha-ketoacids, and the removal of potentially toxic acylcarnitine esters from within mitochondria (Hiatt et al., 1989).

The amino acids valine, alanine and glycine are visible in 1-H NMR spectra of skeletal muscle (see Venkatasubramanian et al., 1986), and convert to glycogen. Cholines can by viewed as 3 distinct peaks by high resolution NMR (phosphocholine, glycerophosphocholine, choline). They may measure an impairment in phospholipid metabolism and are products of the breakdown of the neurotransmitter acetylcholine (ACh). This breakdown is important in order for further muscle contraction to occur.

Taurine is present in high concentrations in skeletal muscle 1-H NMR spectra. It is a very interesting free amino acid for which many biological actions have been proposed (Chesney, 1985; Wright et al., 1986; Huxtable, 1992). Taurine derives from the metabolism of methionine and cysteine (sulfur-containing amino acids). It can therefore arise from dietary intake or endogenous metabolism of sulfur amino acids. At least two separate pathways are involved in the metabolism of cysteine to taurine (see Chesney, 1985). In the CSA pathway, cysteine is converted to cysteine sulfinic acid, cysteic acid and taurine by the enzyme cysteine sulfinic acid decarboxylase. In the cysteamine pathway, cysteine is converted to cysteamine, then hypotaurine and taurine. Both of these pathways require the oxidation of hypotaurine to taurine. Taurine has been implicated in the modulation of neurotransmitter and hormone release, osmoregulation, stimulation of glycolysis and glyconeogenesis, cell proliferation and viability, antioxidation and regulation of phosphorylation, to name a few (see Huxtable, 1992). In muscle, a role in membrane

protection/stabilization (mechanism not understood) is suggested (Wright et al., 1986).

4.2. 31-P NMR of skeletal muscle

Skeletal muscle was the first tissue to be studied using 31-P spectroscopy which provides interesting and valuable information about tissue bioenergetics and metabolism (reviewed by McCully et al., 1994). 31-P NMR spectroscopy allows measurements of variations in concentrations of inorganic phosphate (P_i), PCr, ATP, and small amounts of PME (phosphomonoesters) and PDE (phosphodiesters) at rest, during exercise, and during recovery. Thus, much of our knowledge about the energetics of muscle contraction has been supplied by *in vivo* 31-P studies. Based on the shift frequency of P_i, pH measurements can also be made. Patterns in 31-P NMR spectra have been recognized for several diseases of muscle (Edwards et al., 1982; Argov & Bank, 1991), including DMD (reviewed by Kent-Braun et al., 1994).

In resting dystrophic muscle, PCr are levels are decreased, but ATP levels are normal (Younkin et al., 1987; Kemp et al., 1993). These reports on DMD muscle, and another on *mdx* muscle (Dunn et al., 1991), show increased resting pH levels with disease compared to normal resting muscle, while others reveal no significant abnormality (Griffiths et al., 1985). PDE levels are also elevated in DMD which may reflect breakdown of phospholipids coincident with dystrophy (Younkin et al., 1987). Therefore, it is suggested that DMD patients have less energetic reserve than normal (Younkin et al., 1987), actually not an unexpected finding considering the large energy use involved in tissue damage and repair during pathology.

Abnormal muscle energy metabolism in response to exercise is observed in patients with DMD and in *mdx* mice by 31-P NMR. There appears to be a greater reduction of pH during exercise in DMD (Kemp et al., 1993) and slower metabolic recovery following exercise in *mdx* mice (Dunn et al., 1992; 1993). The differences in pH during exercise provide an indication of impaired ionic regulation in dystrophic muscle (Dunn et al., 1992; 1993; LeRumeur et al., 1995). Additionally, a defect in oxidative metabolism may explain slower recovery (Dunn et al., 1993; LeRumeur et al., 1995).

4.3. 1-H NMR of skeletal muscle

1-H NMR has not been applied extensively to the spectroscopic study of skeletal muscle, but it has important potential for studying muscle metabolism (Arús et al., 1984a). Prominent metabolite peaks from alanine, carnitine, cholines, creatines, glucose, glutamate, glutamine, lactate, taurine, succinate and valine are found in 1-H NMR spectra of mammalian skeletal muscle perchloric acid extracts (Arús et al., 1984b; Venkatasubramanian et al., 1986, Petroff, 1988) and of mammalian muscle biopsies (*ex vivo*) (Yoshizaki et al., 1981; Arús & Bárány, 1986). Changes in the levels of some of the metabolites coincide with muscle disease.

On the basis of 1-H NMR spectra of muscle extracts, it is suggested that two disease states associated with secondary muscle changes (scoliosis and cerebral palsy) have characteristics distinct from healthy muscle (Arús et al., 1984b; Venkatasubramanian et al., 1986). One report indicates that perchloric acid extracts of muscular dystrophic patients can also be distinguished from normal on the basis of a signal attributed to 3-methyl-histidine

which is a marker for contractile protein degradation (Tanguy et al., 1994).

In vivo 1-H NMR spectra of skeletal muscle exhibit signals of water and fats which are far greater than any other metabolite (Williams et al., 1985; Bárány et al., 1989; Bongers et al., 1992; Schick et al., 1993). Studies on human subjects indicate that the lipid resonances between 0.8 and 2.2 ppm appear to be indicators of disease, since these resonances are far larger in diseased muscle and increased intensity of the lipid resonances is related to the severity of muscle involvement (Bárány et al., 1989; Bongers et al., 1992). Lipid signals in muscle spectra of living tissue are largely produced by adipose tissue. Bárány and colleagues (1989) found spectral differences in the lipid composition between healthy muscle and that from patients with neuromuscular diseases. It is important to note that the lipid signals from muscle show components not found in pure fat, and it is suggested that the resonances differentiate lipid within fat cells in muscle from lipids within muscle cells (i.e. intracellular lipid vacuoles) (Bongers et al., 1992; Schick et al., 1993). Early *ex vivo* studies of muscle (Yoshizaki et al., 1981) support these *in vivo* findings and suggest that lipid signals mainly derive from muscle cytosol and are freely mobile as an energy source.

Since the lipid peaks give limited information with present understanding, much work on skeletal muscle *in vivo* has recently been dedicated to suppressing the large lipid peaks so as to detect smaller metabolite signals (Bloch et al., 1995; Shen et al., 1996). For example, lactate editing techniques and increased spectral resolution have improved to the extent that two lactate peaks are distinctly resolved at 1.29 and 1.34 ppm *in vivo* (Shen et

al., 1996). It has been convincingly suggested that these two lactate peaks correspond to two different fiber type populations; glycolytic and oxidative fibers respectively.

Muscle from the *mdx* mouse has been studied by 1-H NMR spectroscopy by one group. By 2 dimensional *in vivo* NMR, *mdx* muscles show an additional peak corresponding to tri-unsaturated fatty acids that are not related to adipose tissue (Gillet et al., 1993). The extra signal in *mdx* muscle could be related to the fluid membrane of fusing myoblasts (Gillet et al., 1993), which are found at a characteristic stage in young regenerating *mdx* muscle. Further study of muscle regenerating after an injury shows that the extra tri-unsaturated fatty acid is a characteristic of the period of intense myoblast fusion (Gillet et al., 1995). No other 1-H NMR studies of *mdx* muscle tissue have been reported. Close examination of the metabolites in *mdx* muscle using high field NMR would characterize further the dystrophic and repair processes and address questions of the chemical constituents of effective repair or severe disease.

4.4. MRI and skeletal muscle

Many MRI studies of normal and pathologic skeletal muscle have been performed. The technique allows muscle to be serially assessed in a non-invasive manner. MRI methods that have been used to grade muscle disease include: 1) analysis of visual changes such as the size of the involved muscle, the number and distribution of diseased muscles and the pattern/severity of fat infiltration (Murphy et al., 1986; Lamminen, 1990; Liu, Jong et al., 1993), 2) analysis of mean T1 and T2 relaxation times (Huang et al., 1994), and 3) quantification of percent fat infiltration by detailed maps of T2 values (Phoenix et al.,

1996). The severity of involvement by MRI measures appears to parallel muscle function upon clinical examination (Murphy et al., 1986; Huang et al., 1994).

Normal muscle appears grey and relatively homogeneous on T1-weighted images, while subcutaneous fat, intermuscular fat and bone marrow are of high signal intensity (Murphy et al., 1986; Suput et al., 1992). Discrimination of individual muscle groups is possible (Murphy et al., 1986). MR images of late-stage DMD muscle have an increased amount of subcutaneous fat (high signal intensity) and homogeneous fat infiltration preferentially into fast muscles (Murphy et al., 1986; Suput et al., 1992). Some sparing of slower muscle (i.e. sartorius, gracilis, semimembranosus and semitendinosus) is evident. T1 values are reported to be decreased in DMD compared to control muscle (Matsumura et al., 1988; Huang et al., 1994), while T2 values are longer in DMD muscle, coincident with increased fatty infiltration (Huang et al., 1994). In addition, and consistent with pathological changes, the distribution of T2 values is narrower in stronger patients and wider in weaker ones (Huang et al., 1994). The application of MRI to skeletal muscle will continue to reveal structural changes associated with disease and treatment. These changes ultimately reflect the chemical constituents in that tissue and advances are being made to the feasibility of monitoring the changes by NMR spectroscopy.

5. OBJECTIVES AND HYPOTHESES

The overall purpose of this thesis is to explore the potential use of 1-H NMR spectroscopy in monitoring the progression of muscular dystrophy and its treatment in *mdx* mice.

The purposes of the studies performed in Chapter 2 were to characterize normal and dystrophic *mdx* muscle biopsies (*ex vivo*) at different ages and stages of dystrophy by high resolution 1-H NMR spectroscopy, and to determine whether spectra correlate with known histological parameters of growth and dystrophy. It was hypothesized that: 1) 1-H NMR would detect changes in muscle status during normal growth in control mice and during the progression of dystrophy in *mdx* mice, and 2) spectral features would correlate to the phenotype of *mdx* muscle as assessed by histological measures. These hypotheses were based on the assumption that biochemical changes in disease can be monitored by examining NMR-visible metabolites by 1-H spectroscopy.

Chapter 3 reports on the effects of two glucocorticoids (deflazacort and prednisone) on control and *mdx* muscle as viewed by high resolution 1-H NMR spectroscopy (*ex vivo*). Findings were interpreted in terms of reports of improved repair with treatment. An additional objective was to study muscle repair at two time points after an imposed injury by analysis of *ex vivo* 1-H NMR spectra. It was hypothesized that: 1) glucocorticoids would produce significant changes in 1-H NMR spectra consistent with increased repair or decreased dystrophy, 2) 1-H NMR would be able to resolve the regenerative state of muscle from that of dystrophy, and 3) control muscle in repair (assessed by histology and 1-H NMR)

would be affected by deflazacort in a similar way to effects on *mdx* muscle.

Normal and *mdx* muscle were characterized by high resolution 1-H NMR spectroscopy of perchloric acid extracts in Chapter 4. Additionally, Chapter 4 reports on 1-H NMR extract analysis of deflazacort-treated muscle. It was hypothesized that: 1) control and *mdx* dystrophic muscles would exhibit different spectral characteristics, and 2) spectra from extracts would have similar changes to those observed in *ex vivo* spectra of deflazacort-treated *mdx* and control animals. Since high resolution NMR of extracts yields more information on muscle metabolites, it was expected that suggestions could be made as to the energy state of *mdx* dystrophic animals.

Chapter 5 reports on preliminary MRI studies which were performed in order to gain an understanding of the potential of *in vivo* 1-H NMR spectroscopy and MR imaging of dystrophic (*mdx*) muscle. It was hypothesized that MRI would distinguish *mdx* dystrophy from control muscle and that regeneration after an injury would be evident on MR images.

The thesis is concluded with a general discussion in Chapter 6. An attempt is made to summarize and integrate the findings reported in Chapters 2 to 5. Additionally, recommendations are made for further studies.

CHAPTER 2

AN *EX VIVO* NUCLEAR MAGNETIC RESONANCE SPECTROSCOPY STUDY OF MUSCLE GROWTH AND *MDX* DYSTROPHY: CORRELATION WITH HISTOPATHOLOGY

1. ABSTRACT

Proton nuclear magnetic resonance spectroscopy (1-H NMR) was used to study skeletal muscle. We tested the hypotheses that: 1) 1-H NMR can detect changes in muscle status during normal growth and during the progression of muscular dystrophy, and 2) spectral features can be correlated to the phenotype of dystrophic muscle as assessed by a morphological measure of accumulated repair. *Ex vivo* spectra of tibialis anterior (TA;n=56) and diaphragms (DIA;n=57) from young (<3wk), adolescent (3-6wk) and adult (>6wk) control and *mdx* dystrophic mice were obtained. Mean heights and areas of peaks at 3.9 ppm (creatines), 3.4 ppm (taurine), 3.2 ppm (taurine and cholines), 3.0 ppm (creatines), 1.3 ppm (lipids and lactate) and 0.9 ppm (lipids and amino acids) were compared among groups. Assignments do not imply these are the sole metabolites contributing to the peaks. Spectra from TA and DIA differed consistently and significantly. Resonances due to taurine and creatines were generally lower in *mdx* young than *mdx* adolescent or adult (i.e. they increased with age). These same resonances were generally lower in *mdx* young than control young. Trials of linear discriminant analysis were between 84 and 100% accurate in differentiating control from *mdx* spectra and in classifying spectra from different ages of *mdx* mice. Correlations between accumulated repair and spectral peaks gave coefficients ranging from $0<R^2<0.71$ on *mdx* data. We conclude that the taurine resonances are particularly useful markers for *mdx* dystrophy. 1-H NMR is sensitive to the distinct and progressive phenotype of *mdx* dystrophy and identifies the *mdx* phenotype before the onset of dystrophic necrosis.

2. INTRODUCTION

Proton nuclear magnetic resonance spectroscopy (1-H NMR) has been used to study biochemical aspects of skeletal muscle (see Chapter 1, section 4.3) and the disease of Duchenne muscular dystrophy (DMD; see Chapter 1, section 1.1). However, the reported NMR studies have not examined spectroscopic features that might best track functional outcomes, namely the stages of muscle growth, the progression of dystrophy and the muscle repair sequelae. It is imperative that status and repair progress be examined in order to monitor changes in the disease during and after various treatments, and that they be correlated accurately to the phenotype of the muscle.

The *mdx* mouse model of dystrophy allows such studies to be made since it is a genetic homologue to DMD (see Chapter 1, section 2.1) and undergoes a well-characterized disease process in limb and diaphragm. Most NMR studies on *mdx* dystrophy report 31-P NMR (Dunn et al., 1992; 1993) and show abnormal pH regulation and muscle energetics. These changes are postulated to be due to a reduction in the capacity to export proton equivalents in *mdx* muscle. One study on *mdx* mouse muscle using *in vivo* 1-H NMR suggests that increased membrane fluidity, detected as a new lipid resonance, marks the formation of new myotubes (Gillet et al., 1993), and is consistent with previous findings on phospholipids in *mdx* muscle *in vitro* (Anderson, 1991). Thus it is reasonable to suggest that 1-H NMR spectroscopy can also identify biochemical features that mark key steps in myogenesis and dystrophic progression in *mdx* mice.

This study tested the hypothesis that 1-H NMR can discriminate between normal and

mdx muscle during growth and the progression of dystrophy. In addition we tested whether 1-H NMR spectra were different in *mdx* limb and diaphragm muscle, in view of their distinct mild and severe phenotypes of dystrophy respectively. Features of 1-H NMR spectra were correlated to the degree of fiber centronucleation in the same samples of *mdx* limb muscles in order to determine whether and how well the changes in spectra might predict changes in histology that indicate accumulated muscle repair.

3. MATERIALS AND METHODS

3.1. Animals and tissue samples

Control (C57Bl/10ScSn) and *mdx* mice were divided into 3 groups: young (<3wk), adolescent (3-6wk) and adult (>6wk), ages that correspond to 3 stages of *mdx* dystrophy (pre-dystrophy, active dystrophy and stable dystrophy). Anaesthetized animals (1:1 ketamine - xylazine) were killed by cervical dislocation. The right tibialis anterior (TA) and the entire diaphragm (DIA) were removed from each mouse, coded, immediately frozen in a vial of PBS/D_2O (phosphate buffered saline in deuterated water; pH=7.4) in $N_2(l)$, and stored in a -70° freezer until use. During dissection care was taken to remove visible adipose tissue, nerves and blood vessels from muscles. For control mice, there were a total of 29 TAs (young=11; adolescent=10; adult=8) and 28 DIAs (young=12; adolescent =7; adult=9). For *mdx* samples, there were a total of 27 TAs (young=8; adolescent=10; adult=9) and 28 DIAs (young=7; adolescent=10; adult=11). Maintenance, breeding and handling of animals was carried out according to the Canadian Council on Animal Care.

At the time of spectroscopy, specimens were thawed at room temperature for 15 min. A small longitudinal piece (approximately 3mm) of muscle tissue was dissected from the whole TA or DIA, excluding most tendon, adipose and nerve tissues. For the DIAs, the muscle tissue was sampled so as to include parts of the costal plus crural regions. Specimens were then placed in a capillary tube filled with PBS/D_20 (Kuesel et al., 1992).

3.2. Nuclear magnetic resonance spectroscopy (NMR)

The 1-H spectra (one dimensional-1D; number of scans-NS=256-640; spectral width-SW=5000 Hz, relaxation delay-RD=2.41s, time domain-TD=4K) were acquired at 25°C with presaturation of the water signal on a narrow bore 360MHz spectrometer (AM360; Bruker; Institute for Biodiagnostics, National Research Council; IBD-NRC). Para-aminobenzoic acid (PABA; 5 or 0.5 mmol/L) was used as a quantitative and chemical shift reference. Following acquisition of spectra, samples were weighed and fixed in 10% formalin for 7-10 days for subsequent histopathological analysis. Resonances were assigned by the spectral pattern in one-dimensional spectra of perchloric acid extracts, by two-dimensional COSY spectra on some samples and by comparison with chemical shift values of pure compounds and literature values (Williams et al., 1985; Peeling & Sutherland, 1992; Moreno et al., 1993; Brière et al., 1995).

3.3. Peak height and area measurements

For TA and DIA spectra, data were acquired on the spectral peak areas and peak heights listed below. Data were processed multiple times in different manners until a reliable, precise method of quantification was achieved. The results from each processing

method (1-6, below) were statistically compared using t-tests. Spectra were: 1) baseline corrected then integrated, 2) phased-only then integrated, 3) processed by 2 separate researchers, 4) processed by the same researcher on 2 separate occasions, 5) processed using *dis-nmr* (Bruker) software, and 6) processed using *x-spec* (version 2.0.7; Bruker) software. In the instances where baseline correction was performed, baseline irregularities were removed by applying a series of linear corrections over the entire spectrum. These corrections produced a flattened baseline.

Areas (integrals) were measured between 4.4 and 3.5 ppm (A1), 3.5 and 3.3 ppm (A2), 3.3 and 3.1 ppm (A3), 3.1 and 2.8 ppm (A4) and 1.8 and 0.8 ppm (A5) for each spectrum (see Fig 2.1), and subsequently normalized to tissue mass and to the area of the PABA reference peak (7.1 to 6.6 ppm). The integrals were defined at exactly the same points in each spectrum. The height of the peaks were measured for resonances at 3.9, 3.4, 3.2 , 3.0, 1.3 ppm and 0.9 ppm (HTs 1-6 respectively; Fig 2.1), and once again normalized to tissue mass and to the height of the PABA peak (6.81 ppm). In addition, ratios of all combinations of peak heights (HT1/HT2, HT1/HT3, etc) and areas (A1/A2, A1/A3, etc) were determined.

Data were then decoded and the mean (± SEM) height, height ratio, area and area ratio were determined for each group. Two-way ANOVA and Duncan's test *post hoc* were used to test for significant differences among age groups (young; adolescent; old) and strains (control; *mdx*). As well, three-way repeated measures ANOVA was used to test for significant differences between peaks from TA and DIA spectra. A probability of $p<0.05$ was

used to reject the null hypothesis.

3.4. Linear discriminant analysis

Trials of linear discriminant analysis (LDA) on processed spectral data were performed (*x-prep* software; IBD-NRC) to attempt strain and age discrimination between control and *mdx* TA muscle spectra. A region of interest from 0.44 ppm to 4.12 ppm was chosen, the raw numerical data were reduced from 600 to 150 data points for each spectrum, and the results were stored as a numerical data matrix.

LDA was performed using the discrimination version-k (*dscr_k*) program (IBD-NRC). A training set of data, consisting of a random selection from the original data matrix of about two-thirds of the processed TA samples from each group, was employed to generate a reduced data set of regions between 0.44 and 4.12 ppm which best described and discriminated among groups of spectra. The program operated iteratively assembling the best 1, 2, 3, ..., n data points which classified all spectra, n usually chosen to be 15. Spectral comparisons were made using: 1) two groups - control vs. *mdx*, 2) three groups - *mdx* young vs. *mdx* adolescent vs. *mdx* adult, 3) four groups - control vs. *mdx* young, *mdx* adolescent and *mdx* adult, and 4) six groups - control young, adolescent and adult vs. *mdx* young, adolescent and adult. A test set, selected from the remaining spectra not used in the training set, was used to verify the descriptive and discriminative validity of the reduced data set according to training. All reported results will be of test data only, as training set data must necessarily be at 100% before reliable test set data can be expected.

Ratios, calculated from a reduced data set that best discriminated among the

groups, were then generated to produce new data matrices comprised of both the ratio data and the original reduced data set. *Dscr_k* was then used as above to generate reduced sets. A genetic algorithm program (*dscr_l*), which used a pre-selected number (15) of regions and iterations as constraints for the production of variably sized data point domains, was employed to discriminate between spectra. Distribution of classification data were tested for significance using Chi-square statistics.

3.5. Histology and morphometry

After acquisition of spectra from each *ex vivo* sample, tissue was fixed (7 days) in buffered formalin. Formalin-fixed samples were rinsed overnight in phosphate buffer containing 5% sucrose, then placed in Tissue-Tek O.C.T. compound, oriented for longitudinal sectioning, and frozen in isopentane at -50°C. Every third 7μm section was collected serially onto glass slides. One slide from each collection was stained with H&E (Hemotoxylin and Eosin), another with PAS (Periodic Acid Schiff) for connective tissue and lipid.

To analyze the coded TAs, a camera lucida was used with a calibrated graphics tablet and the Sigma Scan program (Jandel Scientific, CA) to record myotube length (at 100X) and the length of central nucleation (cnl) within each of the myotubes (at 200X). Cnl was defined as that distance subtended by a segment of central nucleation, plus half the width of the fiber at each end of the segment of central nucleation (Fig 2.2). If the total subtended distances of two consecutive regions of cnl within a myotube intersected, that length was measured as one; if they did not intersect, two lengths were measured. When

peripheral nuclei were observed in a segment, the cnl terminus was considered to be half the distance between the peripheral nucleus and the terminal central nucleus visible in a myotube at 200X. The longitudinal centronucleation index (CNI-L) was calculated by dividing the sum of cnls by the sum of the total myofiber length (including myotubes) in one complete section of muscle. Measurements and calculations were made without exact knowledge as to source, although control samples were easily distinguished from dystrophic muscle sections. The mean (± SEM) CNI-L was determined for each group and 2-way ANOVA were used to determine the effects of strain and age on the CNI-L of TA muscles.

3.6. Correlations

Analysis of correlation between TA-CNI-L and the defined spectral heights, areas and ratios from the same samples of muscle were performed using Excel (Microsoft Corp, Cambridge, MA) and NWA Statpak (Northwest Analytical Inc, Portland OR). In this instance a probability of $p<0.01$ was used to decide significance.

4. RESULTS

4.1. 1-H NMR resonance assignments and spectral characteristics

Typical DIA and TA spectra are shown in Fig 2.1. Peaks at 3.9 ppm and 3.0 ppm were respectively assigned to N-CH_2- and CH_3-N of creatine protons (peak 1 and 4). Peaks at 3.4 ppm and 3.2 ppm were assigned respectively to -CH_2-N and -CH_2-S of taurine protons (peak 2 and 3). The peak at 3.4 ppm may also have contributions from methyl protons of choline-containing compounds. The peak at 1.3 ppm was assigned to -$(CH_2)_n$ protons of

mobile fatty acids, and may be partially due to $-CH_3$ protons of lactate (peak 5). Methyl protons of fatty acids and some amino acids contribute to the peak at 0.9 ppm (peak 6). Assignments do not imply that these are the only substances contributing to any particular peak. The structure of these metabolites are shown in Appendix A.

Tibialis anterior spectra from control and *mdx* muscle (Fig 2.1b and 3) were dominated by resonances at 3.4 ppm (HT2), 3.2 ppm (HT3), 3.9 ppm (HT1) and 3.0 ppm (HT4), 1.3 ppm (HT5) and 0.9 ppm (HT6). Mobile lipids resonances were also observed in the region between 2.2 to 0.8 ppm and at 5.3 ppm. In contrast, diaphragm spectra (Fig 2.1a) were dominated by resonances from mobile lipids centred at 0.9 (HT6), 1.3 (HT5), 2.1, 2.3, and 5.3 ppm. Resonances due to taurine (HT2 and HT3) and creatines (HT1 and HT4) were also observed.

4.2. The processing method

Phased-only spectra gave significantly higher means for peak heights ($p<0.001$) and areas ($p<0.05$) compared to baseline corrected spectra. When the baseline correction/integration procedure was performed on two separate occasions, significant differences resulted ($p<0.02$) in peak heights and areas. However, no significant differences were found when phased-only spectra were integrated on 2 separate occasions or by 2 separate researchers. As well, no significant differences were found using the 2 different software packages on phased-only spectra. In the remainder of this paper, and in subsequent reports, the processing method of only phasing the spectra and then performing integration with *x-spec* software will be reported.

4.3. Peak height and area measurements

The results of statistical analyses (2-way ANOVA) of all significant effects of age, strain, and age X strain interaction of peak area, peak height and ratios (of peak areas and peak heights) are summarized in Table 2.1 (TA, upper table; DIA, lower table). Tables of the mean (± SEM) and significant results of all peak heights, areas and ratios are included at the end of this chapter.

4.3.1. TA Analysis of peak areas of the TA (Table 2.2) showed a significant difference by ANOVA among the 3 age groups for A3 and significant interactions for A1, A2, A3 and A4. Specifically, A2 (Fig 2.4), A3 and A4 were significantly lower (by Duncan's) in *mdx* young than in *mdx* adolescent or *mdx* adult. As well, A1, A2, A3 and A4 were significantly lower in *mdx* young compared to control young (for example, see Fig 2.4).

Ratios of peak area (Table 2.6) were consistently and significantly different among the 3 age groups. Generally, this was seen as a decrease with age in area ratio means in both control and *mdx* TAs. However, ratios A3/A4, A3/A5 and A4/A5 exhibited a greater mean with age in *mdx* TA. Differences between control and *mdx* strains were observed for comparisons between *mdx* young and control young for A1/A5, A2/A5, A3/A5 and A4/A5. As well, *mdx* adult and control adult differed significantly for A1/A5, A2/A3, A2/A4, A2/A5, A3/A5 and A4/A5. The means were lower in *mdx* young compared to control young, but higher in *mdx* adult compared to control adult.

Peak height and height ratios (Tables 2.4 & 2.8) showed characteristic differences among groups that were similar to those for area and area ratios. For example, similar to

A2 and A3, HT2 and HT3 were higher in *mdx* adult compared to *mdx* young, higher in *mdx* adult compared to control adult and lower in *mdx* young compared to control young. In addition to significant area data, HT5 changed significantly with age and HT6 changed significantly with strain.

4.3.2. DIA A1, A2, A3 and A4 exhibited significant differences among DIAs (Table 2.3) of the 3 age groups. In particular, *mdx* DIA A2 (Fig 2.4), A3 and A4 were greater with age, while control A1 was significantly higher in adolescent compared to young or adult control DIA. Significant strain differences were seen for 3 peak areas: A5 was significantly lower in *mdx* young than control young, A1 was significantly lower in *mdx* adolescent than control adolescent, and A4 was significantly higher in *mdx* adult than control adult.

Area ratios (Table 2.7) A1/A2, A1/A3, A1/A4, A1/A5 and A2/A4 exhibited significant differences among the 3 age groups. This was observed as higher means for control and *mdx* adolescent DIAs compared to their young and adult counterparts (A1/A2, A1/A3 and A1/A4), higher means for *mdx* young compared to adolescent or adult (A1/A5) and higher means for *mdx* adult compared to young or adolescent (A2/A4). Significant strain differences were observed for A1/A3, A1/A4, A1/A5 and A2/A4: A1/A3 and A1/A4 were lower in *mdx* adolescent compared to control adolescent, A1/A5 was higher in *mdx* young compared to control young, and area A2/A4 was lower in *mdx* young compared to control young.

Once again, peak height and height ratios (Tables 2.5 & 2.9) showed changes similar in character to those changes in area and area ratios, with the addition of significant

strain effects at HT6 and ratio HT3/HT4. Also, ratios involving HT6 showed significant differences among the 3 ages (HT3/HT6 and HT4/HT6) and 2 strains (HT5/HT6).

4.3.3. TA vs. DIA TA and DIA spectra were clearly different upon visual inspection (Fig 2.1a vs. 2.1b) and by statistical analysis (for example, see Fig 2.4). All peak heights and areas examined by repeated measures 3-way ANOVA (matching TA and DIA spectra from the same mouse) differed significantly between TA and DIA spectra. A1, A2, A3 and A4 were lower in DIA and peak A5 was higher in DIA compared to TA. The ratio means of A1/A2, A1/A3, A1/A4 and A3/A4 were higher in DIA compared to TA, while A1/A5, A2/A3, A2/A4, A2/A5, A3/A5 and A4/A5 were lower in DIA compared to TA.

4.3.4. Summary In summary, the significant peak areas and heights were lower in *mdx* young compared to control young (A1-A4 and HT2 for TA; A5 and HT4 for DIA) and higher in *mdx* adult compared to control adult (HT2, HT3, HT5 and HT6 for TA; A4, A5 and HT3 for DIA). No differences were seen between *mdx* adolescent and control adolescent for the TA, but *mdx* adolescent was lower than control adolescent for the DIA for A1. Significant ratios exhibited the same trends. In addition, the significant peak areas and heights of TA (A2-A4, HT2, HT3 and HT5) and DIA (A2-A4, HT3 and HT4) generally were greater with age in *mdx* spectra, although there was no consistent age-wise trend in the ratio data. Therefore, it appears that the levels of the creatine (peaks 1 & 4) and taurine (peaks 2 & 3) are consistent markers for the continuous and successful repair process in dystrophic *mdx* muscle.

4.4. Linear discriminant analysis

LDA results were best for classifications between 2 and 3 groups of data. Significant results were not obtained for 4 or 6 groups (the groups are described in section 3.4). The 2-group LDA classifications between control and *mdx* mice demonstrated 84.2% accuracy after 7 iterations on the original data matrix. A ratio matrix consisting of the best 12 data points from the original data matrix gave 100% accuracy after 6 iterations. The genetic algorithm program resulted in 89.5% accuracy with 10 regions and 128 iterations. Ratios could not be generated on the data domains that the genetic algorithm program produced. The 3-group classifications between *mdx* young, adolescent and adult mice gave 90% accuracy for 5 iterations on a ratio matrix derived from the best 7 data points from the original data matrix. All of the above test set LDAs significantly discriminated among groups examined ($p<0.005$; Chi-squared statistics).

4.5. Histology and morphometry

The TA and DIA showed two distinct histological phenotypes, as previously reported. Considerable shrinkage of myofibers occurred during NMR (more so at 37°C than 25°C), so reliable measurements of myotube or fiber diameter (that would track growth) were not possible. However, fiber length and centronucleation index measurements were possible for TA specimens as they were determined in a ratio within a tissue sample and in perspective to fiber diameter. Adipose tissue or lipid droplets and deposits were not visible between, around, or within myofibers upon staining with PAS in TA. DIA sections were not sufficiently longitudinal in orientation to allow reliable cnl measurements, due to the

architecture of that muscle, smaller fibers, and the greater severity of pathological changes in the *mdx* DIA than in TA. All DIA samples examined post-NMR were found to have very small pieces of liver attached to the abdominal side of the muscle in section.

CNI-L was significantly different with age ($p<0.01$) and was greater in *mdx* than control TA ($p<0.01$), as expected. There was also a significant age by strain interaction ($p<0.01$) as CNI-L increased much more with age in *mdx* than control TA, as anticipated.

4.6. Correlation analysis

Correlations between TA CNI-L and peak heights, peak areas, and height and area ratios gave correlation coefficients ranging from $0<R^2<0.71$ on the *mdx* data. Of 74 correlations, 18 gave R^2 values of 0.50 or greater (accounting for ≥ 50% of the variance in the samples) and were significantly different from 0 (see Table 4.6.1 for a list of the significant coefficients). Ratios A1/A3 (Fig 2.5) and A1/A2 were particularly well correlated with CNI-L.

Table 4.6.1

PEAK AREA	R^2 VALUE	PEAK HEIGHT	R^2 VALUE
A1	0.50	HT2	0.52
A2	0.51	HT3	0.64
A3	0.61	HT4	0.59
A4	0.61	HT1/HT2	0.62
A1/A2	0.67	HT1/HT3	0.62
A1/A3	0.72	HT2/HT3	0.50
A1/A4	0.51	HT2/HT4	0.62
A2/A4	0.60	HT3/HT4	0.50
A3/A4	0.56	HT3/HT5	0.50

5. DISCUSSION

This study presents a possible new application of 1-H NMR as a technique in monitoring the progress of muscular dystrophy in *mdx* mice which contrasts with normal growth in control muscle. Control and *mdx* muscle spectra are clearly different from one another. Although the pre-dystrophic phase (*mdx* young) is not resolvable by conventional histopathology (Anderson et al., 1987; 1988), 1-H NMR clearly distinguishes pre-dystrophic from age-matched controls, as well as from active (*mdx* adolescent) and stable (*mdx* adult) dystrophic phases. In addition, LDA studies and the correlation of CNI-L (extent of repair) with spectral features contribute valuable new information on the objective discriminating power of 1-H NMR to classify muscle status. Using the information gained from this investigation, studies monitoring muscle regeneration and possible treatment effects on disease and repair will follow.

5.1. The processing method and data analysis

Baseline correction by 2 observers and on 2 occasions gave inconsistent results. Therefore, our results show that baseline correction is a manipulation of the spectra which is not reproducible. It appears that performing a series of linear corrections is very subjective, and the problem is magnified due to the broad overlapping peaks that are present in *ex vivo* 1-H NMR spectra. Even though the points at which the spectrum would be flattened was decided upon prior to the procedure, it was very difficult to duplicate previous measurements. In contrast, phasing the spectra after fourier transformation resulted in consistent and reproducible results. Phasing makes peaks symmetrical about

the baseline in one operation. This method was therefore chosen to analyze this data and all other data in this thesis.

Significant and consistent changes in many peaks were found using two methods to quantify and compare the heights and areas of the spectra (suggested by Kuesel et al., 1992). First, individual peak heights and areas were standardized on the basis of the mass of the tissue and a reference compound (PABA). Second, the ratios of peak heights and areas were determined. Although the latter method has the advantage of eliminating weighing errors and the need for a reference solution, it cannot determine the origin of a change in the peak ratio (i.e. the same effect could be observed by a decrease in one signal or an increase in another). Therefore, ratios may obscure important information. However, since it is difficult to provide external references during *in vivo* spectroscopy, ratios are often the only means of quantification in those experiments. Thus, the finding that ratio comparisons were statistically different (in addition to comparisons of absolute peak measurements) suggests that *in vivo* NMR spectroscopy may also detect tissue changes in muscle during aging and dystrophy.

5.2. Peak height and area measurements

The particular peaks examined in this study were chosen due to their consistent appearance across the groups and due to significant findings in previous *ex vivo* studies (Kuesel et al., 1992; Brière et al., 1995). There was no observable peak unique to *mdx* dystrophy or different age groups, but rather increases and decreases in certain peaks.

5.2.1. Age and strain effects There were many significant age effects (Table 2.1)

in peak areas and heights. It appears that in some of these cases, the growing/aging process in *mdx* muscle is being monitored in the background of dystrophy (i.e. where both control and *mdx* show age effects, but no strain effects are observed by Duncan's tests). However, in cases where strain and aging effects do occur, or when aging effects occur only in *mdx* muscle, it is assumed that progressive dystrophy is being monitored without interfering signals from the normal aging process. It is important that these two separate phenomena (aging vs. dystrophy) be considered as distinct features when we are attempting to monitor the dystrophic process in *mdx* animals, and eventually DMD patients. Therefore, it is suggested that the peaks indicated by asterisks in Table 2.1 are good candidates for monitoring *mdx* dystrophy.

Peaks 2 and 3, due mostly to the resonances of the free intracellular amino acid taurine (Chesney, 1985; Wright et al., 1986; Huxtable, 1992), consistently exhibited age effects in *mdx* muscle and strain effects. These could easily be followed to monitor the progression of dystrophy. Taurine peak levels were significantly less in young *mdx* vs. control, increased with age in *mdx* TA and DIA, and ultimately reached a level greater in *mdx* adult compared to control adult muscle. In *mdx* dystrophy, degeneration begins at a massive rate at the end of the young period, continues throughout the adolescent period with resulting successful regeneration, and finally slows and stabilizes in the adult period (Dangain & Vrbova, 1984; Zacharias & Anderson, 1991). This sequence parallels the changes in taurine levels. The gradual increase in taurine could cause stabilization of dystrophy or could be secondary to other factors that cause stabilization. Since *mdx* muscle

has a greater capacity for repair than control (McIntosh et al., 1994; Louboutin et al., 1995; Pernitsky et al., 1996), the greater amount of taurine in adult *mdx* vs. adult control muscle could be a marker of successful accumulated muscle regeneration. Taurine is not the primary cause of dystrophic muscle lesions, as suggested by Baskin & Dagirmanjian (1973), since a genetic defect in dystrophy causes dystrophin deficiency (Hoffman et al., 1987).

In addition, taurine concentration has been shown to positively correlate with the percentage of slow type 1 fibers (Airaksinen et al., 1990), and type 1 fiber proportions increase with age. In dystrophy, slower type 1 (Dhoot & Pearce, 1984; Carnwath & Shotton, 1987) or IIA (Anderson et al., 1988) fibers increase in proportions, due to the loss of fast (IIB) fibers which are more susceptible to dystrophy in humans (Webster et al., 1988). Because there is a higher potential for regeneration in type 1 fibers, the greater taurine content in *mdx* muscle with age and in *mdx* adult compared to control adult could play a protective role in *mdx* dystrophy, giving older *mdx* muscles stability and generally normal function. This supports the suggestion that taurine is a membrane stabilizer (Wright et al., 1986; DeLuca et al., 1990). As well, the lower taurine peak intensity in DIA compared to TA, could partially contribute to its severe phenotype and reflect the less adequate cumulative repair that occurs in DIA. Taurine administration to patients with myotonic dystrophy can markedly reduce the electrical signs of myotonia (Durelli et al., 1983), thus taurine may also be feasible as a therapeutic protectant in DMD.

5.2.2. Muscle effects The wide lipid resonances between 2.5 and 0 ppm were consistent qualitative and quantitative markers that distinguished TA from DIA, and confirm

an early report which found that lipid signal intensity was greatest in the normal diaphragm compared to limb muscles (Yoshizaki et al., 1981). The origin of the lipid signal is unknown. A small part may be derived from adipose tissue, since the signal is larger in the DIA where fibrosis and small accumulations of adipose tissue are observed. However, there are no lipid deposits intracellularly in fibers or adipose tissue deposits interstitially in the *mdx* TA (judged by PAS staining and routine light microscopy), which still exhibits the lipid signal. Therefore the increased lipid content could be due to: 1) membrane destruction (Yoshizaki et al., 1981) when myofibers degenerate in *mdx* dystrophy, 2) membrane lipid changes that increase mobility, 3) an extra linolenic-like fatty acid peak in regenerating *mdx* myofibers (Gillet et al., 1993) (that cross-peak was not observed by 2-dimensional COSY experiments of our *in vitro* DIA or TA samples; data not shown), 4) mobile neutral lipid domains intercalated within the bilayer lipid (May et al., 1986; Mountford & Wright, 1988), 5) intracellular lipid droplets observed by electron microscopy (Callies et al., 1993), or 6) fiber type proportion in each muscle (fast<intermediate<slow; Yoshizaki et al., 1981).

5.3. LDA

LDA proved very useful for accurately classifying or separating spectra into both 2 (*mdx* vs. control) and 3 (*mdx* young, adolescent and old) groups. Given the positive preliminary results, more data will be acquired to test the validity of this method to discriminate a higher number of groups. The possibility of detecting significant treatment effects on muscle 1-H NMR spectra through classifications and pattern recognition algorithms lends exciting potential to this technology.

5.4. Histology and morphometry

The use of CNI-L as an index of longitudinal repair accumulated during dystrophy proved to be very useful in detecting significant differences between groups of dystrophic and normal mice and among the 3 stages of *mdx* dystrophy, since age, strain and age by strain interactions were all observed. Furthermore, the strong correlation of longitudinal CNI and certain 1-H NMR peak ratios suggests that the cumulative effect of increased numbers of myotubes and centrally-nucleated segments in a muscle may best be appreciated volumetrically in this longitudinal assessment of muscle nucleation, rather than by a cross-sectional index useful in general tissue assessment (for example Karpati et al., 1988; Anderson et al., 1996b).

5.5. Correlation analysis

There was a clear relationship between spectral properties of the proton resonances in affected muscle and cytological markers of the disease. The correlation of peak heights, areas and ratios with CNI-L was very effective in detecting differences in muscle status of the *mdx* TA. The linearity of A1/A3 regression is particularly useful for correlation with CNI-L. Peaks 1-4 (creatines, taurine and cholines) contributed to the correlation studies, while peaks 5 and 6 (lipids) proved to be of little predictive or discriminative value. The correlations also suggest certain peak ratios require further study as predictors of phenotype assignment during repair. In the future, measures of muscle precursor cell proliferation and fusion, such as the number of labelled mononuclear muscle precursors and nuclei in myotubes (by autoradiography), MyoD mRNA levels, and levels and types of myosin heavy

chain isoforms, may prove useful to correlate with NMR.

5.6. Conclusions

The results of this study support the hypothesis that 1-H NMR is a reliable tool in investigation of muscle repair status during muscular dystrophy, and that the key histological feature of muscle regeneration (formation of new muscle) is correlated to spectral peaks. The findings of certain differences in peak heights and areas (particularly taurine and lipid resonances) taken together with LDA findings suggest that the observed spectral changes are related to the extent of repair in the muscles tested. Therefore, the results focus not on the detection of muscular dystrophy, but on muscle repair which occurs differentially among the progressive stages of dystrophy (pre-dystrophy vs. active dystrophy vs. stable dystrophy), different strains (control vs. *mdx*) and different tissues (severe, DIA vs. mild, TA). Proton NMR distinguishes spectra in all the above case comparisons. It cannot be stated for certain whether the changes are specific to the disease of *mdx* dystrophy. Further data on other neuromuscular disease states (with and without repair) are required to test the specificity of our spectral markers for disease. We are optimistic that 1-H NMR will be valuable in following the effects of a current drug treatment trial on *mdx* mice, and of special importance to young DMD boys.

Acknowledgements: Karl Granberg performed the histological, correlation and LDA analyses. Kathleen Brière and Maureen Donnelly spent many hours teaching correct tissue preparation, NMR acquisition and analysis. Thanks also to Tina Hibbs (tissue sectioning) and Roy Simpson (photographic expertise).

6. CHAPTER 2 FIGURES AND TABLES

FIGURE 2.1: Representative 1-H NMR spectra of a) DIA and b) TA, in deuterated PBS, from a young *mdx* mouse. Peak heights 1-6 were determined using the peak picking routine supplied on *x-spec* software (version 2.0.7; Bruker). Peak areas were determined by defining the integral regions (A1: 4.4-3.5 ppm; A2: 3.5-3.3 ppm; A3: 3.3-3.1 ppm; A4: 3.1-2.8 ppm; A5: 1.8-0.8 ppm). Heights and areas were then normalized respectively to the height or area of the PABA peak and to the tissue mass. Height and areas ratios were later determined. See text (section 4.1.) for assignments. Abbreviations: Ans:anserine; Car:carnosine; Chos:cholines; Crs:creatines; Lac:lactate; Lip:lipid; Lys:lysine; Tau:taurine; HDO: deuterated water

FIGURE 2.2: An example of central nucleation in a damaged muscle fiber on an H&E section. A sample segment measurement (according to the method outlined in the text) for cnl is indicated (200X).

FIGURE 2.3: Representative spectra of a) young, b) adolescent, and c) adult *mdx* TA samples in PBS/D_2O. The spectra were plotted in the absolute intensity mode with the resonance at 1.3 ppm given a fixed height. Peaks are assigned as in Fig 1.

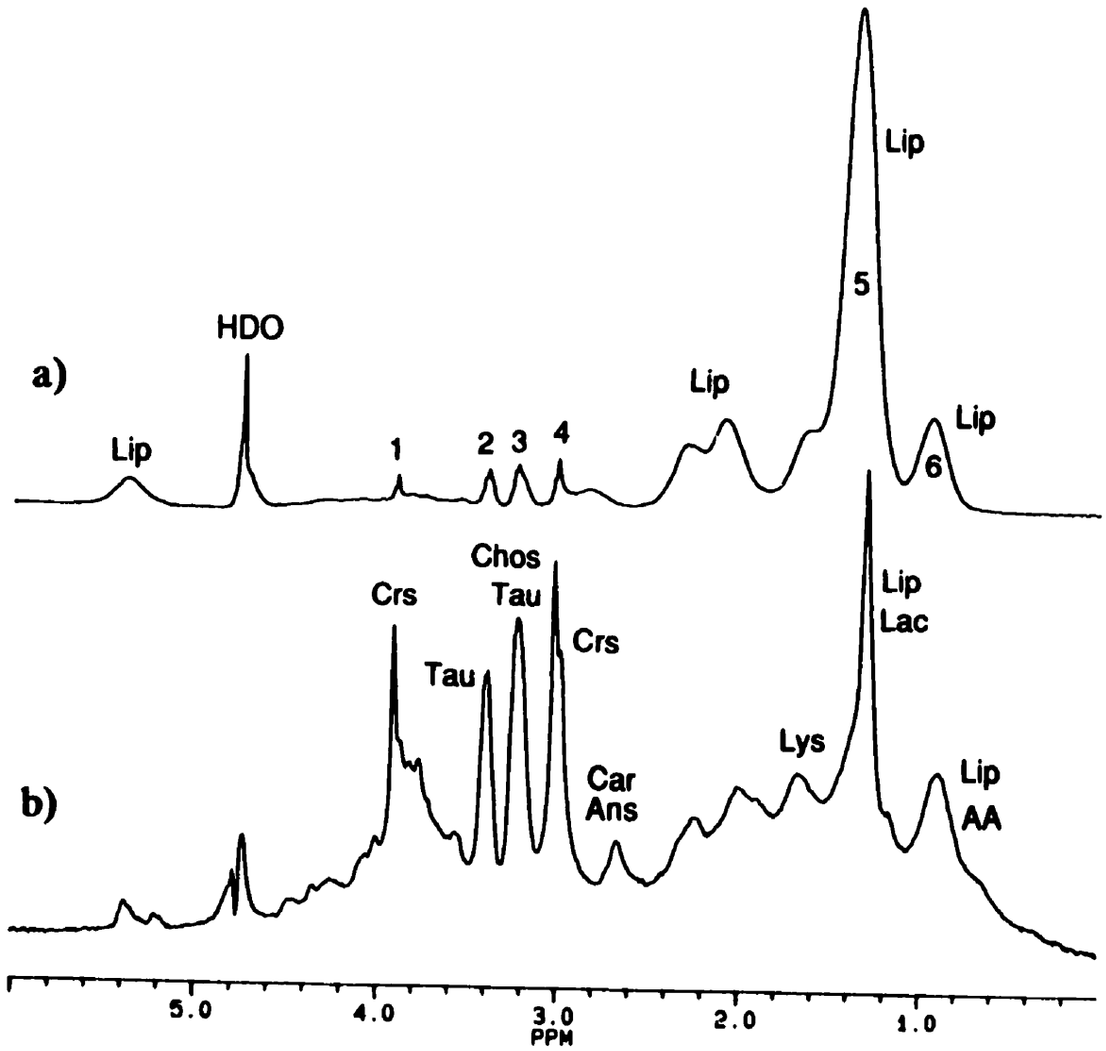
a)
HDO
Lip
1
2
3
4
Lip
5
Lip
6
Lip
b)
Crs
Tau
Chos
Tau
Crs
Car
Ans
Lys
Lip
Lac
Lip
AA
5.0
4.0
3.0
PPM
2.0
1.0

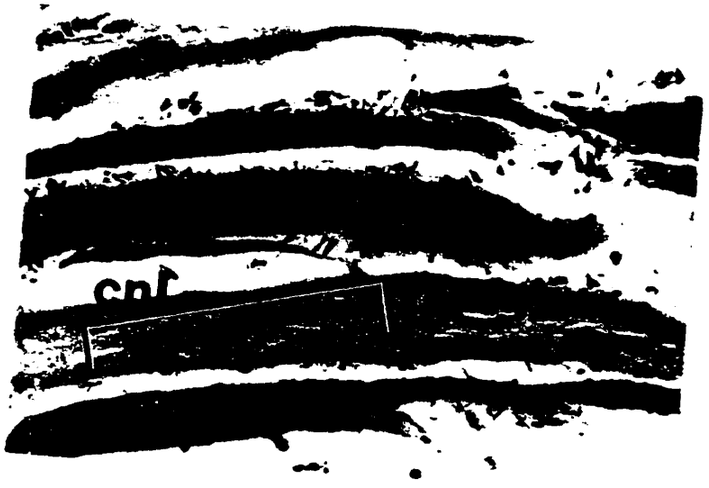

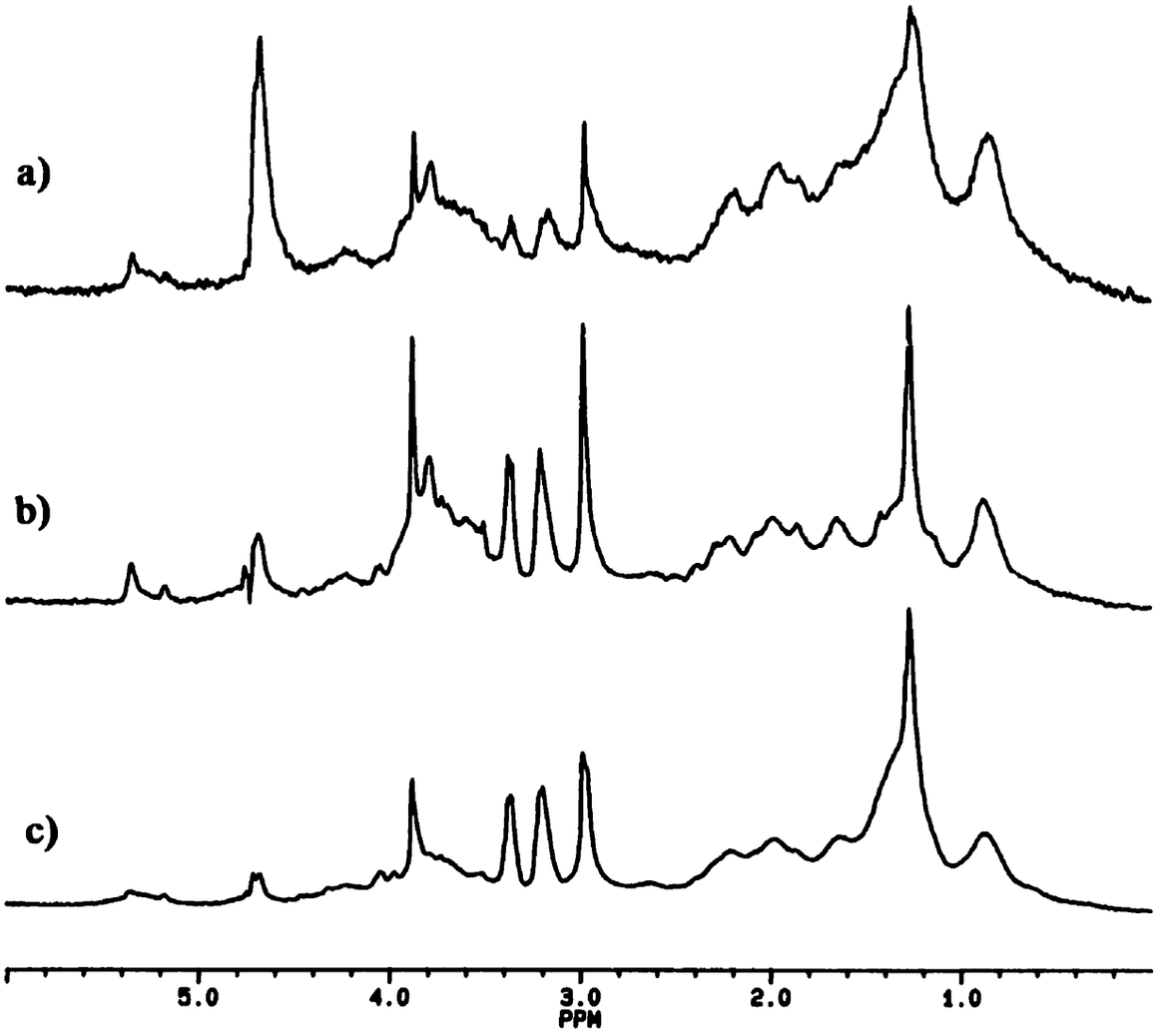
a)
b)
c)
5.0
4.0
3.0
2.0
1.0
PPM

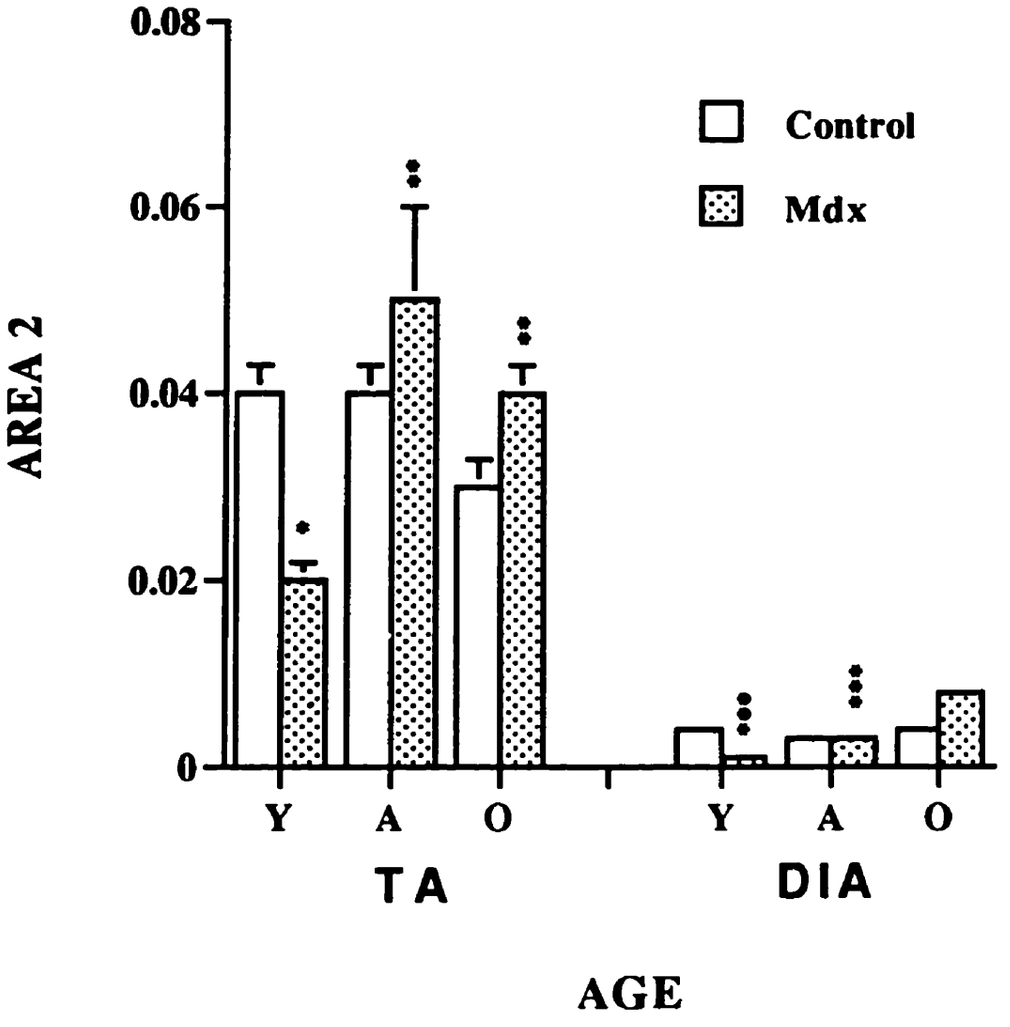
0.08
0.06
0.04
0.02
0
AREA 2
Control
Mdx
Y
A
O
Y
A
O
TA
DIA
AGE

AREA 1 / AREA 3

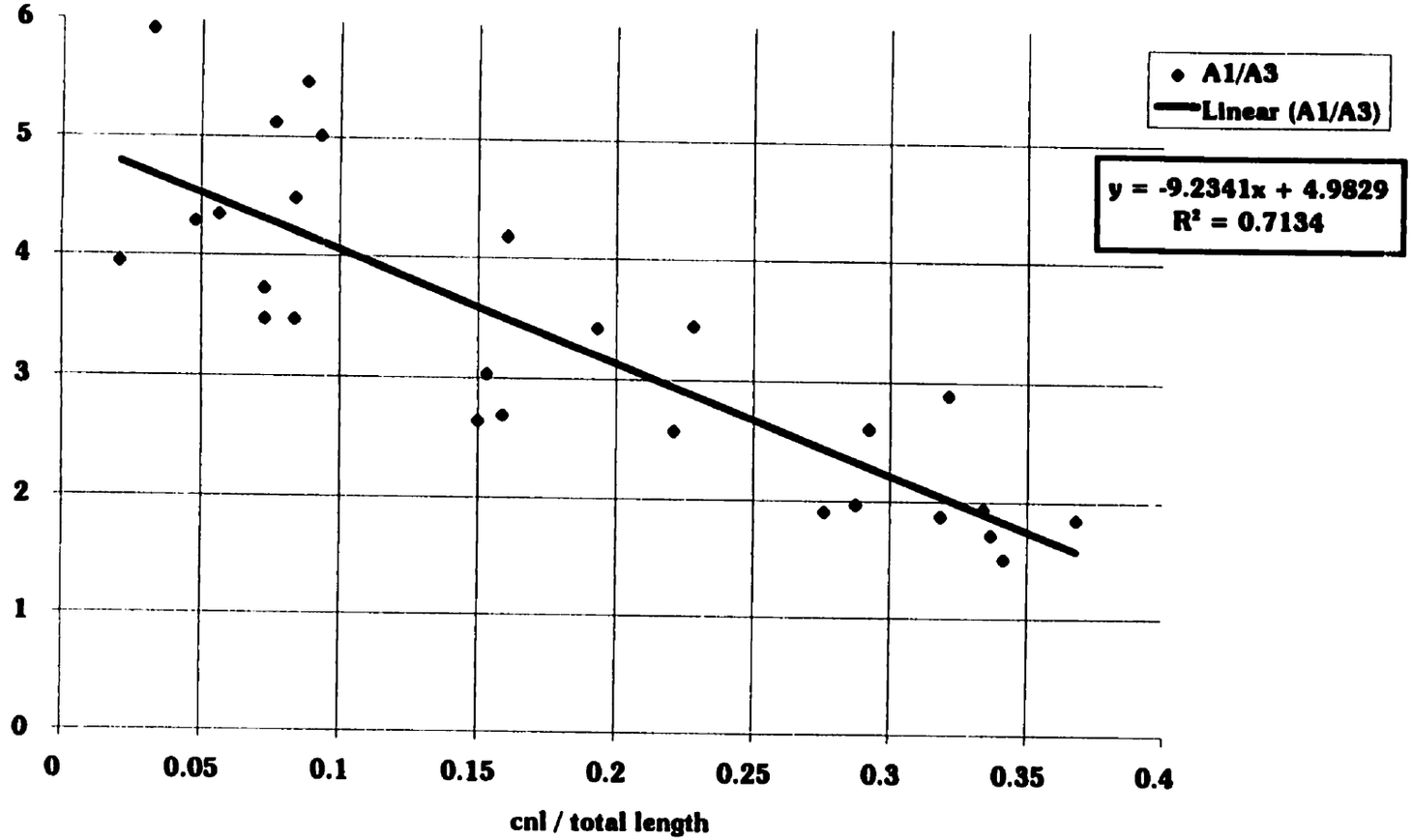
6
5
4
3
2
1
0
0
0.05
0.1
0.15
0.2
0.25
0.3
0.35
0.4
cnl / total length
A1/A3
Linear (A1/A3)
y = -9.2341x + 4.9829
R² = 0.7134

TABLE 2.1: Summary of significant probability values by 2-way ANOVA of peak area and ratio and peak height and ratio from TA and DIA spectra. *: suggested peaks for monitoring *mdx* dystrophy (see text section 5.2.)

TA:

AREA	age	strain	inter	HT	age	strain	inter
1			0.02	2 *			0.002
2 *			0.01	3 *			0.01
3 *	0.03		0.01	5 *	0.05		0.04
4 *			0.02	6		0.004	
1:2 *	0.03			1:2 *	0.001		0.01
1:3	0.0001			1:3	0.0001		
1:4	0.0001			1:5	0.0001		
1:5 *	0.0001		0.001	2:3	0.0001		0.03
2:3 *	0.0001	0.02	0.05	2:4 *	0.001		0.02
2:4 *	0.0001		0.005	2:5 *	0.05		0.01
2:5 *	0.001		0.0001	2:6 *			0.004
3:4 *	0.001			3:4	0.001		
3:5 *	0.002		0.0005	3:6 *			0.02
4:5 *			0.001	5:6 *	0.02		0.04

DIA:

1	0.0001		0.04	3 *	0.01		0.04
2 *	0.01		0.03	4 *	0.003		0.05
3 *	0.001		0.01	6		0.05	
4 *	0.002			1:2 *	0.002		0.02
5		0.01		1:3 *	0.02		
1:2	0.002			1:4 *	0.01		
1:3 *	0.0001		0.02	3:4		0.04	
1:4	0.01	0.05		3:6	0.02		
1:5 *		0.01		4:6	0.01		
2:4 *			0.02	5:6 *		0.03	

TABLE 2.2: Mean peak areas (± SEM) of TIBIALIS ANTERIOR muscle spectra.

Area	Control young	*Mdx* young	Control adolesc	*Mdx* adolesc	Control adult	*Mdx* adult
A1 c	0.28 ± 0.07	0.12 ± 0.005 *	0.17 ± 0.01	0.24 ± 0.05	0.13 ± 0.008	0.16 ± 0.008
A2 c	0.04 ± 0.003	0.02 ± 0.002 *	0.04 ± 0.003	0.05 ± 0.01 ¶	0.03 ± 0.003	0.04 ± 0.003 ¶
A3 a,c	0.05 ± 0.004	0.03 ± 0.001 *	0.05 ± 0.004	0.06 ± 0.01 ¶	0.05 ± 0.004	0.06 ± 0.004 ¶
A4 c	0.08 ± 0.005	0.05 ± 0.003 *	0.07 ± 0.005	0.09 ± 0.02 ¶	0.07 ± 0.005	0.08 ± 0.003 ¶
A5	0.04 ± 0.003	0.03 ± 0.002	0.03 ± 0.002	0.04 ± 0.01	0.04 ± 0.002	0.04 ± 0.002

TABLE 2.3: Mean peak areas (± SEM) of DIAPHRAGM muscle spectra.

Area	Control young	*Mdx* young	Control adolesc	*Mdx* adolesc	Control adult	*Mdx* adult
A1 a,c	0.05 ± 0.006	0.04 ± 0.005	0.12 ± 0.02 ¶,§	0.07 ± 0.01 *	0.03 ± 0.01	0.04 ± 0.004
A2 a,c	0.004 ± 0.001	0.001 ± 0.0008 §	0.003 ± 0.001	0.003 ± 0.001 §	0.004 ± 0.0008	0.008 ± 0.001
A3 a,c	0.012 ± 0.001	0.008 ± 0.001 §	0.01 ± 0.002	0.013 ± 0.002 §	0.013 ± 0.001	0.02 ± 0.001
A4 a	0.009 ± 0.002	0.007 ± 0.001 §	0.009 ± 0.001	0.012 ± 0.002 §	0.015 ± 0.004	0.017 ± 0.002 *
A5 b,c	2.05 ± 0.3	0.64 ± 0.3 *	2.7 ± 0.6	1.4 ± 0.3	1.4 ± 0.4	1.6 ± 0.3

a: age groups differ (ANOVA)
b: strain groups differ (ANOVA)
c: interaction (ANOVA)

*: sig differ from control of same age (Duncan's)
¶: sig differ from young animal of same strain
§: sig differ from adult animal of same strain

TABLE 2.4: Mean peak heights (± SEM) of TIBIALIS ANTERIOR muscle spectra.

HT	Control young	*Mdx* young	Control adolesc	*Mdx* adolesc	Control adult	*Mdx* adult
HT1	0.042 ± 0.006	0.033 ± 0.005	0.039 ± 0.007	0.035 ± 0.004	0.026 ± 0.003	0.039 ± 0.006
HT2 c	0.025 ± 0.003 §	0.015 ± 0.001 *,§	0.023 ± 0.002	0.022 ± 0.002	0.016 ± 0.002	0.027 ± 0.003 *
HT3 c	0.024 ● 0.003	0.016 ± 0.002 §	0.025 ± 0.004	0.022 ● 0.002	0.020 ± 0.003	0.031 ± 0.004 *
HT4	0.053 ± 0.008	0.044 ± 0.008	0.041 ± 0.006	0.040 ± 0.004	0.035 ± 0.005	0.056 ± 0.01
HT5 a,c	0.045 ± 0.006	0.044 ± 0.006 §	0.042 ± 0.005	0.041 ± 0.003 §	0.042 ± 0.004	0.067 ± 0.007 *
HT6 b	0.016 ● 0.001	0.018 ± 0.002	0.014 ● 0.0005	0.016 ± 0.0006	0.014 ± 0.0009	0.018 ± 0.001 *

TABLE 2.5: Mean peak heights (± SEM) of DIAPHRAGM muscle spectra.

HT	Control young	*Mdx* young	Control adolesc	*Mdx* adolesc	Control adult	*Mdx* adult
HT1	0.02 ± 0.004	0.011 ± 0.001	0.017 ± 0.002	0.018 ± 0.004	0.020 ± 0.005	0.022 ± 0.002
HT2	0.016 ± 0.004	0.008 ± 0.005	0.013 ± 0.003	0.015 ± 0.003	0.018 ± 0.004	0.026 ± 0.004
HT3 a,c	0.019 ± 0.004	0.011 ± 0.001 §	0.015 ± 0.003	0.015 ± 0.002 §	0.019 ± 0.003	0.028 ± 0.004 *
HT4 a,c	0.03 ± 0.005	0.014 ± 0.003 *,§	0.022 ± 0.004	0.020 ± 0.003 §	0.032 ± 0.004	0.038 ± 0.004
HT5	0.44 ± 0.07	0.17 ± 0.07	0.53 ± 0.13	0.39 ± 0.10	0.48 ± 0.12	0.44 ± 0.10
HT6 b	0.081 ± 0.011	0.043 ± 0.012	0.12 ± 0.03	0.077 ± 0.018	0.086 ± 0.019	0.076 ± 0.013

a: age groups differ (ANOVA)
b: strain groups differ (ANOVA)
c: interaction (ANOVA)
*: significantly different from control of same age (Duncan's)
§: significantly different from adult animal of same strain (Duncan's)

TABLE 2.6: Mean peak area ratios (± SEM) of TIBIALIS ANTERIOR muscle spectra.

	Control young	*Mdx* young	Control adolesc	*Mdx* adolesc	Control adult	*Mdx* adult
A1/A2	4.7 ±	5.0 ±	4.3 ±	4.5 ±	4.3 ±	4.0 ±
a	0.3	0.2 §	0.2	0.1	0.2	0.3
A1/A3	3.9 ±	4.2 ±	3.4 ±	3.8 ±	2.8 ±	2.9 ±
a	0.3 §	0.1 §	0.2 §	0.1 §	0.1	0.2
A1/A4	2.6 ±	2.6 ±	2.5 ±	2.7 ±	2.0 ±	2.1 ±
a	0.2 §	0.1 §	0.1 §	0.1 §	0.1	0.1
A1/A5	5.6 ±	4.4 ±	5.2 ±	5.6 ±	3.5 ±	4.4 ±
a,c	0.5 §	0.2 *	0.3 §	0.2 §,¶	0.2	0.1 *
A2/A3	0.85 ±	0.84 ±	0.81 ±	0.85 ±	0.64 ±	0.72 ±
a,b,c	0.02 §	0.01 §	0.02 §	0.02 §	0.02	0.02 *
A2/A4	0.57 ±	0.52 ±	0.58 ±	0.60 ±	0.46 ±	0.53 ±
a,c	0.01 §	0.01	0.01 §	0.01 §,¶	0.02	0.02 *
A2/A5	1.2 ±	0.88 ±	1.2 ±	1.3 ±	0.83 ±	1.1 ±
a,c	0.07 §	0.05 *	0.08 §	0.05 ¶	0.06	0.06 *,¶
A3/A4	0.67 ±	0.62 ±	0.72 ±	0.71 ±	0.71 ±	0.73 ±
a	0.01	0.01	0.01	0.02 ¶	0.02	0.03 ¶
A3/A5	1.4 ±	1.0 ±	1.5 ±	1.5 ±	1.3 ±	1.5 ±
a,c	0.09	0.06 *	0.09	0.08 ¶	0.07	0.06 *,¶
A4/A5	2.1 ±	1.7 ±	2.1 ±	2.1 ±	1.8 ±	2.1 ±
c	0.1 §	0.1 *	0.1 §	0.07 ¶	0.08	0.08 *,¶

a: age groups differ (ANOVA)
b: strain groups differ (ANOVA)
c: interaction (ANOVA)
*: significantly different from control of same age (Duncan's)
¶: significantly different from young animal of same strain (Duncan's)
§: significantly different from adult animal of same strain (Duncan's)

TABLE 2.7: Mean peak area ratios (± SEM) of DIAPHRAGM muscle spectra.

	Control young	*Mdx* young	Control adolesc	*Mdx* adolesc	Control adult	*Mdx* adult
A1/A2 a	34.6 ± 12.2	35.5 ± 5.2	48.3 ± 5.8 §	35.7 ± 9.7	7.8 ± 4.5	7.0 ± 1.7
A1/A3 a,c	4.8 ± 0.8	5.9 ± 0.8 §	10.1 ± 2.6 §,¶	5.4 ± 0.5 *,§	2.7 ± 1.0	2.3 ± 0.3
A1/A4 a,b	9.2 ± 3.1	6.7 ± 1.1	15.1 ± 4.2 §,¶	6.7 ± 1.1 *	3.9 ± 2.1	3.4 ± 0.9
A1/A5 b	0.03 ± 0.01	0.11 ± 0.03 *	0.05 ± 0.004	0.06 ± 0.01 ¶	0.04 ± 0.02	0.05 ± 0.01 ¶
A2/A3	0.28 ± 0.06	0.14 ± 0.04	0.29 ± 0.09	0.21 ± 0.06	0.32 ± 0.04	0.38 ± 0.03
A2/A4 c	0.55 ± 0.08	0.18 ± 0.07 *,§	0.40 ± 0.15	0.22 ± 0.05 §	0.37 ± 0.09	0.51 ± 0.07
A2/A5	0.004 ± 0.002	0.004 ± 0.001	0.001 ± 0.0004	0.003 ± 0.002	0.007 ± 0.004	0.01 ± 0.003
A3/A4	3.9 ± 2.1	1.2 ± 0.2	1.1 ± 0.2	1.2 ± 0.1	1.2 ± 0.3	1.4 ± 0.2
A3/A5	0.01 ± 0.003	0.02 ± 0.005	0.01 ± 0.002	0.01 ± 0.002	0.02 ± 0.008	0.02 ± 0.008
A4/A5	0.007 ± 0.003	0.02 ± 0.006	0.005 ± 0.002	0.01 ± 0.003	0.03 ± 0.01	0.02 ± 0.009

a: age groups differ (ANOVA)
b: strain groups differ (ANOVA)
c: interaction (ANOVA)
*: significantly different from control of same age (Duncan's)
¶: significantly different from young animal of same strain (Duncan's)
§: significantly different from adult animal of same strain (Duncan's)

TABLE 2.8: Mean peak ht ratios (± SEM) of TIBIALIS ANTERIOR muscle spectra.

	Con yng	*Mdx* yng	Con adol	*Mdx* adol	Con adt	*Mdx* adt
Ht1/Ht2 a,c	1.74 ± 0.05	2.32 ± 0.16 *	1.70 ± 0.22	1.61 ± 0.07 ¶	1.61 ± 0.08	1.42 ± 0.09 ¶
Ht1/Ht3 a	1.78 ± 0.06	2.03 ± 0.18	1.55 ± 0.08	1.61 ± 0.06 ¶,§	1.29 ± 0.05 ¶	1.25 ± 0.08 ¶
Ht1/Ht4	0.82 ± 0.04	0.81 ± 0.04	0.77 ± 0.03	0.87 ± 0.03	0.75 ± 0.04	0.73 ± 0.04
Ht1/Ht5 a	0.95 ± 0.06 §	0.79 ± 0.12	0.88 ± 0.06 §	0.84 ± 0.03 §	0.60 ± 0.05	0.59 ± 0.06
Ht1/Ht6	2.55 ± 0.24	1.92 ± 0.29	2.72 ± 0.45	2.17 ± 0.19	1.74 ± 0.17	2.14 ± 0.29
Ht2/Ht3 a,c	1.02 ± 0.02 §	0.92 ± 0.03	0.97 ± 0.05 §	1.00 ± 0.02 §	0.81 ± 0.02	0.88 ± 0.02
Ht2/Ht4 a,c	0.47 ± 0.01	0.37 ± 0.04 *	0.53 ± 0.01	0.55 ± 0.02 ¶	0.47 ± 0.03	0.53 ± 0.04 ¶
Ht2/Ht5 a,c	0.54 ± 0.03 §	0.36 ± 0.04 *	0.55 ± 0.04 §	0.52 ± 0.02 ¶	0.38 ± 0.04	0.43 ± 0.05
Ht2/Ht6 c	1.49 ± 0.15	0.88 ± 0.09 *	1.61 ± 0.15 §	1.36 ± 0.13 ¶	1.08 ± 0.13	1.51 ± 0.17 ¶
Ht3/Ht4 a	0.46 ± 0.01 §	0.45 ± 0.06 §	0.52 ± 0.02	0.55 ± 0.02	0.58 ± 0.02	0.60 ± 0.05
Ht3/Ht5	0.53 ± 0.03	0.38 ± 0.03	0.58 ± 0.04	0.53 ± 0.02	0.47 ± 0.05	0.49 ± 0.06
Ht3/Ht6 c	1.47 ± 0.15	0.92 ± 0.09 §	1.75 ± 0.23	1.36 ± 0.13	1.35 ± 0.16	1.73 ± 0.21
Ht4/Ht5	1.18 ± 0.10	0.90 ± 0.14	1.09 ± 0.09	0.97 ± 0.05	0.82 ± 0.09	0.85 ± 0.11
Ht4/Ht6	3.21 ± 0.35	2.38 ± 0.48	2.99 ± 0.39	2.48 ± 0.19	2.37 ± 0.28	3.05 ± 0.48
Ht5/Ht6 a,c	2.75 ± 0.24	2.42 ± 0.17 §	2.97 ± 0.28	2.57 ± 0.19 §	2.88 ± 0.19	3.61 ± 0.27

a: age groups differ (ANOVA)

c: interaction (ANOVA)

*: sig. different from control of same age

¶: sig. different from young animal of same strain

§: sig. different from adult animal of same strain

TABLE 2.9: Mean peak height ratios (± SEM) of DIAPHRAGM muscle spectra.

	Con yng	*Mdx* yng	Con adol	*Mdx* adol	Con adt	*Mdx* adt
Ht1/Ht2 **a,c**	1.22 ± 0.07	1.54 ± 0.19 *,§	1.48 ± 0.17 §	1.30 ± 0.09 §	1.15 ± 0.07	0.90 ± 0.07
Ht1/Ht3 **a**	1.03 ± 0.06	1.06 ± 0.08 §	1.07 ± 0.06	1.19 ± 0.09 §	1.00 ± 0.11	0.78 ± 0.05
Ht1/Ht4 **a**	0.65 ± 0.06	0.81 ± 0.05 §	0.71 ± 0.05	0.83 ± 0.06 §	0.58 ± 0.08	0.59 ± 0.05
Ht1/Ht5	0.061 ± 0.017	0.097 ± 0.021	0.030 ± 0.023	0.066 ± 0.017	0.13 ± 0.08	0.12 ± 0.05
Ht1/Ht6	0.29 ± 0.07	0.32 ± 0.05	0.15 ± 0.05	0.29 ± 0.06	0.50 ± 0.27	0.44 ± 0.11
Ht2/Ht3	0.86 ± 0.05	0.77 ± 0.10	0.76 ± 0.10	0.99 ± 0.09	0.88 ± 0.09	0.89 ± 0.05
Ht2/Ht4	0.56 ± 0.10	0.51 ± 0.06	0.51 ± 0.07	0.67 ± 0.06	0.51 ± 0.06	0.69 ± 0.08
Ht2/Ht5	0.058 ± 0.023	0.045 ± 0.024	0.027 ± 0.031	0.062 ± 0.020	0.11 ± 0.07	0.14 ± 0.05
Ht2/Ht6	0.26 ± 0.09	0.18 ± 0.09	0.12 ± 0.07	0.27 ± 0.07	0.42 ± 0.22	0.52 ± 0.13
Ht3/Ht4 **b**	0.64 ± 0.07	0.80 ± 0.07	0.70 ± 0.04	0.71 ± 0.05	0.59 ± 0.06	0.76 ± 0.06
Ht3/Ht5	0.059 ± 0.018	0.093 ± 0.018	0.036 ± 0.018	0.061 ± 0.016	0.11 ± 0.05	0.15 ± 0.05
Ht3/Ht6 **a**	0.28 ± 0.07	0.31 ± 0.05	0.16 ± 0.03	0.27 ± 0.06	0.43 ± 0.18	0.57 ± 0.13
Ht4/Ht5	0.085 ± 0.017	0.11 ± 0.02	0.051 ± 0.02	0.078 ± 0.017	0.15 ± 0.08	0.18 ± 0.05
Ht4/Ht6 **a**	0.42 ± 0.07	0.39 ± 0.06	0.23 ± 0.03 §	0.35 ± 0.06	0.65 ± 0.26	0.69 ± 0.12
Ht5/Ht6 **b**	5.28 ± 0.31	3.63 ± 0.36 *	5.39 ± 0.42	4.80 ± 0.21 ¶	5.16 ± 0.52	5.21 ± 0.44 ¶

a: age groups differ (ANOVA)
b: strain groups differ (ANOVA)
c: interaction (ANOVA)

*: sig. different from control of same age
¶: sig. different from young animal of same strain
§: sig. different from adult animal of same strain

CHAPTER 3

GLUCOCORTICOIDS CHANGE MAGNETIC RESONANCE SPECTRA OF DYSTROPHIC MUSCLE: AN *EX VIVO* STUDY

1. ABSTRACT

Glucocorticoids have been successfully used to alleviate the progression of Duchenne muscular dystrophy in clinical trials, but the mechanism of their action is unknown. We were interested in studying whether proton NMR could detect treatment effects that were previously determined to be due to increased proliferation and fusion of muscle precursors. It was hypothesized that: 1) glucocorticoids would produce significant changes in 1-H NMR spectra consistent with increased repair or decreased dystrophy, and 2) spectra from muscles with a short recovery after an injury would be different from those after a longer recovery period. Control and *mdx* mice were treated for 4 weeks with placebo, deflazacort, or prednisone, then received a crush-injury to one tibialis anterior (TA). Diaphragm (DIA) and crushed and uncrushed TAs were dissected 2 or 4 days later, and *ex vivo* 1-H NMR spectra were collected at 500MHz. Six peaks were analyzed in detail and compared between groups by ANOVA and t-tests. Linear discriminant trials of the entire spectral pattern were performed. Peaks due to taurine and creatine protons showed significant differences among steroid-treated and placebo *mdx* groups. This was especially evident in comparisons between deflazacort and placebo in the uncrushed TA. In addition, linear discriminant trials distinguished prednisone from deflazacort from placebo groups 95% accurately in the uncrushed TA. As well, certain peak ratios exhibited significant differences corresponding to the regenerative state of the muscle. Spectral characteristics of DIA and limb muscles were reliably different. The results suggest that 1-H NMR detects an improved muscle phenotype which results from treating dystrophic mice with deflazacort.

2. INTRODUCTION

Mdx dystrophy has been studied by *in vivo* NMR, with the finding of an added lipid resonance in two dimensional spectroscopy (Gillet et al., 1993). However, no NMR studies have been made of treatment effects on dystrophy, and until recently, the progression of *mdx* dystrophy had not been studied by 1-H NMR. In Chapter 2, it was shown that: 1) 1-H NMR separates control from *mdx* muscle spectra and distinguishes the three phases of *mdx* dystrophy, 2) dystrophic diaphragm and leg muscle spectra are consistently different from one another, and 3) muscle spectra are correlated significantly and highly to the phenotype of the muscle, in particular to the centronucleation index in muscles, an indicator of accumulated repair in skeletal muscle.

The above baseline studies allowed us to proceed to the next step of monitoring the disease of *mdx* dystrophy after treatment. The hypotheses of this study were: 1) 1-H NMR can detect drug treatment effects (deflazacort vs. prednisone vs. placebo; see Chapter 1, sections 1.3 and 2.4 for a review of glucocorticoids) in *mdx* mice based on the cellular changes occurring within the muscles during dystrophy, inflammation and regeneration, 2) 1-H NMR can distinguish regenerating from non-regenerating control and *mdx* muscle, and 3) the diaphragm (severe) and limb (mild) spectra are distinct from one another (as found previously). These studies are extremely important steps in the ultimate goal of monitoring drug treatments and muscle regeneration non-invasively *in vivo*.

3. MATERIALS AND METHODS

3.1. Animals

Control (C57Bl/10ScSn) and *mdx* mice were maintained and housed according to the Canadian Council of Animal Care at the University of Manitoba Animal Care Facility (Winnipeg, Manitoba). Treatment by subcutaneous injections of deflazacort (HD: 1.2mg/kg body weight or LD: 0.67mg/kg body weight; Marion Merrell Dow Inc., Laval, Québec), prednisone (PR: 1.0mg/kg body weight; Sigma Chemical Co., Mississauga, ON) or placebo (PL: Methocel; CIBA Vision, Mississauga, ON) began at three weeks of age for *mdx* animals and at 5 weeks for control animals, and continued daily for 4.5 weeks. After 4 weeks of treatment, the mice were subjected to a crush-injury of the right tibialis anterior (TA) muscle (McIntosh et al., 1994) under anaesthetic (1:1 ketamine - xylazine). Animals were killed by cervical dislocation under anaesthesia after 2 or 4 days of recovery. The following treatment-groups were studied:

1) *mdx* mice were injected with HD (n=6), LD (n=5), PR (n=5) or PL (n=6) and allowed to recover for 4 days after the crush injury. Treatment effects were analyzed (section 4.2.1). Detailed histology and morphometry of these tissues are reported elsewhere (Anderson et al., 1996b). In addition, gastrocnemius muscles from the same study were analyzed by infrared spectroscopy (Shaw et al., 1996).

2) *mdx* mice were injected with HD (n=5) or PL (n=5) and allowed to recover for 2 days after the crush-injury. Treatment effects were measured (section 4.2.1). In addition, statistics were combined with those of #1 in order to determine regeneration effects (section 4.2.2).

3) control mice were injected with HD (n=5) or PL (n=4) and allowed to recover for 4 days post muscle crush. Treatment (section 4.2.1) and regeneration effects (section 4.2.2) were measured.

3.2. Tissue samples

Half of each diaphragm (DIA), half of each uncrushed TA (LTA) and half of each crushed TA (RTA-4days recovery or RTA-2days recovery) were dissected out, placed individually in PBS/D_2O (pH 7.4) and snap frozen in liquid nitrogen. Samples were stored in a -70°C freezer until the time of spectroscopy. DIA samples from #1 and #2 (above, section 3.1) were pooled for statistics. The following table (Table 3.3.1) summarizes the numbers of muscles in each group.

Table 3.2.1

		High dose deflazacort (HD)	Low dose deflazacort (LD)	Prednisone (PR)	Placebo (PL)
Mdx	DIA	11	5	5	11
	LTA	6	5	5	6
	RTA - 4 days	6	5	5	6
	RTA - 2 days	5	0	0	5
Control	DIA	5	0	0	4
	LTA	5	0	0	4
	RTA - 4 days	5	0	0	4

NMR samples were thawed at room temperature for 15 min. A small longitudinal piece (approximately 3mm) of muscle tissue was dissected from the TA or DIA, excluding most tendon, as well as adipose and nerve tissues. For the DIAs, the muscle tissue was sampled so as to include parts of both the costal plus crural regions. Samples were then placed in a glass capillary tube filled with PBS/D_2O (Kuesel et al., 1992). The capillary tube was placed in a 5mm NMR tube filled with 5mmol/L paraminobenzoic acid (PABA; in PBS/D_2O; Aldrich) which served as a quantitative standard and chemical shift reference. Following acquisition of spectra, samples were blotted, weighed and fixed in 10% formalin for 7-10 days for subsequent histopathological examination. Hemotoxylin and eosin stained slides were examined to confirm that the tissue was characteristic of the particular muscle and that no fat accumulations or tendon were present. All mice and samples were handled in a double-blinded fashion, and the code was only broken after spectral processing and statistical analyses were completed.

3.3. 1-H NMR

1-H spectra were acquired at 25°C with presaturation of the water signal on a AMX500 Bruker Spectrospin spectrometer after 10 minutes of temperature equilibration. One dimensional 1-H spectra (640 acquisitions; 4K data points; acquisition time 0.340 sec; spectral width 6024.10Hz) were obtained for all samples. Ninety degree pulses were used which were typically 12.3μsec and the presaturation time was 2.0 sec.

3.4. Peak height and area measurements

The one-dimensional FIDs were zero-filled to 8K and Fourier transformed following

exponential multiplication (LB=1). Selected spectral peak areas and peak heights were obtained using *x-spec* software (version 2.0.7; Bruker) according to a carefully pre-established protocol (Chapter 2). Briefly, areas were measured by defining integral regions between 4.4 and 3.4 ppm (A1), 3.5 and 3.3 ppm (A2), 3.3 and 3.1 ppm (A3), 3.1 and 2.8 ppm (A4) and 1.8 and 0.8 ppm (A5). Heights were measured using the peak picking routine for resonances at 3.9, 3.4, 3.2, 3.0, 1.3 ppm and 0.9 ppm (HTs 1-6 respectively). Each area and height from each spectrum was then normalized to tissue mass and the PABA reference peak. Ratios of all combinations of areas and heights were also determined on each separate spectrum. Resonances were assigned according to our previous study (Chapter 2).

Data were decoded and the mean (± SEM) were determined for control and *mdx* mice of each muscle group (DIA, LTA, RTA-4d and RTA-2d) and each treatment group (HD, LD, PR, PL), and tested for significant effects of drug treatment (see section 4.2.1), regeneration (see section 4.2.2) and phenotype (see section 4.2.3) by 2-way ANOVA (NWA Statpak, Portland, OR). Specific t-tests were then performed on the peaks which were found significant by 2-way ANOVA in order to determine selected differences of particular interest (i.e. between PL and HD). A probability of $p<0.05$ was used to reject the null hypothesis.

3.5. Linear discriminant analysis (LDA)

LDA trials were performed on processed spectra collected from the first trial of the study to attempt treatment discrimination (HD, LD, PR, PL) in *mdx* LTA, RTA and DIA. Phased spectra were saved as ASCII files with 2K data points in *xspec* (version 2.0.7;

Bruker). These files were then imported into *gram*, a spectral processing software package, where they were smoothed, aligned, normalized to the PABA peak and baseline corrected. The region from 4.4 to 0 ppm was chosen for examination by LDA. Spectra were grouped into LTA, RTA and DIA data files and were labelled according to the treatment group they belonged. A genetic algorithm written by S. Nikulin (Nikulin et al., 1995) was then utilized in order to find regions that best discriminated among treatment groups. Four regions were searched for using 50 iterations.

4. RESULTS

4.1. 1-H NMR spectral characteristics

Spectral features of LTA (Fig 3.1) and RTA (Fig 3.2) samples were qualitatively similar. Identical peaks were evident in DIA spectra (Fig 3.3), although, in contrast to limb, they were lower in intensity at 3.9, 3.4, 3.2 and 3.0 ppm and larger at 1.3 and 0.9 ppm. Since spectra exhibited similar characteristics as reported in Chapter 2, the identical peak heights and areas were chosen for quantification of the metabolites of interest in this study.

Quantitative (see section 4.2, below) and qualitative inspection showed that differences in peak intensity existed between treatment groups. For the LTA (Fig 3.1) and RTA (Fig 3.2), the lipid peaks between 2 and 0 ppm appeared larger in the PL and PR groups compared to the HD group. Similarly, the lipid peaks in the DIA (Fig 3.3) were largest in the PL group.

4.2. Peak height and area measurements

All mean height, area, height ratios and area ratios are reported (Tables 3.6-3.21) and the results of statistical analyses are reported in Tables 3.1 and 3.2. Integral regions in the DIA spectra were very variable with large SEMs. For the control samples, most DIA spectra could not be integrated (poor resolution of very small samples). Therefore, the control DIA group was not included in any statistical analyses.

4.2.1. Effects of treatment (HD, LD, PR, PL; see TABLE 3.1 and Fig 3.4)

Control muscles: Four ratio measurements showed significant treatment x muscle interactions by ANOVA (Table 3.1). Specifically (t-tests), in the LTA, HT2/HT4 (Fig 3.4) was less in HD compared to PL. In the RTA-4d, A2/A3 was greater in HD vs. PL.

***Mdx* muscles:** Twelve measurements (heights, areas or ratios) exhibited a significant treatment effect or interaction by ANOVA for *mdx* muscles (Table 3.1). T-tests were performed on these 12 measurements. The following results were obtained:

1) LD spectra were not statistically different from PL spectra.

2) In DIA spectra, no statistical differences were found between the mean values for PR vs. PL and HD vs. PL.

3) In the LTA, means for HD spectra were significantly greater for HT2, HT3, HT2/HT4 (Fig 3.4), HT2/HT6, HT3/HT6 and A2/A3 and significantly less for A1/A2 compared to PL spectra. Also in the LTA, means for PR spectra were significantly more for HT2, HT2/HT4 (Fig 3.4) and A2/A3 compared to PL spectra. HD and PR spectra were statistically different from one another only for A2/A3 in the LTA.

4) In the RTA-2d, HD changed peak areas A2, A3 and A4/A5 compared to PL.

5) In the RTA-4d, there was only one instance where HD was different from PL; HT2/HT4 (Fig 3.4) was greater in HD vs. PL.

Thus, the peaks with contributions from taurine resonances (particularly A2, A3, HT2, HT3 and HT2/HT4) were most discriminating among treatment groups.

4.2.2. Effects of regeneration (LTA, RTA-2d, RTA-4d; TABLE 3.2 and Fig 3.5)

Control muscles: In placebo-treated control mice, 18 measurements exhibited significant regeneration effects or phenotype interactions by ANOVA (Table 3.2). Specifically (t-tests), HT2/HT6, HT3/HT6 and HT4/HT6 were greater in LTA compared to RTA-4d and HT5, HT6, A1/A2, A1/A3, A1/A4 and A3/A4 were less in LTA compared to RTA-4d.

***Mdx* muscles:** In placebo-treated *mdx* mice, 20 measurements exhibited significant regeneration effects or interactions by ANOVA (Table 3.2 and see Fig 3.5 for a representation of selected significant differences). The following results were obtained:

1) The LTA differed from the RTA-4d for A1, A2, A3, A5 and HT2/HT4 (less in LTA compared to RTA-4d).

2) The LTA differed from the RTA-2d in 9 instances. HT1/HT4, HT2/HT4, HT3/HT4, A1/A3, A1/A4 and A2/A4 were all less in LTA compared to RTA-2d, while HT1/HT5, HT4/HT5 and A4/A5 were greater in LTA vs. RTA-2d.

3) There were also cases where RTA-2d differed from RTA-4d. HT1/HT4, HT2/HT4, HT3/HT4, A1/A3 and A1/A4 were less in RTA-4d vs. RTA-2d.

Therefore, the similar changes in peaks (specifically, A2, A3, A2/A4, A4/A5, HT2/HT4) in

the phases of *mdx* dystrophy (Chapter 2) and different stages of *mdx* regeneration after an imposed injury (this study), suggest that 1-H NMR detects the process of muscle regeneration.

4.2.3. Effects of muscle type (LTA, DIA) Twenty-six (26) of a possible 36 height, area, height ratio and area ratio means were significantly different between DIA and TA by t-tests for *mdx* spectra. Specifically, the mean of HT4 was greater in LTA than DIA, and HT5 and HT6 were lower in LTA vs. DIA. All height ratios were significantly different between TA and DIA except HT1/HT4. Most height ratios were greater in LTA compared to DIA, except HT2/HT4, HT3/HT4 and HT5/HT6, which were lower in LTA compared to DIA. The mean of A3 was less in LTA vs. DIA spectra. All area ratios were significantly different between LTA and DIA except A1/A3 and A3/A5. A1/A5, A2/A3, A2/A5 and A4/A5 were greater in LTA compared to DIA, and A1/A2, A1/A4, A2/A4 and A3/A4 were lower in LTA compared to DIA spectra. Therefore, many differences between LTA and DIA were noted in *mdx* spectra.

4.3. LDA statistics

Output of LDA tests is in the form of classification tables (Tables 3.3-3.5). Values on the diagonal indicate the number of cases where classification agrees with the known identity of the tissue, while off-diagonal values denote misclassifications. The LDA classification for the LTA demonstrated 95% accuracy (Table 3.3). Only one misclassification resulted; a LD tissue was mistaken for a PR tissue. The four regions the genetic algorithm used for discrimination of LTA spectra were: 1) 4.4 ppm (+ 14 points), 2) 3.62 ppm (+1 point), 3) 3.47 ppm (+ 12 points), and 4) 0.23 ppm (+7 points). Classification for the RTA

demonstrated 54.2% accuracy (Table 3.4). In this case, the PL group was classified with 100% accuracy, while the HD, PR and LD groups were largely misclassified. The RTA classification procedure used: 1) 3.75 ppm (+14 points), 2) 1.99 ppm (+2 points), 3) 1.55 ppm (+2 points), and 0.95 ppm (+1 point). For the DIA, the LDA classification was 81.7% accurate (Table 3.5). LD, PR and PL groups demonstrated misclassifications, while the HD group was classified 100% correct. The genetic algorithm classified DIA spectra according to the areas: 1) 3.23 ppm (+1 point), 2) 3.05 ppm (+1 point), 3) 0.85 ppm (+22 points), and 4) -0.02 ppm (+1 point).

5. DISCUSSION

To our knowledge, this is the first study that has attempted to follow treatment effects of *ex vivo* dystrophic samples using 1-H NMR. We conclude that: 1) 1-H NMR detects differences between drug treatments reliably in the *mdx* LTA, but not in the *mdx* DIA or RTA, 2) the distinct stages of synchronous regeneration are detected in RTA muscles, and 3) proton spectra reliably distinguish the two different phenotypes of *mdx* dystrophy (DIA vs. limb). The results suggest that the observed spectral changes are related to muscle repair capacity, not degenerative changes. This study has identified possible spectral regions of interest for monitoring muscle status after glucocorticoid treatment by 1-H NMR *in vivo*.

5.1. Treatment effects

5.1.1. Control results There were very few instances of treatment effects in control

muscles by spectroscopy (see Table 3.1). Spectra of non-regenerating control muscle (LTA) exhibited a significant treatment effect only for HT2/HT4, and this effect was opposite to that seen in *mdx* (see Fig 3.4). These data are in agreement with examination of identical tissues which show no obvious treatment effects in control tissue (unpublished observations). Therefore, HD has no beneficial or useful effect in normal uninjured control muscle. In fact, previous reports state that glucocorticoids have a catabolic effect on normal rat muscle (Kelly et al., 1986; Dekhuijzen et al., 1993; Dekhuijzen et al., 1995) and this would account for the opposite trend we observed in control versus *mdx* data.

HD affects proliferation and fusion in *mdx* muscle (Anderson et al., 1996b). Early growth of normal muscle involves cell proliferation and fusion, and some treatment effects might be anticipated in very young control animals. In addition, an insult to control muscle (the crush injury) induces proliferation and fusion. Treatment effects were therefore expected in regenerating control muscle, based on the hypotheses that NMR monitors repair and that HD improves repair capacity. Treatment of controls only changed the ratio A2/A3 in regenerating muscle. Upon histological observation, it appears that HD has very little effect on regenerating control muscle after 4 days of recovery (unpub. observations). Therefore, it is possible that, although the processes of regeneration appear similar in control and *mdx* muscle by histology, the biochemistry (by high resolution NMR) is distinct in the two strains which results in slightly different regenerative processes. This may render regenerating control muscle less susceptible to the beneficial effects of glucocorticoids on muscle repair, and a higher (or different) dose may be required if muscle regeneration is to

be enhanced in previously normal muscle.

5.1.2. Diaphragm results Statistics on peak height and area measurements detected no differences among spectra of DIA samples in the 4 treatment groups in *mdx* DIA (unable to do statistics on small groups of control DIA). However, LDA classification was 81.7% accurate. The HD group was classified 100% correctly, while the other 3 groups were misclassified. It is interesting to note that the regions selected by LDA to classify groups included points at 3.23 ppm (taurine area), 3.05 ppm (creatine area) and 0.85 ppm (amino acid and lipid region). Therefore, LDA is more specific compared to morphometry, histology or peak height and area measurements, and points to a role for taurine in improving the phenotype of muscle. However, it is unknown if the favourable results by LDA equate improved diaphragm function.

LDA found LD, PR and PL treatments to be very similar, in agreement with morphometry (Anderson et al., 1996b). This may partly explain the lack of statistical findings by peak height and area measurements. In addition, the *mdx* DIA is inhomogeneous in comparison to the general cumulative repair in the TA. The extent of disease progression in the DIA at the start of the study is much larger than in TA (Stedman et al., 1991; Dupont-Versteegden & McCarter, 1992). Thus, a real treatment-induced change (i.e. new muscle fibers) over and above the pathological changes (i.e. degeneration and necrosis) that were well-advanced by the onset of treatment may be difficult to resolve by 1-H NMR of DIA.

5.1.3. LTA results Upon a cursory look at Table 3.1, it is obvious that the significant treatment effects for *mdx* muscles are generally seen as greater values with

glucocorticoid treatment (except for lipid peaks). Therefore, the spectra can be arranged HD > PR > PL and LD (for example see Fig 3.4). This grouping, backed by histological analysis of identical samples (Anderson et al., 1996b), suggests that HD has a greater effect on muscle repair than PR, and that 1-H NMR monitors this regenerative process. Therefore, due to the decreased side-effects and increased effects on muscle repair, deflazacort should be the drug of choice for DMD treatment, assuming treatment effects on humans are the same as in *mdx* mice.

LDA classified LTA samples from the four treatment groups 95% correctly. This fact, taken together with peak height and area measurements, give confidence to the conclusion that treatments can be monitored in this dystrophic tissue. Early treatment of DMD patients is crucial so that muscles do not approach advanced stages of the disease where monitoring would be more difficult and treatment effects less, as seen in these DIA-treated muscles.

5.1.4. RTA results Treatment effects occurred in the RTA-2d for A2, A3 and A4/A5 and in the RTA-4d for HT2/HT4. It could be that HT2/HT4 (Fig 3.4) is the most sensitive to small changes in repair capacity in the ongoing background of dystrophy. In contrast, A2 and A3, which are less with HD compared to PL, could monitor proliferation. The levels are probably decreased due to the biochemistry involved in increased proliferation in HD vs. PL at 2d after crush. Therefore, in interpreting NMR data, it is imperative to be aware of the tissue's stage of regeneration (by histology and morphometry). Classification for the RTA-4d demonstrated 54.2% accuracy. However, the PL group was classified 100% correctly, while

there was much overlap among the other 3 groups. Therefore, monitoring treatment is still a possibility, but changes in early regenerating muscle (see section 5.2) are not as clear as in the LTA and DIA.

5.2. Regeneration effects

The crush injury is a useful technique that allows study of induced synchronous repair, as compared to low-level asynchronous repair in uncrushed *mdx* muscles. The sequelae in *mdx* crushed muscle are well characterized (McIntosh et al., 1994; McIntosh & Anderson, 1995). It was expected that spectral differences between LTA and RTA would exist, since it was theorized that 1-H NMR detects changes in metabolites due to repair, and not due to dystrophic lesions. Any differences may relate to the relative concentrations of the compounds in healthy muscle (LTA) vs. undifferentiated or necrotic/inflamed muscle at 2 or 4 days post-injury.

In placebo-treated animals, on the basis of significant peaks (see Fig 3.5), the spectra can be arranged *mdx* RTA-2d and control RTA-4d > *mdx* RTA-4d > *mdx* LTA. Histologically, control RTA-4d is close to *mdx* RTA-2d in regenerative stage (McIntosh & Anderson, 1995; Pernitsky et al., 1996), although this has been debated (Pastoret & Sebille, 1995; Grounds & McGeachie, 1992). In *mdx* RTA-2d and control RTA-4d, very active phases of muscle precursor cell proliferation and fusion occur, and the levels of significant NMR-visible metabolites appear to be affected similarly (i.e. greater amounts). There were more differences between *mdx* RTA-2d and LTA than between *mdx* RTA-4d and LTA. This would suggest that the *mdx* RTA-4d spectra are not as active and are reaching a similar

level of regeneration as in the *mdx* LTA. As well, the crushed area is quite small in *mdx* TA after 4 days of recovery ($5.4 \pm 1.5 \times 10^{-4}$ μm; McIntosh et al., 1994) and the chance of obtaining a homogenous sampling from only crushed muscle is quite small. It may be that perchloric acid extractions of selected crushed and adjacent zones (see McIntosh et al., 1994 for definitions) will be able to give a more accurate picture of the spectral characteristics of regenerating muscle at given intervals post-injury.

When significant results from *mdx* RTA-2d and control RTA-4d spectra were compared, it was found that A1/A3 and A1/A4 were the only ratios with significant differences between regeneration groups in common. It is proposed that these 2 peak ratios are monitoring muscle precursor proliferation and early fusion events, not the degeneration/regeneration process of dystrophy.

5.3. Muscle effects

It was previously shown that the DIA was different from the TA in 3 different age groups in control and *mdx* mice. This study confirmed those results. The wide lipid resonances between 2.5 and 0 ppm were consistent qualitative and quantitative markers that distinguished LTA from DIA, as found previously. Since it is quite difficult to monitor the DIA *in vivo* due to continuous respiratory movements of the muscles in the thorax, the lipid resonances probably would not be useful in monitoring treatment even if they did discriminate treatment effects in the DIA. As well, many other peaks and ratios discriminate muscle phenotypes and could therefore be more useful to monitor treatment effects in the context of phenotype for muscles accessible to 1-H NMR.

5.4. Taurine

Closer examination of the taurine peaks (any peak height, area or ratio including peak 2 or 3) is both feasible and informative based on the above findings and on previous findings in aging normal and dystrophic muscles (Chapter 2). Increased intensity of taurine protons in HD are spectral features which distinguish PL from PR and HD treatments in the LTA. This may reflect increased membrane stability and accumulated repair with treatment in *mdx* (confirmed by morphometry; Anderson et al., 1996b), and are consistent with the changes in taurine levels during the progression of *mdx* dystrophy (Chapter 2). Therefore, taurine probably plays a role in skeletal muscle fiber membrane protection, as suggested by Wright et al. (1986). In HD-treated *mdx* after 2 days of regeneration, taurine levels were reduced, probably due to increased proliferation preceding fusion with treatment at this time.

In addition to membrane stability, greater taurine levels may also reflect increased fusion (Huxtable, 1992) of muscle precursors into myotubes. This agrees with findings of greater taurine levels in actively fusing *mdx* muscles after 4 days of recovery compared to stable *mdx* muscles (LTA). In conclusion, it is suggested that during muscle regeneration, taurine levels are depleted during myoblast (and other cell) proliferation, rise dramatically in amount with events of myoblast fusion into myotubes, and continue to remain high, conferring protection and stabilization to myofibers.

5.5. Conclusions

The results from this study strongly support that 1-H NMR can monitor treatment effects in muscular dystrophy which are a result of increased muscle repair. As well,

important data and strategies for analysis required in order to proceed toward *in vivo* NMR analysis of treatment effects on progression of human DMD were identified. We have identified a potential region from 3-4 ppm, which includes taurine proton resonances, which may be a valuable marker in such investigations. This region was found important for correlation with centronucleation index and as a possible marker for muscle regeneration (the ultimate goal of ideal treatment). Future assessments by *in vivo* 1-H NMR spectroscopy will require confirmation using smaller field-strength clinical instruments *in situ* in human limb.

Acknowledgements: Spectra were acquired at the Prairie Regional NMR Facility, University of Manitoba. Thanks to Terry Wolowiec for teaching proper acquisition procedures on the spectrometer and for all the time spent on consultations. Cinthya Vargas sectioned most tissue blocks post-NMR. Thanks to Dr. Tony Shaw who assisted in LDA analysis and figure preparation.

6. CHAPTER 3 FIGURES AND TABLES

FIGURE 3.1: *Mdx* average spectra from the uncrushed tibialis anterior (LTA). Spectra collected from the high dose deflazacort (HD) group are represented in blue (n=6), the low dose deflazacort (LD) group is in green (n=5), the prednisone-treated group (PR) is in red (n=5) and the placebo group (PL) is in yellow (n=6). SEMs are not included in these figures. Assignments are as shown in Chapter 2, Figure 2.1 (3.9 ppm - creatines; 3.4 ppm - taurine; 3.2 ppm - taurine, cholines; 3.0 ppm - creatines; 1.3 ppm -lipid and lactate; 0.9 ppm - amino acids and lipid). Assignments do not imply these are the only metabolites contributing to the peaks. LDA classified the groups 95% correctly and the regions selected were at 4.4 ppm, 3.62 ppm, 3.47 ppm and 0.23 ppm (see section 4.3 and Table 3.3).

FIGURE 3.2: *Mdx* average spectra from the crushed tibialis anterior (RTA). Spectra and peaks are assigned as above. The groups were classified 54.2% correctly by LDA and the regions selected were at 3.75 ppm, 1.97 ppm, 1.55 ppm and 0.95 ppm (see Table 3.4).

FIGURE 3.3: *Mdx* average spectra from the diaphragm (DIA). Spectra and peaks are assigned as above. LDA classified groups 81.7% correctly and the regions selected were at 3.23 ppm, 3.05 ppm, 0.85 ppm and -0.02 ppm (see Table 3.5).

FIGURE 3.4: Mean ± SEM of the ratio of HT2/HT4 showing PL, HD and PR-treated LTA, RTA and DIA spectra in control and *mdx* mice. • significantly different from PL.

FIGURE 3.5: Mean ± SEM of selected height and area ratios of PL-treated LTA, RTA-2d and RTA-4d control and *mdx* spectra. A1/A3 and A1/A4 values are $x10^2$. In all cases for *mdx* RTA-2d differed from RTA-4d. • significantly different from LTA.

High Dose Deflazacort
Prednisone
Low Dose Deflazacort

Uncrushed
TA Spectra

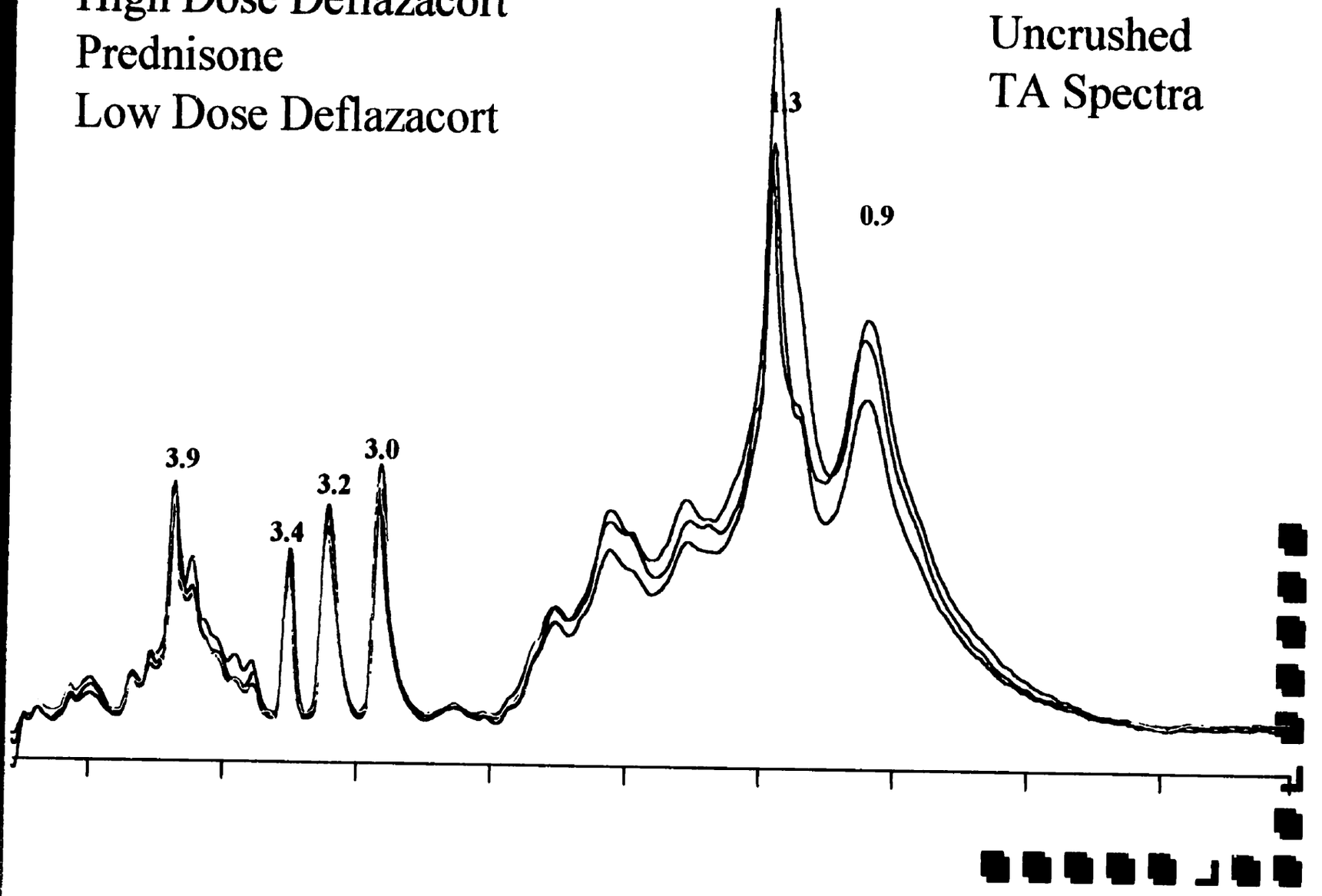

High Dose Deflazacort
Prednisone
Low Dose Deflazacort

Crushed
TA Spectra

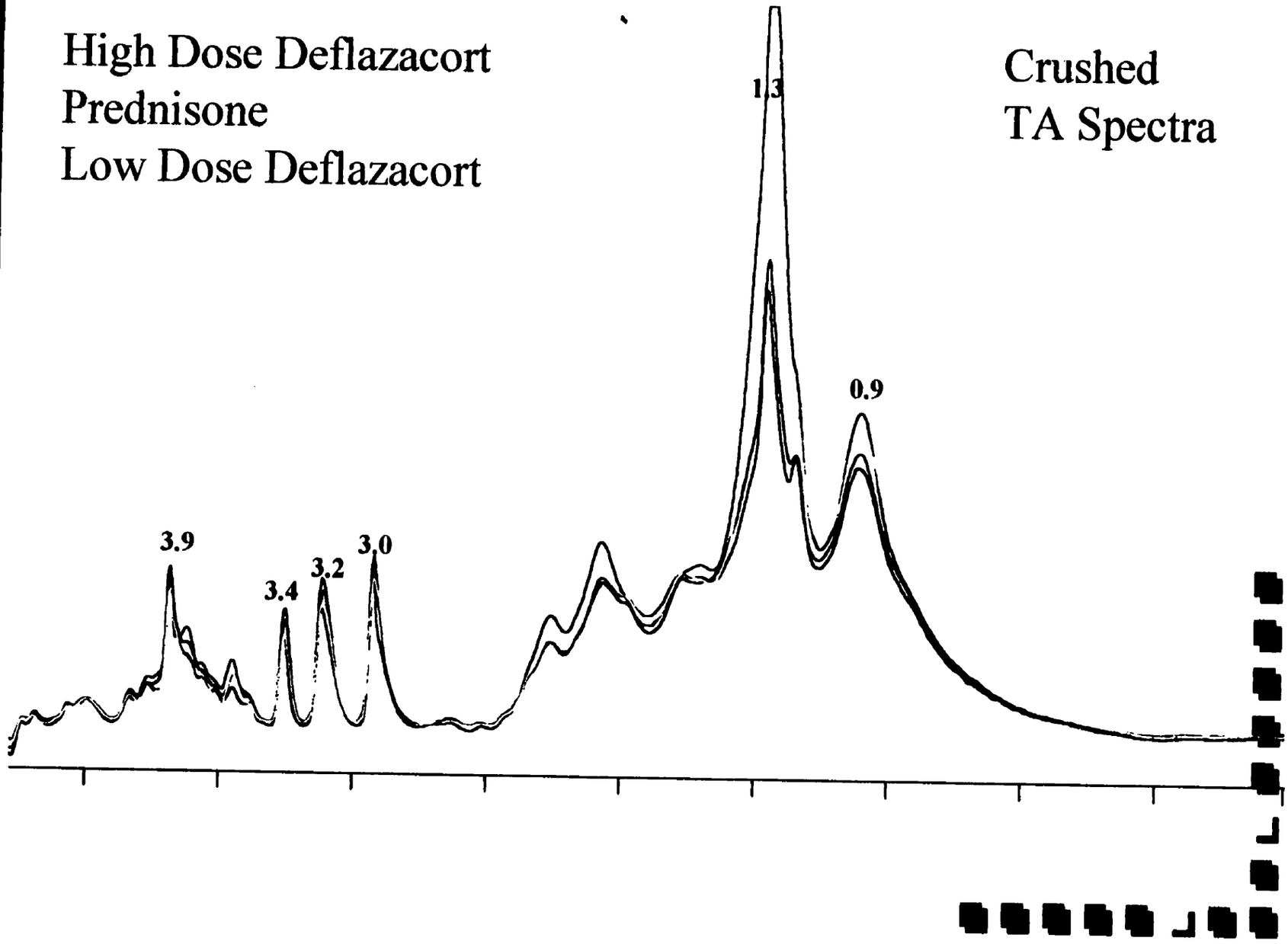

High Dose Deflazacort
Prednisone
Low Dose Deflazacort

Diaphragm
Spectra

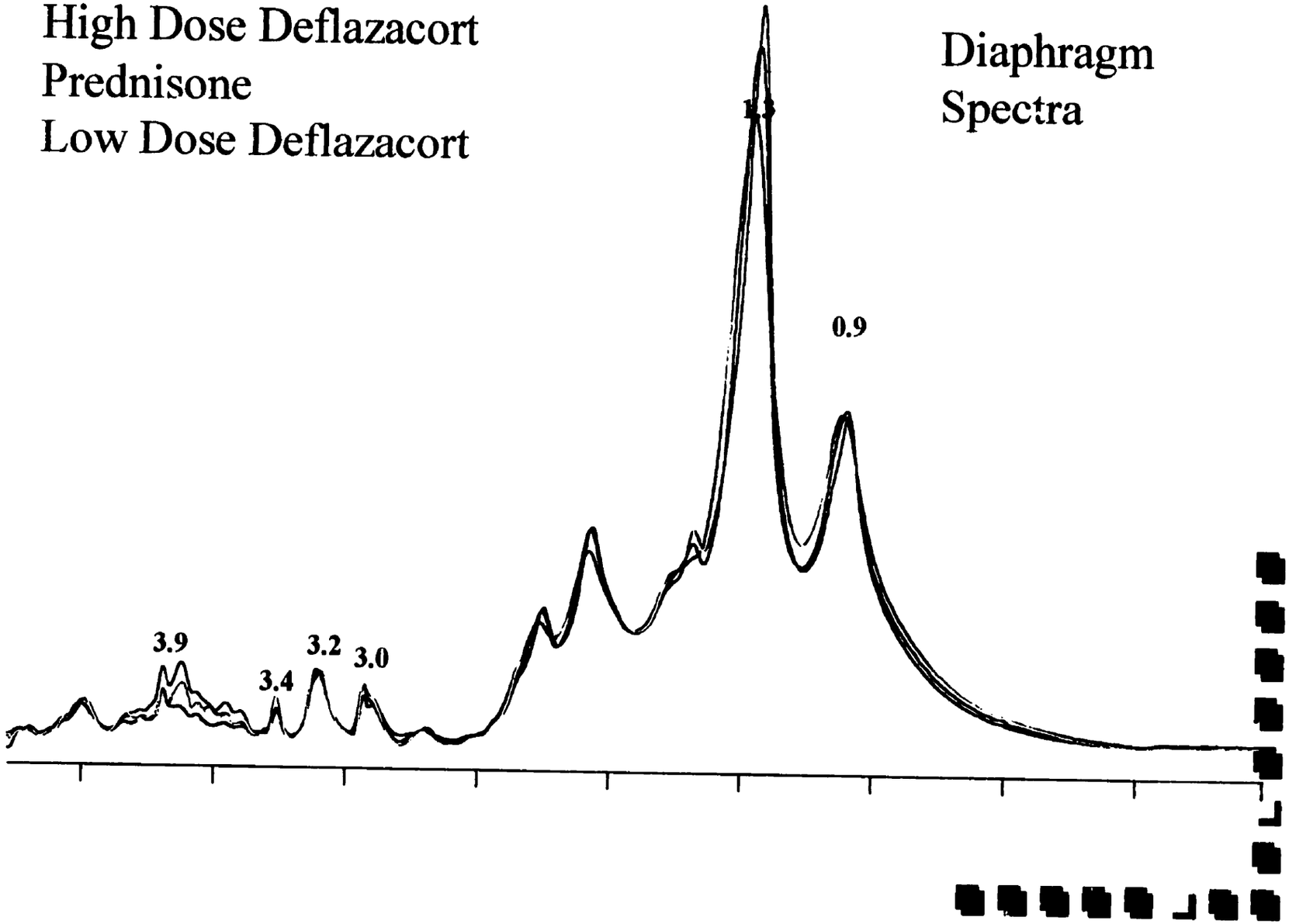

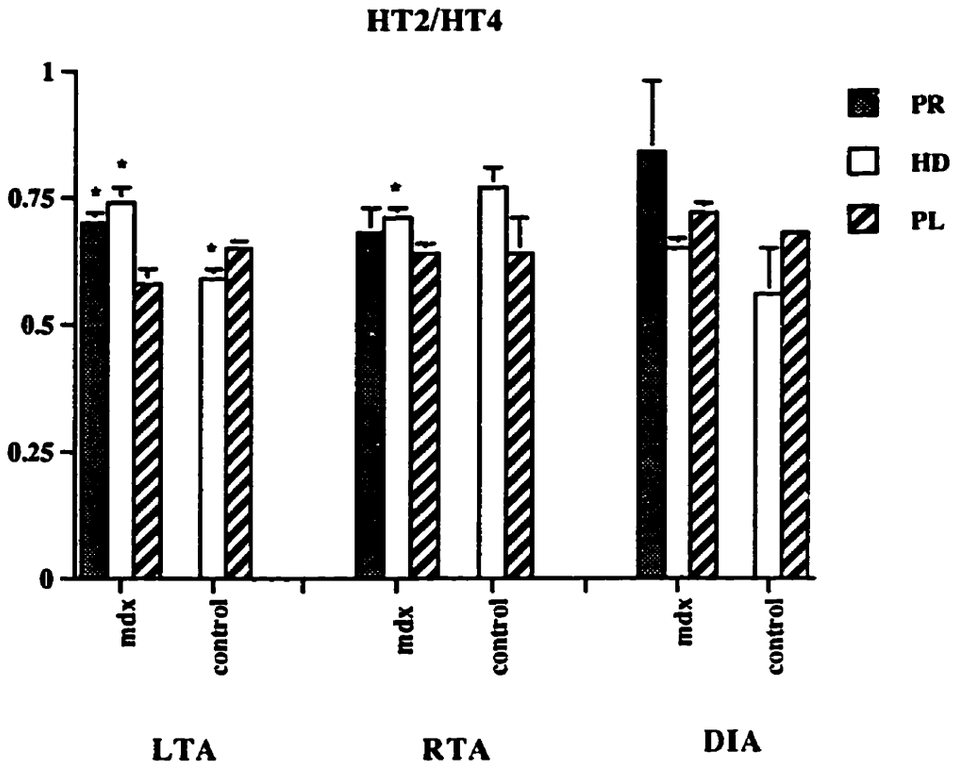
HT2/HT4
1
0.75
0.5
0.25
0
PR
HD
PL
mdx
control
mdx
control
mdx
control
LTA
RTA
DIA

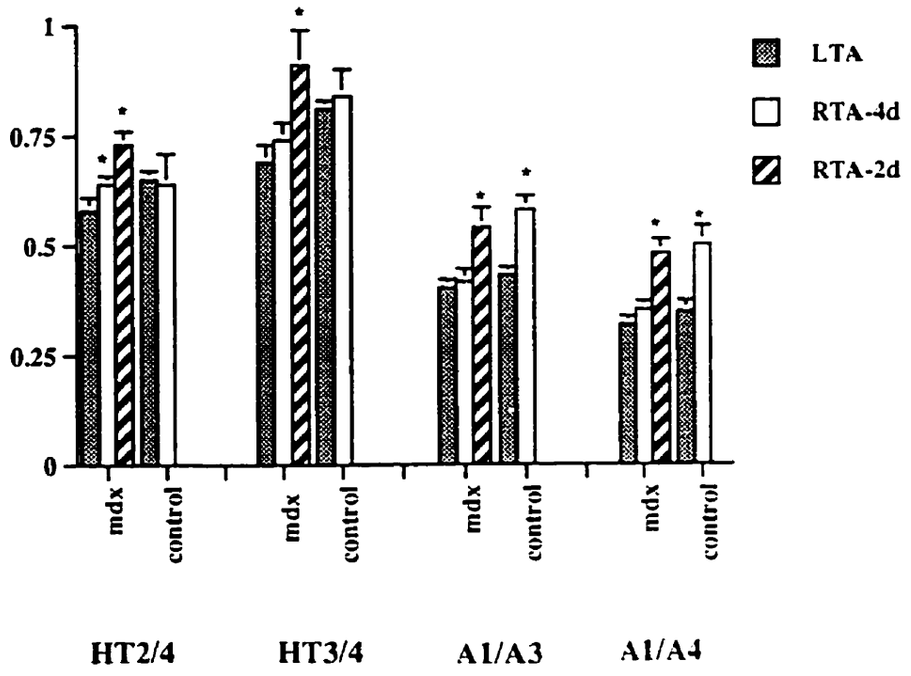
1
0.75
0.5
0.25
0
LTA
RTA-4d
RTA-2d
mdx
control
mdx
control
mdx
control
mdx
control
HT2/4
HT3/4
A1/A3
A1/A4

TABLE 3.1: Summary of treatment effects of peak heights, areas and ratios and the direction of the effect.

HTS	*Mdx* (HD, LD, PR, PL)	Control (HD, PL)	AREAS	*Mdx* (HD, LD, PR, PL)	Control (HD, PL)
Ht1	*	---	A1	---	---
Ht2	* a(↑) b(↑)	---	A2	* e(↓)	---
Ht3	* a(↑)	---	A3	* e(↓)	---
Ht4	---	---	A4	---	---
Ht5	---	---	A5	---	---
Ht6	---	---			
Ht1/2	---	---	A1/A2	* a(↓)	*
Ht1/3	*	---	A1/A3	---	---
Ht1/4	---	---	A1/A4	---	---
Ht1/5	---	---	A1/A5	---	---
Ht1/6	---	---			
Ht2/3	---	---	A2/A3	* a(↑) b(↑) c(↑)	* d(↑)
Ht2/4	* a(↑) b(↑) d(↑)	* a(↓)	A2/A4	---	*
Ht2/5	---	---	A2/A5	---	---
Ht2/6	* a(↑)	---			
Ht3/4	---	---	A3/A4	---	---
Ht3/5	---	---	A3/A5	---	---
Ht3/6	* a(↑)	---			
Ht4/5	---	---	A4/A5	* e(↓)	---
Ht4/6	---	---			
Ht5/6	---	---			

*: treatment effect or interaction (by 2-way ANOVA)
a: HD significantly differs from PL in the LTA t-tests)
b: PR significantly differs from PL in the LTA (t-tests)
c: HD significantly differs from PR in the LTA (t-tests)
d: HD significantly differs from PL in the RTA-4d (t-tests)
e: HD significantly differs from PL in the RTA-2d (t-tests)
↑/↓: increase or decrease in HD vs. PL(a), PR vs. PL(b), HD vs. PR(c) or HD vs. PL(d,e)

TABLE 3.2: Summary of regeneration effects of peak heights, areas and ratios and the direction of the effect.

HTS	*Mdx* (LTA, 2d, 4d)	Control (LTA, 4d)	AREAS	*Mdx* (LTA, 2d, 4d)	Control (LTA, 4d)
Ht1	---	---	A1	* a(↓)	---
Ht2	---	---	A2	* a(↓)	---
Ht3	---	---	A3	* a(↓)	---
Ht4	---	---	A4	---	---
Ht5	---	* a(↓)	A5	* a(↓)	---
Ht6	---	* a(↓)			
Ht1/2	---	---	A1/A2	*	* a(↓)
Ht1/3	---	---	A1/A3	* b(↓) c(↓)	* a(↓)
Ht1/4	* b(↓) c(↓)	*	A1/A4	* b (↓) c(↓)	* a(↓)
Ht1/5	* b(↑)	---	A1/A5	---	---
Ht1/6	*	*			
Ht2/3	---	---	A2/A3	---	*
Ht2/4	* a(↓) b(↓) c(↓)	*	A2/A4	* b(↓)	*
Ht2/5	---	*	A2/A5	*	---
Ht2/6	---	* a(↑)			
Ht3/4	* b(↓) c(↓)	*	A3/A4	---	* a(↓)
Ht3/5	*	---	A3/A5	*	---
Ht3/6	*	* a(↑)			
Ht4/5	* b(↑)	*	A4/A5	* b(↑)	*
Ht4/6	*	* a(↑)			
Ht5/6	---	---			

*: treatment effect or interaction (by 2-way ANOVA)
a: LTA significantly differs from RTA-4d (t-tests) - placebo
b: LTA significantly differs from RTA-2d (t-tests) - placebo
c: RTA-4d significantly differs from RTA-2d (t-tests) - placebo
↑/↓: increase or decrease in LTA vs. RTA-4d(a), LTA vs. RTA-2d(b) or RTA-4d vs. RTA-2d(c)

TABLE 3.3: LTA CLASSIFICATION TABLE

Desired class	1 - HD	2 - PR	3 - LD	4 - PL	% correct (of)
1 - HD	6	0	0	0	100 (6)
2 - PR	0	4	0	0	100 (4)
3 - LD	0	1	4	0	80 (5)
4 - PL	0	0	0	6	100 (6)
Totals	6	5	4	6	overall 95%

TABLE 3.4: RTA CLASSIFICATION TABLE

Desired class	1 - HD	2 - PR	3 - LD	4 - PL	% correct (of)
1 - HD	1	1	4	0	16.7 (6)
2 - PR	0	4	0	1	80 (5)
3 - LD	4	0	1	0	20 (5)
4 - PL	0	0	0	6	100 (6)
Totals	5	5	5	7	overall 54.2%

TABLE 3.5: DIA CLASSIFICATION TABLE

Desired class	1 - HD	2 - PR	3 - LD	4 - PL	% correct (of)
1 - HD	6	0	0	0	100 (6)
2 - PR	0	4	0	1	80 (5)
3 - LD	0	1	4	0	80 (5)
4 - PL	0	2	0	4	66.7 (6)
Totals	6	7	4	5	overall 81.7%

TABLE 3.6: Mean peak heights (± SEM) of control and *mdx* muscles treated with high dose deflazacort (HD). Key: dia=diaphragm; LTA=uncrushed tibialis anterior; 4d=crushed TA with 4 days recovery; 2d=crushed TA with 2 days recovery

HTS	*Mdx* dia(6)	*Mdx* LTA(6)	*Mdx* 4d(6)	*Mdx* 2d(5)	Con dia(5)	Con LTA(5)	Con 4d(4)
Ht1	0.026± 0.002	0.047± 0.007	0.041± 0.007	0.004± 0.001	0.004± 0.001	0.013± 0.006	0.007± 0.001
Ht2	0.018± 0.001	0.035± 0.005	0.031± 0.003	0.003± 0.001	0.002± 0.001	0.008± 0.003	0.004± 0.0002
Ht3	0.025± 0.001	0.038± 0.006	0.036± 0.004	0.003± 0.001	0.003± 0.0004	0.006± 0.001	0.005± 0.0003
Ht4	0.028± 0.002	0.047± 0.007	0.041± 0.004	0.004± 0.001	0.004± 0.001	0.007± 0.02	0.005± 0.0006
Ht5	0.104± 0.024	0.068± 0.005	0.079± 0.012	0.014± 0.002	0.050± 0.008	0.023± 0.004	0.035± 0.006
Ht6	0.052 0.006	0.037± 0.003	0.043± 0.003	0.007± 0.001	0.017± 0.002	0.010± 0.001	0.015± 0.002

TABLE 3.7: Mean peak heights (± SEM) of *mdx* muscles treated with low dose deflazacort (LD).

Heights	*Mdx* dia (5)	*Mdx* LTA (5)	*Mdx* 4d (5)
Ht1	0.030± 0.004	0.037± 0.005	0.039± 0.004
Ht2	0.022± 0.003	0.026± 0.004	0.025± 0.003
Ht3	0.026± 0.002	0.029± 0.004	0.027± 0.003
Ht4	0.027± 0.003	0.037± 0.005	0.036± 0.003
Ht5	0.123± 0.014	0.052± 0.007	0.061± 0.007
Ht6	0.058± 0.004	0.035± 0.003	0.039± 0.004

TABLE 3.8: Mean peak heights (± SEM) of *mdx* muscles treated with prednisone (PR).

Heights	*Mdx* dia (5)	*Mdx* LTA (5)	*Mdx* 4d (5)
Ht1	0.024± 0.003	0.040± 0.003	0.045± 0.004
Ht2	0.021± 0.003	0.029± 0.003	0.029± 0.002
Ht3	0.023± 0.002	0.033± 0.003	0.034± 0.002
Ht4	0.024± 0.003	0.041± 0.004	0.044± 0.005
Ht5	0.105± 0.017	0.070± 0.008	0.117± 0.025
Ht6	0.051± 0.003	0.042± 0.002	0.049± 0.006

TABLE 3.9: Mean peak heights (± SEM) of control and *mdx* muscles treated with placebo (PL).

HTS	*Mdx* dia(6)	*Mdx* LTA(6)	*Mdx* 4d(6)	*Mdx* 2d(5)	Con dia(1-3)	Con LTA(4)	Con 4d(4)
Ht1	0.023± 0.002	0.034± 0.005	0.037± 0.004	0.004± 0.001	0.006	0.007± 0.0007	0.008± 0.002
Ht2	0.016± 0.001	0.021± 0.003	0.024± 0.002	0.003± 0.001	0.003	0.005± 0.0004	0.004± 0.0009
Ht3	0.022± 0.002	0.024± 0.003	0.028± 0.003	0.004± 0.001	0.003± 0.0004	0.006± 0.0005	0.005± 0.001
Ht4	0.023± 0.002	0.036± 0.006	0.038± 0.003	0.004± 0.001	0.003± 0.001	0.008± 0.0007	0.006± 0.0008
Ht5	0.115± 0.028	0.058± 0.010	0.076± 0.016	0.011± 0.002	0.044± 0.018	0.020± 0.005	0.033± 0.004
Ht6	0.052± 0.003	0.037± 0.003	0.041± 0.004	0.006± 0.001	0.015± 0.004	0.009± 0.001	0.016± 0.001

TABLE 3.10: Mean peak height ratios (±SEM) of control and *mdx* muscles treated with HD.

Height ratios	*Mdx* dia(11)	*Mdx* LTA(6)	*Mdx* 4d(6)	*Mdx* 2d(5)	Con dia(3)	Con LTA(5)	Con 4d(5)
Ht1/2	1.41± 0.07	1.36± 0.05	1.39± 0.08	1.53± 0.06	1.90± 0.37	1.60± 0.15	1.47± 0.07
Ht1/3	1.03± 0.03	1.24± 0.04	1.22± 0.08	1.40± 0.07	1.13± 0.07	1.25± 0.11	1.18± 0.05
Ht1/4	0.99± 0.05	1.01± 0.04	0.98± 0.03	1.26± 0.09	1.07± 0.17	0.94± 0.07	1.15± 0.06
Ht1/5	0.26± 0.06	0.69± 0.08	0.56± 0.09	0.34± 0.09	0.09± 0.13	0.34± 0.09	0.21± 0.03
Ht1/6	0.44± 0.06	1.27± 0.17	0.97± 0.13	0.58± 0.10	0.25± 0.21	0.68± 0.13	0.45± 0.03
Ht2/3	0.73± 0.01	0.91± 0.02	0.87± 0.02	0.85± 0.04	0.64± 0.15	0.78± 0.02	0.81± 0.03
Ht2/4	0.65± 0.02	0.74± 0.03	0.71± 0.02	0.73± 0.02	0.56± 0.09	0.59± 0.02	0.77± 0.04
Ht2/5	0.25± 0.05	0.51± 0.06	0.40± 0.06	0.30± 0.08	0.07± 0.16	0.25± 0.08	0.16± 0.03
Ht2/6	0.38± 0.04	0.94± 0.13	0.75± 0.08	0.46± 0.11	0.17± 0.26	0.49± 0.13	0.34± 0.03
Ht3/4	0.96± 0.03	0.82± 0.02	0.82± 0.03	0.90± 0.04	0.97± 0.11	0.76± 0.02	0.95± 0.06
Ht3/5	0.25± 0.05	0.56± 0.07	0.45± 0.07	0.26± 0.08	0.08± 0.06	0.32± 0.11	0.20± 0.03
Ht3/6	0.43± 0.05	1.03± 0.14	0.85± 0.08	0.43± 0.08	0.21± 0.10	0.63± 0.17	0.39± 0.04
Ht4/5	0.28± 0.06	0.69± 0.08	0.56± 0.08	0.30± 0.10	0.10± 0.12	0.41± 0.15	0.18± 0.06
Ht4/6	0.46± 0.08	1.26± 0.17	0.99± 0.11	0.49± 0.11	0.26± 0.19	0.81± 0.22	0.41± 0.06
Ht5/6	2.25± 0.26	1.83± 0.09	1.87± 0.23	1.96± 0.25	2.92± 0.32	2.28± 0.20	2.36± 0.35

TABLE 3.11: Mean peak height ratios (± SEM) of *mdx* muscles treated with LD.

Height ratios	*Mdx* dia (5)	*Mdx* LTA (5)	*Mdx* 4d (5)
Ht1/2	1.43± 0.03	1.44± 0.06	1.60± 0.01
Ht1/3	1.13± 0.06	1.27± 0.04	1.43± 0.03
Ht1/4	1.10± 0.03	1.00± 0.02	1.08± 0.03
Ht1/5	0.25± 0.04	0.71± 0.04	0.67± 0.06
Ht1/6	0.51± 0.05	1.05± 0.10	1.02± 0.09
Ht2/3	0.82± 0.03	0.89± 0.01	0.90± 0.02
Ht2/4	0.76± 0.01	0.70± 0.04	0.68± 0.02
Ht2/5	0.18± 0.03	0.49± 0.03	0.42± 0.04
Ht2/6	0.37± 0.04	0.73± 0.09	0.64± 0.06
Ht3/4	0.98± 0.04	0.79± 0.04	0.76± 0.02
Ht3/5	0.22± 0.03	0.56± 0.03	0.47± 0.04
Ht3/6	0.45± 0.03	0.83± 0.09	0.71± 0.05
Ht4/5	0.23± 0.03	0.71± 0.05	0.62± 0.05
Ht4/6	0.46± 0.04	1.05± 0.11	0.95± 0.08
Ht5/6	2.10± 0.15	1.49± 0.18	1.58± 0.16

TABLE 3.12: Mean peak height ratios (± SEM) of *mdx* muscles treated with PR.

Height ratios	*Mdx* dia (5)	*Mdx* LTA (5)	*Mdx* 4d (5)
Ht1/2	1.42± 0.21	1.39± 0.04	1.52± 0.07
Ht1/3	1.02± 0.07	1.23± 0.04	1.31± 0.06
Ht1/4	1.01± 0.03	0.97± 0.03	1.02± 0.04
Ht1/5	0.25± 0.05	0.59± 0.09	0.47± 0.11
Ht1/6	0.47± 0.06	0.96± 0.09	1.00± 0.18
Ht2/3	0.78± 0.08	0.89± 0.02	0.86± 0.01
Ht2/4	0.84± 0.14	0.70± 0.02	0.68± 0.05
Ht2/5	0.20± 0.05	0.43± 0.07	0.30± 0.07
Ht2/6	0.42± 0.09	0.70± 0.07	0.65± 0.10
Ht3/4	1.00± 0.08	0.79± 0.02	0.79± 0.06
Ht3/5	0.25± 0.04	0.49± 0.09	0.35± 0.08
Ht3/6	0.46± 0.05	0.79± 0.09	0.75± 0.11
Ht4/5	0.25± 0.04	0.61± 0.10	0.48± 0.12
Ht4/6	0.47± 0.06	0.99± 0.10	1.01± 0.21
Ht5/6	2.02± 0.24	1.67± 0.16	2.31± 0.20

TABLE 3.13: Mean peak height ratios (±SEM) of control and *mdx* muscles treated with PL.

Height ratios	*Mdx* dia(11)	*Mdx* LTA(6)	*Mdx* 4d(6)	*Mdx* 2d(5)	Con dia(2)	Con LTA(4)	Con 4d(4)
Ht1/2	1.44± 0.04	1.67± 0.12	1.50± 0.06	1.50± 0.10	1.89	1.47± 0.05	1.86± 0.16
Ht1/3	1.09± 0.04	1.50± 0.12	1.30± 0.09	1.28± 0.08	1.58	1.19± 0.05	1.41± 0.13
Ht1/4	1.07± 0.04	1.02± 0.04	0.95± 0.04	1.26± 0.09	1.28	0.96± 0.03	1.19± 0.17
Ht1/5	0.23± 0.05	0.61± 0.03	0.54± 0.08	0.42± 0.09	0.08	0.44± 0.11	0.26± 0.10
Ht1/6	0.41± 0.05	0.90± 0.08	0.94± 0.15	0.77± 0.15	0.27	0.82± 0.12	0.46± 0.09
Ht2/3	0.73± 0.02	0.84± 0.03	0.87± 0.03	0.87± 0.03	0.84	0.81± 0.01	0.76± 0.03
Ht2/4	0.72± 0.02	0.58± 0.03	0.64± 0.02	0.73± 0.03	0.68	0.65± 0.01	0.64± 0.07
Ht2/5	0.15± 0.03	0.38± 0.03	0.36± 0.05	0.33± 0.07	0.04	0.29± 0.07	0.13± 0.04
Ht2/6	0.29± 0.04	0.55± 0.06	0.63± 0.10	0.59± 0.13	0.14	0.55± 0.06	0.25± 0.04
Ht3/4	0.99± 0.01	0.69± 0.04	0.74± 0.04	0.91± 0.08	0.94± 0.14	0.81± 0.01	0.84± 0.06
Ht3/5	0.20± 0.04	0.45± 0.05	0.41± 0.06	0.33± 0.07	0.09± 0.13	0.36± 0.09	0.17± 0.05
Ht3/6	0.38± 0.04	0.65± 0.06	0.72± 0.12	0.60± 0.12	0.23± 0.20	0.68± 0.07	0.33± 0.05
Ht4/5	0.20± 0.04	0.66± 0.07	0.56± 0.08	0.39± 0.10	0.09± 0.17	0.45± 0.11	0.20± 0.05
Ht4/6	0.39± 0.05	0.96± 0.10	0.98± 0.15	0.70± 0.17	0.24± 0.26	0.84± 0.10	0.38± 0.03
Ht5/6	2.30± 0.23	1.50± 0.17	1.79± 0.19	1.82± 0.04	2.75± 0.66	2.11± 0.38	2.20± 0.35

TABLE 3.14: Mean peak areas (± SEM) of control and *mdx* muscles treated with HD.

Areas	*Mdx* dia(6)	*Mdx* LTA(6)	*Mdx* 4d(6)	*Mdx* 2d(5)	Con dia(1-3)	Con LTA(5)	Con 4d(5)
A1	0.487± 0.036	0.465± 0.037	0.512± 0.102	0.103± 0.008	0.221± 0.072	0.088± 0.012	0.131± 0.006
A2	0.058± 0.006	0.077± 0.007	0.080± 0.015	0.011± 0.001	0.017± 0.004	0.012± 0.003	0.015± 0.001
A3	0.134± 0.012	0.113± 0.009	0.121± 0.022	0.016± 0.002	0.515± 0.015	0.020± 0.004	0.024± 0.002
A4	0.125± 0.013	0.139± 0.012	0.151± 0.029	0.019± 0.002	0.042± 0.012	0.026± 0.005	0.027± 0.002
A5	0.919± 0.126	0.621± 0.084	0.741± 0.109	0.197± 0.049	0.856± 0.346	0.225± 0.034	0.331± 0.061

TABLE 3.15: Mean peak areas (± SEM) of *mdx* muscles treated with LD.

Areas	*Mdx* dia (5)	*Mdx* LTA (5)	*Mdx* 4d (5)
A1	0.517± 0.091	0.467± 0.063	0.502± 0.059
A2	0.062± 0.009	0.069± 0.011	0.068± 0.005
A3	0.139± 0.027	0.119± 0.016	0.118± 0.013
A4	0.126± 0.024	0.138± 0.017	0.139± 0.013
A5	1.076± 0.167	0.572± 0.066	0.687± 0.100

TABLE 3.16: Mean peak areas (± SEM) of *mdx* muscles treated with PR.

Areas	*Mdx* dia (5)	*Mdx* LTA (5)	*Mdx* 4d (5)
A1	0.660± 0.108	0.434± 0.036	0.455± 0.059
A2	0.093± 0.025	0.065± 0.005	0.063± 0.007
A3	0.173± 0.020	0.107± 0.009	0.101± 0.012
A4	0.154± 0.020	0.126± 0.004	0.117± 0.012
A5	1.340± 0.245	0.601± 0.106	0.903± 0.268

TABLE 3.17: Mean peak areas (± SEM) of control and *mdx* muscles treated with PL.

Areas	*Mdx* dia(6)	*Mdx* LTA(6)	*Mdx* 4d(6)	*Mdx* 2d(5)	Con dia(1-3)	Con LTA(5)	Con 4d(5)
A1	0.560± 0.126	0.361± 0.026	0.538± 0.091	0.122± 0.018	0.197± 0.065	0.179± 0.056	0.138± 0.010
A2	0.064± 0.013	0.050± 0.003	0.079± 0.013	0.015± 0.002	0.021	0.025± 0.008	0.016± 0.003
A3	0.153± 0.035	0.090± 0.008	0.132± 0.023	0.023± 0.003	0.039	0.041± 0.012	0.027± 0.004
A4	0.120± 0.023	0.115± 0.011	0.153± 0.023	0.026± 0.004	0.026± 0.002	0.051± 0.013	0.030± 0.003
A5	1.601± 0.611	0.540± 0.029	0.794± 0.064	0.214± 0.047	0.898± 0.402	0.299± 0.070	0.406± 0.057

TABLE 3.18: Mean peak area ratios (± SEM) of control and *mdx* muscles treated with HD.

Area ratios	*Mdx* dia(11)	*Mdx* LTA(5)	*Mdx* 4d(6)	*Mdx* 2d(5)	Con dia(3)	Con LTA(5)	Con 4d(5)
A1/A2	9.17± 0.72	6.12± 0.26	6.48± 0.32	9.77± 1.13	12.75± 3.95	8.57± 1.07	8.69± 0.41
A1/A3	4.06± 0.29	4.11± 0.09	4.21± 0.15	6.53± 0.80	4.19± 0.30	4.80± 0.52	5.57± 0.42
A1/A4	4.39± 0.31	3.37± 0.16	3.38± 0.08	5.78± 0.79	5.09± 0.84	3.61± 0.32	4.98± 0.30
A1/A5	0.52± 0.05	0.78± 0.07	0.70± 0.07	0.61± 0.09	0.28± 0.20	0.45± 0.10	0.45± 0.08
A2/A3	0.45± 0.02	0.67± 0.02	0.66± 0.03	0.67± 0.05	0.33± 0.17	0.57± 0.02	0.64± 0.03
A2/A4	0.48± 0.02	0.55± 0.02	0.52± 0.01	0.59± 0.04	0.40± 0.08	0.43± 0.03	0.57± 0.03
A2/A5	0.06± 0.01	0.13± 0.01	0.11± 0.01	0.07± 0.01	0.02± 0.04	0.06± 0.02	0.05± 0.01
A3/A4	1.08± 0.03	0.82± 0.02	0.80± 0.03	0.88± 0.02	1.21± 0.22	0.76± 0.03	0.90± 0.04
A3/A5	0.14± 0.02	0.19± 0.02	0.17± 0.02	0.10± 0.02	0.07± 0.05	0.11± 0.03	0.08± 0.02
A4/A5	0.13± 0.02	0.24± 0.03	0.21± 0.02	0.002± 0.0004	0.06± 0.06	0.14± 0.04	0.003± 0.0003

TABLE 3.19: Mean peak area ratios (± SEM) of *mdx* muscles treated with LD.

Areas	*Mdx* dia (5)	*Mdx* LTA (5)	*Mdx* 4d (5)
A1/A2	8.30± 0.43	6.81± 0.26	7.38± 0.70
A1/A3	3.81± 0.17	3.94± 0.11	4.25± 0.15
A1/A4	4.15± 0.10	3.37± 0.08	3.58± 0.18
A1/A5	0.49± 0.05	0.81± 0.05	0.75± 0.06
A2/A3	0.46± 0.03	0.58± 0.01	0.59± 0.03
A2/A4	0.50± 0.03	0.50± 0.02	0.49± 0.02
A2/A5	0.06± 0.01	0.12± 0.01	0.10± 0.01
A3/A4	1.09± 0.04	0.86± 0.03	0.84± 0.02
A3/A5	0.13± 0.01	0.21± 0.01	0.18± 0.01
A4/A5	0.12± 0.01	0.24± 0.01	0.21± 0.01

TABLE 3.20: Mean peak area ratios (± SEM) of *mdx* muscles treated with PR.

Areas	*Mdx* dia (5)	*Mdx* LTA (5)	*Mdx* 4d (5)
A1/A2	7.77± 0.82	6.64± 0.33	7.17± 0.24
A1/A3	3.72± 0.23	4.06± 0.11	4.45± 0.10
A1/A4	4.21± 0.24	3.42± 0.20	3.85± 0.15
A1/A5	0.52± 0.07	0.75± 0.09	0.61± 0.10
A2/A3	0.51± 0.09	0.61± 0.03	0.62± 0.01
A2/A4	0.58± 0.11	0.51± 0.02	0.54± 0.01
A2/A5	0.07± 0.02	0.11± 0.02	0.09± 0.02
A3/A4	1.14± 0.02	0.84± 0.05	0.86± 0.02
A3/A5	0.14± 0.02	0.19± 0.02	0.14± 0.02
A4/A5	0.12± 0.01	0.22± 0.03	0.16± 0.03

TABLE 3.21: Mean peak area ratios (± SEM) of control and *mdx* muscles treated with PL.

Area ratios	*Mdx* dia(11)	*Mdx* LTA(6)	*Mdx* 4d(6)	*Mdx* 2d(5)	Con dia(2)	Con LTA(4)	Con 4d(4)
A1/A2	8.66± 0.32	7.29± 0.43	6.90± 0.51	8.05± 0.66	13.74	7.16± 0.19	10.56± 0.30
A1/A3	3.90± 0.17	4.03± 0.13	4.17± 0.30	5.40± 0.46	7.36	4.32± 0.18	5.81± 0.31
A1/A4	4.63± 0.20	3.19± 0.19	3.54± 0.19	4.81± 0.32	7.25	3.48± 0.26	5.01± 0.43
A1/A5	0.41± 0.05	0.67± 0.04	0.67± 0.08	0.62± 0.07	0.26± 0.17	0.61± 0.11	0.33± 0.05
A2/A3	0.45± 0.02	0.56± 0.03	0.61± 0.03	0.67± 0.04	0.54	0.60± 0.01	0.57± 0.02
A2/A4	0.53± 0.01	0.44± 0.02	0.52± 0.05	0.60± 0.01	0.72	0.48± 0.02	0.50± 0.04
A2/A5	0.05± 0.01	0.09± 0.01	0.10± 0.01	0.08± 0.01	0.01	0.09± 0.02	0.04± 0.01
A3/A4	1.19± 0.04	0.79± 0.03	0.87± 0.09	0.90± 0.04	1.35	0.80± 0.03	0.88± 0.03
A3/A5	0.11± 0.02	0.17± 0.01	0.16± 0.02	0.12± 0.02	0.03	0.14± 0.03	0.07± 0.02
A4/A5	0.09± 0.01	0.21± 0.02	0.19± 0.02	0.13± 0.02	0.04± 0.06	0.18± 0.04	0.08± 0.02

CHAPTER 4

1-H NMR SPECTROSCOPY OF DYSTROPHIC *MDX* SKELETAL MUSCLE PERCHLORIC ACID EXTRACTS: CHANGES WITH DEFLAZACORT TREATMENT

1. ABSTRACT

The *mdx* mouse suffers from dystrophin-deficient myopathy identical to that observed in Duchenne muscular dystrophy (DMD). Glucocorticoids are the only treatments that alleviate the progression of DMD, and increase proliferation, fusion and growth of *mdx* muscle. We were interested in studying whether high-resolution proton nuclear magnetic resonance spectroscopy (1-H NMR) of tissue extracts could detect the different phenotypes of control and *mdx* muscle and of muscles that were treated with glucocorticoids. It was hypothesized that: 1) control and *mdx* muscles would exhibit different spectral characteristics, and 2) spectra from extracts of deflazacort-treated animals would be different from the placebo group. Control and *mdx* (5.5 wks) limb and diaphragm (DIA) muscles were extracted with perchloric acid and prepared for 1-H NMR spectroscopy at 500MHz. Another group of control (5 wks) and *mdx* (3 wks) animals were treated with deflazacort or placebo for 4.5 weeks, at which time limb and DIA were collected and prepared for spectroscopy. The concentrations of valine, lactate, alanine, glutamate, succinate, glutamine, creatines, taurine, carnitine, glycine and glucose were measured from the spectra and compared between groups by t-tests. Lower levels of taurine and carnitine were observed in *mdx* limb and DIA compared to control. Additionally, glutamate, alanine and succinate were decreased in the *mdx* DIA, but increased with deflazacort-treatment in *mdx* DIA muscles. Results indicate that these peaks may be useful markers for monitoring the effectiveness of treatment and point to alterations in energy metabolism in *mdx* dystrophy.

2. INTRODUCTION

Nuclear magnetic resonance spectroscopy (NMR) is a tool which has potential for diagnosing and monitoring disease (Peeling & Sutherland, 1992; Cazzaniga et al., 1994; Brière et al., 1995). Duchenne muscular dystrophy (DMD) has been studied by 31-P, 13-C and 1-H NMR (Younkin et al., 1987; Bongers et al., 1992; Dunn et al., 1992; 1993; Schick et al., 1993; Heinriksen, 1994). *In vivo* 1-H NMR studies of pathological skeletal muscle focus on changes in the lipid resonances between 0.8 and 2.2 ppm. These resonances are larger in diseased muscle, relate to the severity of muscle involvement (Bárány et al., 1989; Bongers et al., 1992), and differ in composition with disease (Bárány et al., 1989). Little work has been performed on smaller metabolite signals (i.e. taurine, alanine, carnitine) in dystrophic muscle, particularly because the signals are difficult to distinguish by *in vivo* NMR.

The analysis of acid extracts of tissues by high-resolution 1-H NMR allows quantification of smaller metabolite concentrations, aids in assignment of metabolites, and allows verification of *in vivo* and *ex vivo* spectroscopic results (Bell et al., 1994). Precise regional localization and correlation with histology is possible. In addition, extract analysis may be able to resolve the appearance of new metabolites or changes in metabolite concentrations (other than lipids) due to pathological conditions, and subsequently allow monitoring of treatment strategies. We are not aware of any 1-H NMR studies which have examined perchloric acid (PCA) extracts of DMD muscle or its animal model (the *mdx* mouse).

Recent *ex vivo* 1-H NMR findings from our laboratory (Chapters 2 & 3) show that:

1) spectra from control and *mdx* skeletal muscle are different, 2) the stages of *mdx* dystrophy can be monitored, 3) different muscle types (diaphragm vs. tibialis anterior) exhibit distinct spectral patterns, 4) 1-H NMR detects differences between glucocorticoid treatments in *mdx* limb muscle, and 5) the distinct stages of synchronous regeneration are detected in injured *mdx* muscle.

In this study, 1-H NMR was used to determine the concentration of water soluble metabolites in PCA extracts of control and *mdx* muscle in order to further elucidate the metabolism of living normal and dystrophic *mdx* muscle tissue. Subsequently, 1-H NMR was used to study extracts of muscles which were treated with deflazacort. The hypotheses of the studies were that: 1) spectra from control and *mdx* animals would differ upon 1-H NMR examination of PCA extracts, and 2) spectra from control and *mdx* animals treated with deflazacort would differ from untreated counterparts.

3. MATERIALS AND METHODS

3.1. Animals

Control (C57Bl/10ScSn) and *mdx* mice were maintained and housed according to the Canadian Council of Animal Care at the University of Manitoba Animal Care Facility (Winnipeg, Manitoba). In the first part of the study, control (n=6) and *mdx* (n=5) mice aged 5.5 weeks were killed by cervical dislocation under anaesthetic and the limb muscles (tibialis anterior and gastrocnemius) and diaphragm (DIA) were collected. In the second part of the study, 5 week old control and 3 week old *mdx* mice were treated with either deflazacort

(1.2mg/kg body weight; Marion Merrell Dow Inc., Laval, Québec; n=6 for *mdx* and 5 for control) or placebo (Methocel, CIBA Vision, Mississauga, ON; n=5 for *mdx* and 4 for control) for 4.5 weeks. At the completion of the treatment period, the DIA and limb muscles were collected.

3.2. Tissue preparation

Muscle tissues were rapidly removed from animals, frozen in liquid nitrogen, weighed and stored in a -70°C freezer until performing the extraction procedure (Peeling & Sutherland, 1992; 1993). Each sample was homogenized (POLYTRON, Kinematica Aggregate, Switzerland) on ice in 0.3M cold perchloric acid (1ml per 100mg tissue). The homogenate was centrifuged for 20 minutes at 6000rpm at 0°C and the clear supernatant was collected in a clean tube and refrigerated. The precipitate was extracted again with 1ml of cold 0.3M perchloric acid, the sample was centrifuged in the same manner as previous and the supernatants were pooled. Samples were then neutralized with cold 1.5M KOH to pH 7.0 (± 0.2), centrifuged, and the supernatant was collected, leaving the salt particles behind. After lyophilizing overnight, 1ml of D_2O was added to the dry extracts which were then brought to pH 7.25 (± 0.2) with NaOD and DCl. Samples were lyophilized again and stored. The day before performing spectroscopy, 0.60 ml of 1.5mM TSP (sodium 3-trimethysilylpropionate; a chemical shift reference) in D_2O was added to the dry extract, the pH was checked and the sample was pipetted into a clean 5mm NMR tube.

3.3. Spectroscopy and analysis

1-H NMR spectra were obtained at 300K with a Bruker AMX-500 spectrometer

locked to the D_2O resonance. For each sample, 160 FIDs were accumulated in 16K of memory using a sweep width of 7042.25 Hz (acquisition time of 1.16 seconds). Exponential multiplication (LB=1) and Fourier transformation were applied to give the NMR spectrum.

The assignment of the peaks in the PCA extracts to the major metabolites of interest (valine, lactate, alanine, glutamate, succinate, glutamine, creatines, carnitine, taurine, glycine, glucose) were made on the basis of literature chemical shift values for extracts of skeletal muscle (Arús et al., 1984a; Arús & Bárány, 1986; Venkatasubramanian et al., 1986), lymphocytes (Sze & Jardetzky, 1990; 1994), colon (Moreno & Arús, 1996) and pure compounds, and had the expected pH behaviour and J-couplings. Metabolite concentrations were determined by comparing the integrated intensities of the resonances of interest with the TSP signal, correcting for the number of contributing protons and for the tissue weight. The resonances integrated are those assigned in Figure 4.1.

Statistical comparisons were performed by unpaired t-tests. Results are expressed as mean ± standard error of the mean (SEM).

4. RESULTS

4.1. Spectral characteristics

The metabolites of interest in PCA extracts (see Figs 4.1, 4.2 and 4.3 and Appendix A) were clearly differentiated and assigned to valine (CH_3 doublet; 1.05 ppm), lactate (CH_3 doublet; 1.33 ppm and CH quartet; 4.11 ppm), alanine (CH_3 doublet; 1.47 ppm), glutamate (CH_2 triplet of doublets; 2.35 ppm), succinate (CH_2 singlet; 2.41 ppm), glutamine (CH_2

complex; 2.45 ppm), creatines (CH_3 singlet; 3.04 ppm and CH_2 singlet; 3.93 ppm), carnitine ($N\text{-}CH_3$ singlet; 3.23 ppm), taurine ($S\text{-}CH_2$ triplet; 3.26 ppm and $N\text{-}CH_2$ triplet; 3.42 ppm), glycine (CH_2 singlet; 3.56 ppm) and glucose (CH doublet; 4.65 ppm) at a pH of 7.25 (± 0.2). Two resonances contributing to taurine (3.26 and 3.42 ppm), creatine (3.04 and 3.93 ppm) and lactate (1.33 and 4.12 ppm) were integrated as an internal check, and concentrations were found to differ by less than 0.04μmol/g for the two lactate peaks, 0.18μmol/g for creatines and 0.07μmol/g for taurine. Statistics were performed on the peak at 1.33 ppm for lactate, 3.04 ppm for creatines and 3.26 ppm for taurine.

Minor variations in chemical shifts of the taurine and carnitine peaks were observed. In these instances, the $S\text{-}CH_2$ of taurine shifted toward 3.23 ppm, the $N\text{-}CH_2$ group of taurine resonated around 3.32 ppm and carnitine shifted toward 3.21 ppm. Slight variations in pH values are the cause of the shifting. A clear carnitine peak could not be distinguished in the 3.23 ppm region for 2 spectra in part 1 of the study. In part 2 of the study, carnitine, valine, glutamate, succinate, glutamine and glycine often could not be distinguished from the baseline, probably because the mass of those samples was less than 30mg and/or due to poor shimming (i.e. a poor signal to noise ratio). In addition, control spectra from part 2 of the study were contaminated with alcohols (methanol and ethanol) from an unknown source. The peaks of interest were integrated regardless of chemical shift or contamination because signal intensity should not be affected by pH (Nakajima et al., 1994). The majority of the acquired spectra were very clean and distinct peaks could be identified.

4.2. Part 1 - Control vs. *mdx*

Figures 4.1 and 4.2 show spectra of typical control and *mdx* limb muscle extracts. No extra or different peaks were present in *mdx* muscle, but there were changes in the concentration of some metabolites. For the limb muscle extracts (Table 4.1), peaks attributed to carnitine and taurine were significantly less in *mdx* compared to control muscles. This area is enlarged in Fig 4.2. In DIA muscle extracts (Table 4.2), alanine, glutamate, succinate, creatine, taurine and glycine peaks were significantly less in *mdx* (Fig 4.3) compared to control muscles. The glutamate-succinate-glutamine region is enlarged in Fig 4.3.

4.3. Part 2 - Placebo vs. deflazacort

No extra peaks were observed with deflazacort-treatment, but changes in the concentrations of some metabolites were evident. Control and *mdx* spectra could not be directly compared in this part because they were not age-matched. However, it was still possible to determine effects of treatment in both strains.

In control limb (Table 4.3), the concentrations of creatine and taurine were greater in deflazacort-treated muscles. In control DIA (Table 4.4), lactate, alanine and glutamate were less in deflazacort-treated muscles. In *mdx* limb (Table 4.5), the concentrations of lactate, glutamate and glutamine were less in deflazacort-treated muscles. In *mdx* DIA (Table 4.6), valine and glutamate were significantly greater, while carnitine was significantly less in deflazacort-treated muscles.

5. DISCUSSION

This report shows that high-resolution 1-H NMR is a sensitive method for distinguishing differences in metabolite levels between PCA extracts of control and dystrophic *mdx* muscles. In addition, spectroscopic differences exist between muscles of mice treated with deflazacort or placebo. The differences in metabolite concentrations measured by 1-H NMR must be due to differences in cellular composition and metabolism, but are not easily interpreted and the causes are undoubtedly complex. The results indicate that *mdx* muscles exhibit alterations in energy metabolism as previously reported by 31-P NMR (Dunn et al., 1993; McCully et al., 1994; Camiña et al., 1995) and that treatment with deflazacort partially corrects this disorder.

5.1. Part 1 - Control vs. *mdx*

5.1.1. Limb results Carnitine and taurine were significantly different between control and *mdx* limb muscle extracts. A corresponding peak, which has contributions from both taurine and carnitine protons in *ex vivo* 1-H NMR spectra, consistently differed between control and *mdx* muscle (Chapters 2 & 3). Therefore, 1-H NMR spectroscopic results of PCA extracts are consistent with *ex vivo* findings.

Since taurine plays a role in cell proliferation and viability (Wright et al., 1986; Huxtable, 1992), decreased taurine levels in *mdx* limb (and DIA) likely reflect a very active response to dystrophy at 5.5 weeks of age. Similar results were found in young and adolescent *mdx* muscles by *ex vivo* NMR (Chapter 2). It is expected that taurine levels will be greater in tissue extracts from older *mdx* mice, reflecting increased membrane stability

and decreased proliferation in these muscles.

Carnitine is an essential molecule for transport of long-chain fatty acids into the mitochondria and therefore, plays a key role in regulating fatty acid oxidation in the mitochondria (Hiatt et al., 1989). Studies on DMD (Thomson & Smith, 1978; Berthillier et al., 1982; Camiña et al., 1995) and other forms of neuromuscular disorders (Venkatasubramanian et al., 1986) show decreased levels of muscle carnitine compared to controls. In DMD, levels are decreased to a greater extent in early dystrophy (Berthillier et al., 1982), and thus do not relate to the severity of the disease. In addition, carnitine is decreased in rat skeletal muscle during regeneration induced by bupivacaine (Czyzewski et al., 1983). These results, taken together with our NMR findings of decreased carnitine in the actively-regenerating *mdx* mouse, suggest that: 1) decreases in muscle carnitine content may relate to muscle fiber regeneration rather than to a specific biochemical defect, or 2) disruption of lipid metabolism or mitochondrial function occurs in dystrophy. If the latter is true, metabolic alterations could be secondary to membrane alterations caused by the lack of dystrophin (Camiña et al., 1995), but are not the cause of necrosis since necrotic fibers are not observed in primary carnitine myopathies (Engel et al., 1977; Rebouche & Engel, 1984). It is important to follow this metabolite over time by 1-H NMR to determine whether it approaches normal levels in older stable *mdx* muscle, especially because 31-P NMR studies suggest that old *mdx* muscle adapts to a initial defect in oxidative metabolism (Dunn et al., 1993).

5.1.2. DIA results As observed in the limb muscle, taurine and carnitine stores

were decreased in the *mdx* DIA compared to the control DIA. The carnitine difference was not statistically significant, probably due to a low n value. It is suggested that these metabolites are valuable markers for *mdx* regeneration for the same reasons as stated above (section 5.1.1) and in Chapters 2 and 3.

Additionally, alanine, glutamate and succinate concentrations were less in *mdx* compared to control DIA. The additional significant findings are likely due to the fact that the *mdx* DIA is more affected by the dystrophic process at 5.5 weeks of age than age-matched limb muscles (Stedman et al., 1991; Dupont-Versteegden & McCarter, 1992; Louboutin et al., 1993), making NMR-visible differences even greater between control and *mdx* DIA than between control and *mdx* limb muscle. The reduced metabolite values in *mdx* DIA extracts may be due to decreased energy metabolism, as suggested by Decrouy et al. (1993), or to decreased muscle mass (i.e. more fibrosis and adipose tissue; less myofibers) in *mdx* DIA compared to control DIA. Since *mdx* muscle glucose levels were not significantly different from control muscle by our 1-H NMR analysis, reduced energy metabolism in *mdx* muscle is probably due to decreased oxidative utilization of glucose and free fatty acids (Even et al., 1994; Mokhatarian & Even, 1996). It is postulated that dystrophin in normal muscle might associate with metabolic enzyme complexes and determine the overall efficiency of metabolic pathways (Chinet et al., 1994).

5.2. Part 2 - Placebo vs. deflazacort

5.2.1. Limb results The significant decrease of glutamate and glutamine in treated *mdx* limb is difficult to interpret. It was expected that these metabolites would not be

reduced in amount, since deflazacort increases myogenesis (Anderson et al., 1996b). It may be that small sample weights and a low number of samples skewed the results. Alternatively, deflazacort may increase the amount of degeneration in *mdx* limb muscles (with a subsequent increase in muscle precursor proliferation; Anderson et al., 1996b). Thus, glutamate and glutamine may be markers for increased degeneration, especially since they become depleted in catabolic states (Rennie et al., 1996).

5.2.2. DIA results In non-regenerating skeletal muscle, glucocorticoid treatment is catabolic and causes muscle wasting and weakness (Kelly et al., 1986). In addition, deflazacort treatment results in general fiber atrophy and changes in control DIA contractility, more so than prednisone (Dekhuijzen et al., 1993). These reports support our findings of reduced amounts of alanine and glutamate in control treated DIA. Thus, glucocorticoids do not have a beneficial effect in non-pathologic muscle. The presence of constant low-level regeneration in *mdx* muscle must render it susceptible to the beneficial effects of glucocorticoids.

1-H NMR spectroscopy of muscle PCA extracts were better at monitoring treatment changes in the DIA than in *ex vivo* spectroscopy (Chapter 3), probably because the sample was more homogenous in solution than in its thin delicate *ex vivo* state. Glutamate, glutamine and valine concentrations were greater in treated DIA, and approached control levels. Deflazacort decreased the number of dystrophic lesions in the DIA (Anderson et al., 1996b). Therefore, the increase in glutamate, glutamine and valine may be useful markers of decreased dystrophy. Since dystrophin-revertants are few before and after treatment in

these *mdx* muscles (unpublished observations), linkage of glycolysis and the citric acid cycle to cytoskeletal organization (Chinet et al., 1994) probably does not account for the greater metabolite concentrations with deflazacort.

5.3. Summary

In the future, it is important to assess the potential of using the differences in taurine, carnitine, glutamate, succinate and glutamine as diagnostic aids with *in vivo* NMR spectroscopy, remembering that the field strength of clinical magnets is considerably less than used in this study. It is probably not practical to examine changes in alanine, valine, lactate or creatine concentrations *in vivo*. Alanine and valine are present in very small amounts and integration in noisy *in vivo* spectra is probably not possible. Normally, lactate is over-shadowed by broad lipid resonances *in vivo*. Spectral editing is possible (Bloch et al., 1995; Shen et al., 1996), but that process may also obliterate other metabolites of interest. Recent evidence points to the existence of an inhomogeneous pool of creatine in skeletal muscle and that additional compounds may be present in this region of the spectrum (Styles et al., 1996). For the reasons mentioned above, interpretation in changes in creatine, alanine, valine or lactate were not attempted.

On the other hand, it is felt that carnitine and taurine are valuable markers for regeneration, while glutamate, glutamine and succinate mark degeneration. These metabolites should be studied in more detail by 1-H NMR spectroscopy over the entire course of *mdx* dystrophy. The dependence of metabolite levels on the success of treatment suggests that *in vivo* 1-H NMR spectroscopy might eventually be an effective means of non-

invasively monitoring the degree of pathology in DMD patients.

Acknowledgements: Spectra were acquired at the Prairie Regional NMR Facility, University of Manitoba, with the assistance of Terry Wolowiec. Maureen Donnelly provided the PCA extraction protocol. Thanks to Cinthya Vargas for assisting in the extraction procedure.

6. CHAPTER 4 FIGURES AND TABLES:

FIGURE 4.1: A representative 1-H NMR spectrum of a PCA extract of control limb muscle. Integrated peaks are indicated. 1-valine; 2-lactate; 3-alanine; 4-glutamate; 5-succinate; 6-glutamine; 7-creatines; 8-carnitine; 9-taurine; 10-taurine; 11-glycine; 12-creatines; 13-lactate; 14-glucose. See text and Appendix A for the NMR-visible protons and structure.

FIGURE 4.2: A representative 1-H NMR spectrum of a PCA extract of *mdx* limb muscle. Similar peaks are present as in the control spectrum (Fig 4.1). The region from 3.6 to 3.2 ppm is enlarged to show taurine (9 and 10) and carnitine (8) peaks. The concentration of these metabolites were reduced in *mdx* limb compared to control limb. TSP-reference solution.

FIGURE 4.3: A representative 1-H NMR spectrum of a PCA extract of *mdx* DIA muscle. The region from 2.5 to 2.3 ppm is enlarged in order to show the glutamate (4), succinate (5) and glutamine (6) peaks. The concentration of these metabolites were reduced in *mdx* DIA compared to control DIA. The concentration of glutamate increased with deflazacort treatment in the *mdx* DIA. TSP-reference solution.

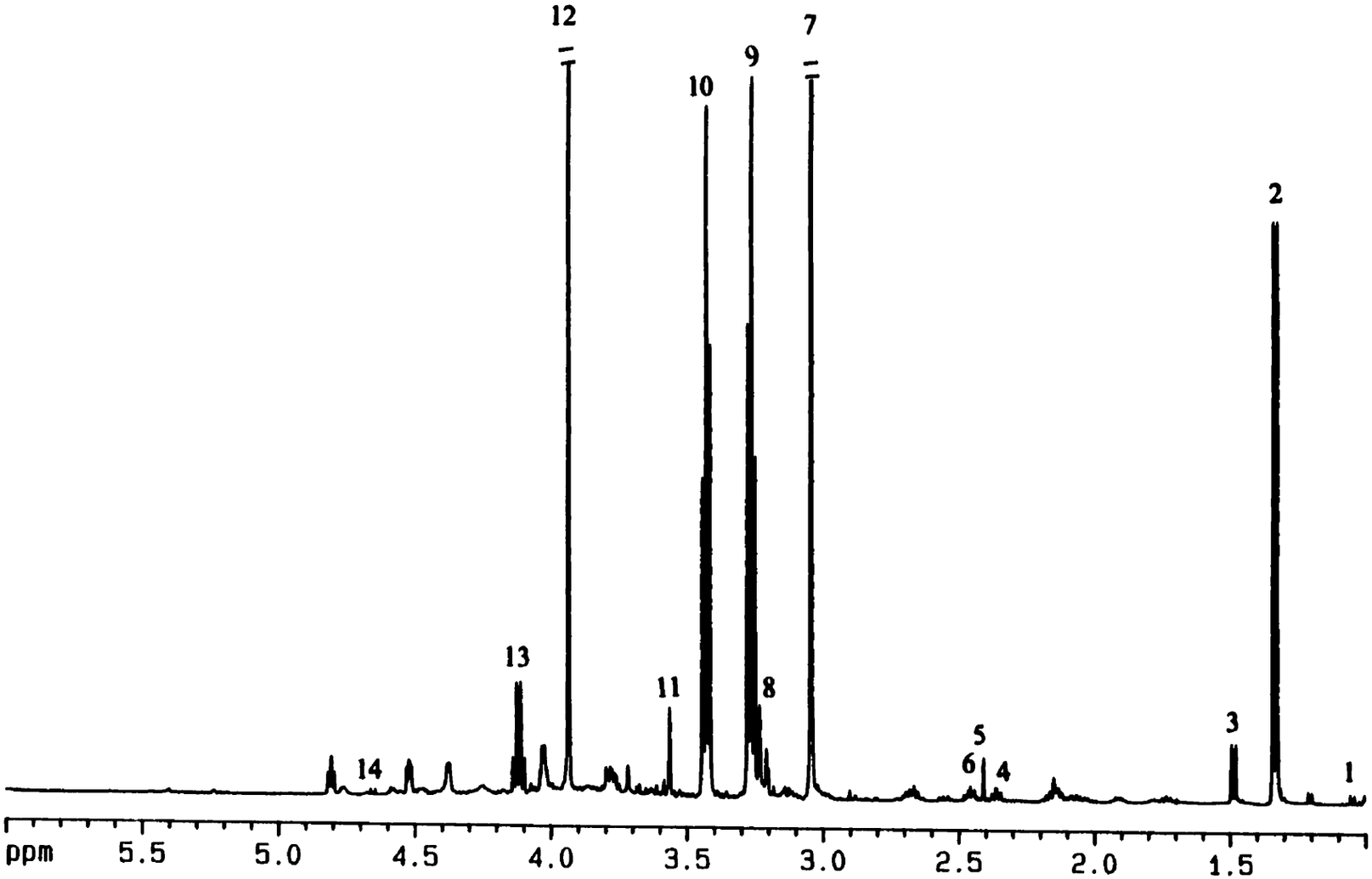
12
7
9
10
2
13
11
8
5
3
6
4
14
1
ppm
5.5
5.0
4.5
4.0
3.5
3.0
2.5
2.0
1.5

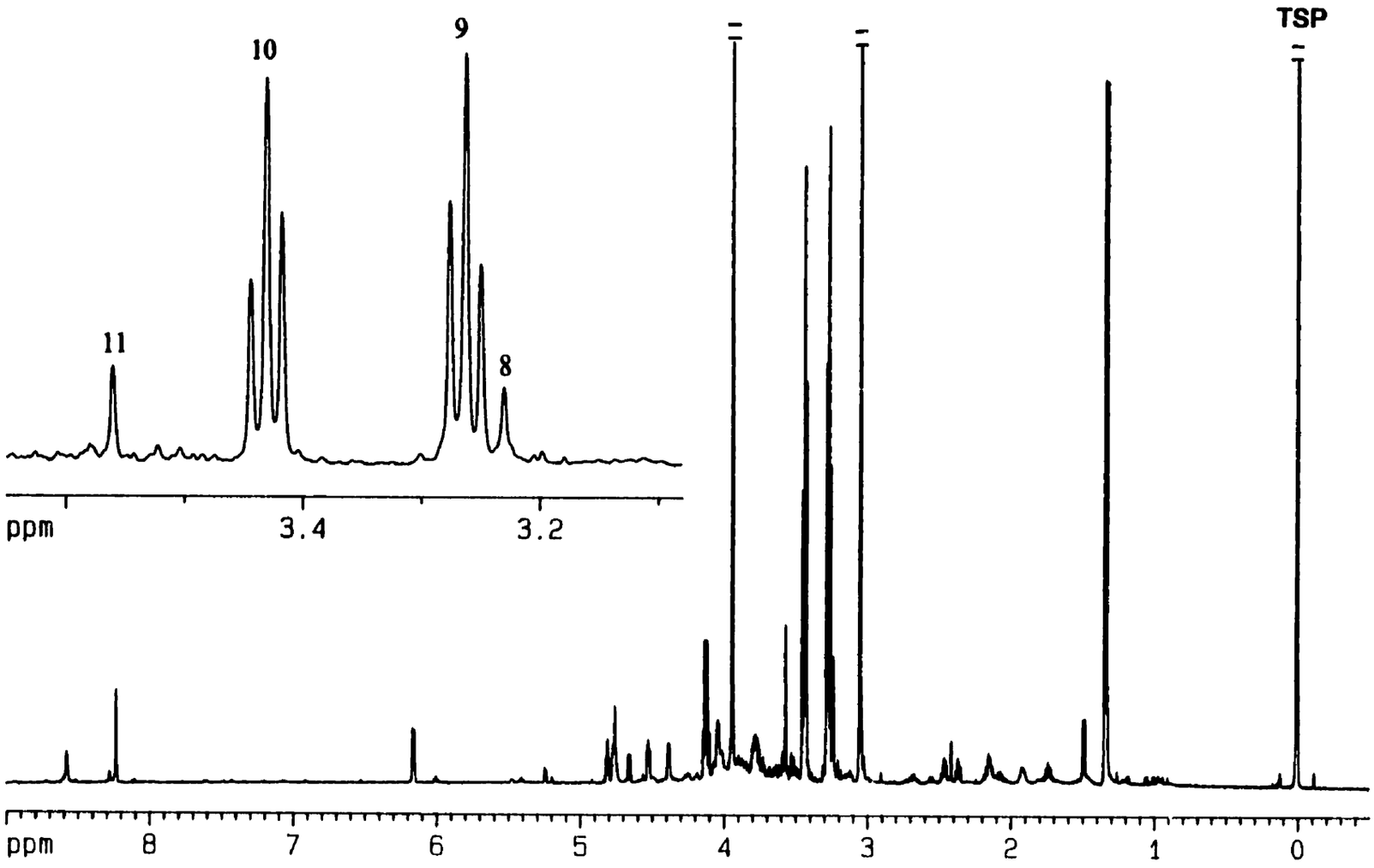
11
10
9
8
TSP
ppm
3.4
3.2
ppm
8
7
6
5
4
3
2
1
0

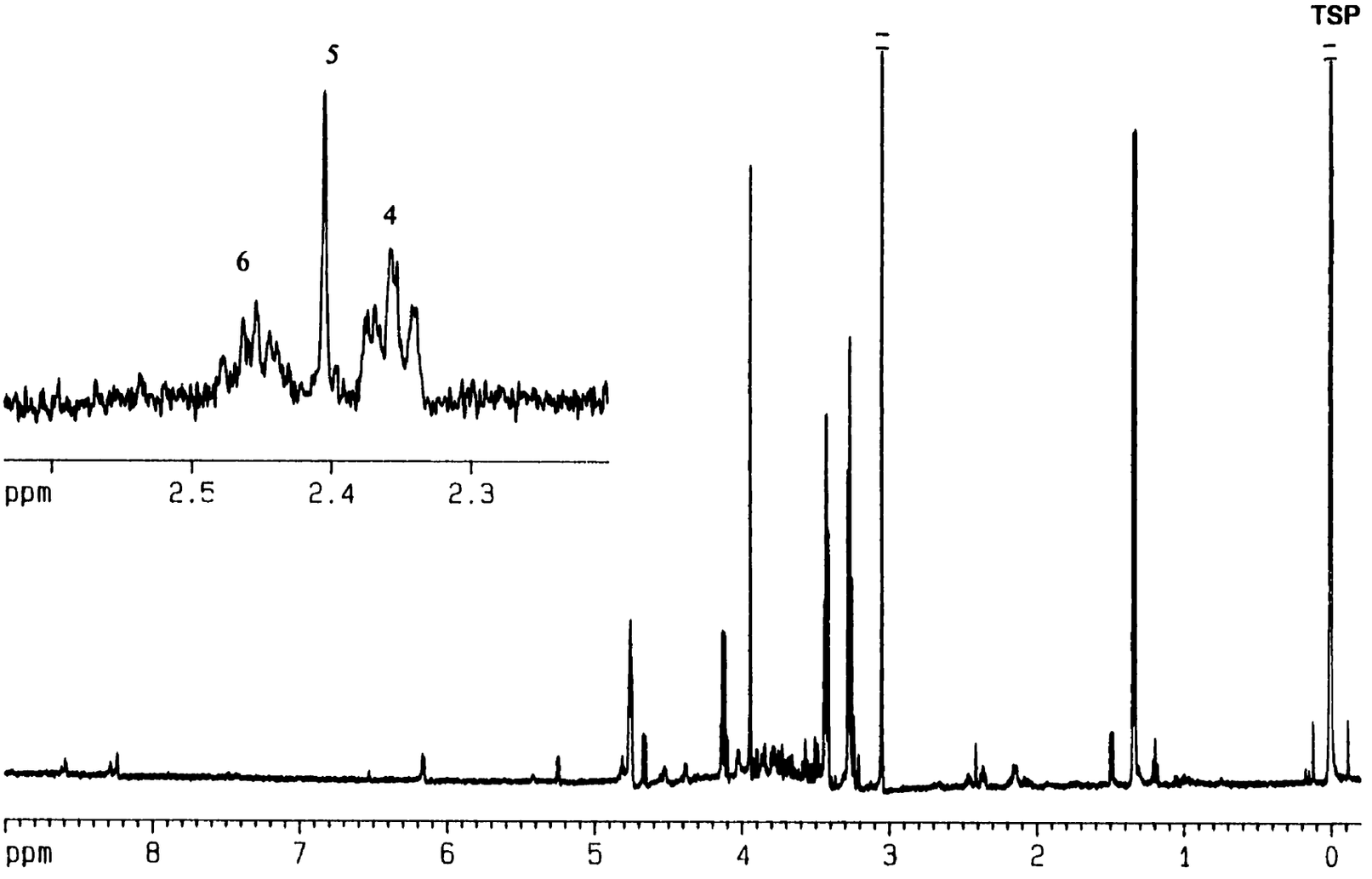
TSP
5
4
6
ppm
2.5
2.4
2.3
ppm
8
7
6
5
4
3
2
1
0

TABLE 4.1: Mean (±SEM) concentrations (μmol/g) of metabolites of interest from 1-H NMR spectra of perchloric acid extracts of LIMB muscles from 5.5 week old control and *mdx* mice. • denotes significance by t-tests ($p<0.05$).

Metabolite	*Mdx*		Control	
valine	0.0085± 0.0027	n=6	0.0067± 0.0011	n=10
lactate	1.5440± 0.2122	n=8	1.4292± 0.1743	n=12
alanine	0.1371± 0.0097	n=8	0.1318± 0.0108	n=11
glutamate	0.0974± 0.0096	n=8	0.1049± 0.0088	n=12
succinate	0.0350± 0.0054	n=8	0.0427± 0.0052	n=12
glutamine	0.1202± 0.0109	n=8	1.1336± 0.0130	n=11
creatines	1.5016± 0.1330	n=8	1.7239± 0.1277	n=12
carnitine (*;p=0.02)	0.0510± 0.0055	n=8	0.0655± 0.0033	n=9
taurine (*;p=0.05)	2.1686± 0.2009	n=8	2.6132± 0.1760	n=11
glycine	0.2885± 0.0290	n=8	0.2895± 0.0214	n=11
glucose	0.1114± 0.0195	n=8	0.1140± 0.0179	n=10

TABLE 4.2: Mean (±SEM) concentrations (μmol/g) of metabolites of interest from 1-H NMR spectra of perchloric acid extracts of DIAPHRAGM muscles from 5.5 week old control and *mdx* mice. * denotes significance by t-tests ($p<0.05$).

Metabolite	*Mdx*		Control	
valine	0.0271± 0.0038	n=4	0.0321± 0.0094	n=3
lactate	0.7996± 0.0614	n=4	1.0720± 0.1753	n=3
alanine (*;p=0.05)	0.1545± 0.0164	n=4	0.1952± 0.0089	n=3
glutamate (*;p=0.04)	0.1862± 0.0144	n=4	0.2447± 0.0254	n=3
succinate (*;p=0.04)	0.0725± 0.0097	n=4	0.1392± 0.0351	n=3
glutamine	0.1430± 0.0138	n=4	0.1632± 0.0111	n=3
creatines (*;p=0.003)	0.6014± 0.0533	n=4	0.9378± 0.0466	n=3
carnitine	0.0571± 0.0092	n=4	0.0817± 0.0053	n=2
taurine (*;p=0.05)	1.3341± 0.1356	n=4	1.8526± 0.0824	n=2
glycine (*;p=0.05)	0.1229± 0.0098	n=4	0.1615± 0.0193	n=2
glucose	0.2121± 0.0355	n=4	0.2603± 0.0311	n=3

TABLE 4.3: Mean (±SEM) concentrations (μmol/g) of metabolites of interest from 1-H NMR spectra of perchloric acid extracts of deflazacort- or placebo-treated control LIMB muscles (9.5 weeks of age). * denotes significance by t-tests (p<0.05).

Metabolite	Control deflazacort	Control placebo
valine	0.0533 n=1	- - -
lactate	3.1824± 0.1523 n=5	2.6507± 0.2879 n=4
alanine	0.1782± 0.0121 n=4	0.1489 n=1
glutamate	0.1598± 0.0072 n=3	0.1374 n=1
succinate	0.0445± 0.0004 n=2	- - -
glutamine	0.1086± 0.0110 n=2	- - -
creatines (*;p=0.01)	1.7254± 0.0509 n=5	1.3341± 0.1314 n=4
carnitine	- - -	- - -
taurine (*;p=0.01)	2.7111± 0.0756 n=5	1.9067± 0.3196 n=4
glycine	0.2542± 0.0137 n=4	- - -
glucose	0.2758± 0.0251 n=4	0.1451 n=1

TABLE 4.4: Mean (±SEM) concentrations (μmol/g) of metabolites of interest from 1-H NMR spectra of perchloric acid extracts of deflazacort- or placebo-treated control DIAPHRAGM muscles (9.5 weeks of age). * denotes significance by t-tests ($p<0.05$).

Metabolite	Control deflazacort		Control placebo	
valine	0.0703± 0.0259	n=3	0.1016± 0.0055	n=2
lactate (*;p=0.02)	1.1317± 0.1504	n=5	1.6098± 0.0661	n=4
alanine (*;p=0.05)	0.1100± 0.0450	n=5	0.2061± 0.0022	n=4
glutamate (*;p=0.05)	0.1589± 0.0298	n=4	0.2977± 0.0158	n=4
succinate	0.0559± 0.0273	n=3	0.0702± 0.0034	n=4
glutamine	0.1536± 0.0598	n=3	0.1850± 0.0199	n=4
creatines	0.9165± 0.1052	n=5	1.0246± 0.0245	n=4
carnitine	0.0453	n=1	- - -	
taurine	1.9532± 0.1916	n=5	2.1785± 0.0388	n=4
glycine	0.1550± 0.0174	n=3	- - -	
glucose	0.2115± 0.0732	n=4	0.2770± 0.0148	n=4

TABLE 4.5: Mean (±SEM) concentrations (μmol/g) of metabolites of interest from 1-H NMR spectra of perchloric acid extracts of deflazacort- or placebo-treated *mdx* LIMB muscles (7.5 weeks of age). * denotes significance by t-tests ($p<0.05$).

Metabolite	*Mdx* deflazacort		*Mdx* placebo	
valine	- - -		0.0212± 0.0126	n=3
lactate (*;p=0.04)	1.4612± 0.2095	n=4	3.0998± 0.6865	n=5
alanine	0.1465± 0.0408	n=4	0.1252± 0.0252	n=4
glutamate (*;p=0.02)	0.0251± 0.0045	n=2	0.0562± 0.0070	n=4
succinate	0.0147± 0.0129	n=2	0.0323± 0.0143	n=4
glutamine (*;p=0.05)	0.0329± 0.0081	n=3	0.0890± 0.0244	n=3
creatines	1.9375± 0.0938	n=4	1.9970± 0.2552	n=5
carnitine	0.0609± 0.0024	n=4	0.0628± 0.0153	n=2
taurine	3.0605± 0.1595	n=4	3.3245± 0.7940	n=4
glycine	0.3418± 0.0208	n=4	0.4251± 0.0830	n=3
glucose	0.0922± 0.0709	n=3	0.2844± 0.1022	n=4

TABLE 4.6: Mean (±SEM) concentrations (μmol/g) of metabolites of interest from 1-H NMR spectra of perchloric acid extracts of deflazacort- or placebo-treated *mdx* DIAPHRAGM muscles (7.5 weeks of age). * denotes significance by t-tests ($p<0.05$).

Metabolite	*Mdx* deflazacort		*Mdx* placebo	
valine (*;p=0.03)	0.0666± 0.0026	n=2	0.0409± 0.0062	n=4
lactate	1.4284± 0.0482	n=4	1.5682± 0.1249	n=5
alanine	0.1753± 0.0108	n=3	0.1888± 0.0067	n=5
glutamate (*;p=0.02)	0.2271± 0.0182	n=4	0.1715± 0.0123	n=4
succinate	0.0961± 0.0160	n=4	0.0905± 0.0100	n=4
glutamine	0.1888± 0.0134	n=4	0.1576± 0.0186	n=4
creatines	0.8017± 0.0876	n=4	0.8286± 0.0670	n=5
carnitine (*;p=0.03)	0.0462± 0.0069	n=2	0.0651± 0.0040	n=5
taurine	1.6966± 0.0792	n=4	1.8400± 0.1378	n=5
glycine	0.1803	n=1	0.1674± 0.0160	n=5
glucose	0.3390± 0.0449	n=4	0.4018± 0.0407	n=5

CHAPTER 5

MAGNETIC RESONANCE IMAGING OF REGENERATING DYSTROPHIC *MDX* MUSCLE

1. ABSTRACT

Magnetic resonance imaging (MRI) allows serial visualization of living muscle. In this study, MRI was used to follow dystrophy and regeneration in the *mdx* mouse, a genetic homologue to human Duchenne muscular dystrophy (DMD). It was hypothesized that MRI would distinguish *mdx* dystrophy from control muscle and that regenerating areas (spontaneous and after an imposed injury) would be evident. T2-weighted images of hindlimb muscles were obtained on anaesthetized mice in a horizontal bore 7.1T experimental magnet. *Mdx* muscle images appeared inhomogeneous in comparison to control images. Foci of high intensity areas in *mdx* MR images corresponded to dystrophic lesions as observed in the same muscles after histological sectioning. In addition, it was possible to chronologically follow the extent of injury and repair after an imposed crush to *mdx* muscle (at 0, 1, 2, 3, 4, 7, 9, and 21 days after crush). There were no apparent side-effects of repeated MRI at 7.1T on mice or muscle. These results should make it possible to obtain meaningful magnetic resonance spectra from a volume of muscle deemed appropriate by magnetic resonance images (i.e. regenerating, degenerating, normal muscle).

2. INTRODUCTION

Magnetic resonance imaging (MRI) is an important diagnostic imaging modality that is widely used clinically. It has been used in preliminary studies of Duchenne muscular dystrophy (DMD). DMD is characterized by adipose and fibrous replacement of degenerated muscle fibers (Partridge, 1993), thus MRI studies have focused on monitoring the severity of the disease by the degree of fat infiltration (Murphy et al., 1986; Lamminen, 1990; Phoenix et al., 1996). However, the degree of fat infiltration may not be the most successful measure for monitoring the effects of treatment in the early stages of DMD, before adipose and fibrotic tissues are deposited.

In contrast to DMD, its animal equivalent, the *mdx* mouse (Bulfield et al., 1984), presents very little adipose tissue infiltration and responds to dystrophy by successful limb muscle repair (Dangain & Vrbova, 1984; Anderson et al., 1987; 1988; Carnwath & Shotton, 1987). Therefore, this study used the *mdx* mouse for MRI studies. The purpose was to create visual MRI maps of regenerating *mdx* muscle as a first step in the ultimate goals of monitoring treatment and studying regeneration by *in vivo* spectroscopy. Proton maps allow meaningful spectra to be obtained from a volume of appropriate muscle (i.e. regenerating, degenerating, normal). It was hypothesized: 1) that MRI would distinguish *mdx* dystrophy from control muscle, and 2) areas regenerating after an injury would be evident on MR images.

3. MATERIALS AND METHODS

3.1. Animals

The lower limb was studied by MRI in control (C57Bl/10ScSn) and *mdx* mice aged 2 - 2.5 months. Maintenance and handling of animals was carried out according to the Canadian Council on Animal Care.

Limb muscles from control (n=3) and *mdx* (n=3) mice were examined by cross and longitudinal MR images. Immediately after imaging, one *mdx* mouse was sacrificed by cervical dislocation under anaesthetic, and the posterior compartment muscles (soleus, gastrocnemius, tibialis posterior, plantaris) were frozen for histology.

Mdx (n=8) limb muscles were examined at 0, 1, 2, 3, 4, 7, 9 and 21 days after a crush injury (McGeachie & Grounds, 1987; McIntosh et al., 1994) to the gastrocnemius muscle. The gastrocnemius (rather than the tibialis anterior) was crushed due to the larger size of the muscle and greater ease in positioning it for MR examination. Sutures were placed in the fascia on either side of the crushed muscle for structural reference in MR images, since silk sutures were black in images (Fig 5.2). At least 2 images from different mice were collected at each time point. Two mice were studied at each time point over the entire period, while one mouse was killed at recovery days 0, 1, 2, 4 and 7 immediately after MRI. The posterior compartment muscles of these mice were embedded for histology.

3.2. MRI

MR imaging was performed on a Bruker MSL-X Biospec 7/21 Spectrometer after the method of Grauman et al. (1986). Animals were anaesthetized with ketamine - xylazine (1:1;

0.01cc/10g body weight) and positioned on their stomach with the hindlimb outstretched and gently taped in place. A 1.5 x 2.0cm surface coil was situated directly above the belly of the gastrocnemius muscle. The centre of the coil was positioned over the centre of the crush by careful measurement. The mouse was then placed in the centre of the horizontal bore magnet.

Five to six T2-weighted spin-echoes of each limb were collected which had a matrix size of 256 x 256 (field of view = 3cm x 3cm). The TE times were normally 13.1, 26.2, 39.3, 52.4 and 65.5. Images from the 4th echo are shown (TR=1500). The acquisition time was 28 minutes. Slice thickness was 1mm, with a 1mm gap between slices.

3.3. Histology

The posterior compartment muscles of one uninjured *mdx* mouse and of *mdx* mice allowed to recover for 0, 1, 2, 4 and 7 days after the injury were quickly dissected, placed in Tissue-Tek O.C.T. compound and oriented for cross-sectioning. They were then frozen in isopentane on dry ice at -50° C. The entire muscle block was sectioned (6μm sections) serially onto glass slides, making note of any lost sections. The sections were then stained with Hemotoxylin and Eosin (H&E). Using this method, we were able to roughly determine the extent of the crush and of dystrophic lesions in cross sections.

4. RESULTS

Mice could be placed in the magnet multiple times under anaesthetic with no obvious detrimental effects. This allowed monitoring of two *mdx* mice over the entire pre-crush and

recovery period. Examination time could not exceed 2 hours in duration, at which time mice came out of the anaesthetic.

4.1. Control and *mdx* images

Discrimination of individual muscles was possible in longitudinal images of control and mdx hindlimb muscles (Fig 5.1a & 5.1b). The soleus muscle was identified as a thin strip in the midline running from the Achilles tendon to the triangular area of the popliteal fossa (white area). The gastrocnemius surrounds this muscle superficially, laterally and medially. In addition, the hamstring muscles were viewed above and attaching on either side of the popliteal area. Control and *mdx* muscles appeared relatively homogenous in longitudinal section.

Individual muscles were harder to discriminate in cross sectional images of control and *mdx* hindlimb (Fig 5.1c & 5.1d). The cavity of the tibia was clearly identified. No fat was present in bone marrow inside the cavity of the tibia at this age in the mice. Control images of muscle were homogenous, while *mdx* images of the same muscles appeared inhomogeneous. Focal areas of high signal intensity were observed in *mdx* muscle (Fig 5.1d, arrows). Histological sections of the posterior compartment muscles from this mouse showed dystrophic lesions (Figs 5.3a & 5.3b) corresponding to the lighter intensity areas, which extended approximately over the 1mm thickness of the MRI slice (about 140, 6μm sections). There was little or no adipose tissue in the *mdx* muscle sections, although subcutaneous fat and popliteal tissues did show up in MRIs.

4.2. Images from crush-injured muscles

The extent of the crush-injury could be viewed both in longitudinal and cross-sectional MR images (Fig 5.2; arrows) as high-intensity areas, likely due to edema at the injury site soon after crush. There was little difference between the injured areas at 1 and 2 days post crush-injury. However, by 3 days post-crush, the extent of the injured area had decreased and was a bright shell around a darker central region, suggesting that edema resolves rapidly with phagocytosis of the crush site. This continued over 4, 7 and 9 days, until at 21 days (Fig 5.2 bottom) the injured area could hardly be distinguished on the image. Small focal areas of high intensity were observed in the parts of the limb not directly affected by the injury, and were once again consistent with dystrophic lesions on histological examination. The histological features of the crush-injured area were as previously reported (McIntosh et al., 1994). A section from the crush-injured muscle after 2 days of recovery is shown (Fig 5.3c).

5. DISCUSSION

This is the first study to report that the extent of dystrophic and imposed lesions can be localized and assessed by MRI of *mdx* muscles. Results are confirmed by histological observation of tissues from identical muscles. These proton images of skeletal muscle should allow precise localization of dystrophic and regenerating foci for studies by *in vivo* magnetic resonance spectroscopy.

The method of quantifying percent fat infiltration is reliable and helps to determine

the severity of advanced disease (Murphy et al., 1986; Phoenix et al., 1996). However, visual grading techniques are probably not rigorous enough to distinguish between small differences in muscle composition, such as may be found in response to treatment. Eventually it is hoped that treatment will occur before adipose deposition occurs in DMD. Therefore, mapping *mdx* dystrophy, which has no interfering adipose tissue, is an important step to the overall goal of monitoring treatment changes in early DMD. The presence of dystrophic lesions was not reported in any MRI studies of DMD patients, probably because dystrophy was examined in advanced stages. In addition, it is difficult to confirm the meaning of MRI visible changes in DMD without biopsy analysis of the area sampled by magnetic resonance.

Not only can dystrophic areas be identified by MRI, but the extent of an imposed injury can also be visualized. Dystrophic lesions include degenerating myofibers, phagocytic cells, proliferating muscle precursor cells and fusing myoblasts at many different stages. Alternatively, a crush-injury allows study of a synchronous muscle repair sequence, and has been well-characterized (i.e. McGeachie & Grounds, 1987; Grounds & McGeachie, 1992; McIntosh et al., 1994; Pernitsky et al., 1996). Therefore, localization of the injury can now be used in conjunction with magnetic resonance spectroscopy (MRS). Spectra should be interpreted based on the predominant event at the particular time point examined (i.e. degeneration and inflammation at 0-1 days; muscle precursor cell proliferation at 2 and 3 days; fusion into myotubes at 4-7 days; normal phenotype with centrally-nucleated fibers at 21 days).

Ideally, spectroscopic imaging would have been performed on the localized crush-injured dystrophic muscles. Spectroscopic imaging divides an area of interest into small voxels (2.5 x 2.5mm), resulting in a proton spectral map of the area of interest. Theoretically, spectra from: 1) dystrophic lesions, 2) muscle regenerating after an imposed injury, and 3) normal muscle could be obtained during one imaging session of a single animal. We performed many trials in an attempt at these ends. The best result is shown in Figure 5.4. This took 46 minutes and resulting spectra were not informative. Spectra were very noisy, making peak assignment and quantification impossible. Spectral resolution should be possible at this magnetic field strength *in vivo*. However, it was concluded that the receiver coil was not of an appropriate size for examination of mouse limbs (i.e. it was too large). The result was poor signal to noise. In addition, suppression of the large lipid signal spanning the 1.3 ppm area should be used in order to visualize the smaller metabolite peaks (e.g. taurine). The potential of this method is obvious and will be pursued.

This study provides a baseline for further magnetic resonance imaging and spectroscopy studies of dystrophy. The ability to non-invasively follow the progression of *mdx* dystrophy and treatment effects should prove very informative. Although subject muscles will be larger, it remains to be seen whether dystrophic lesions will be resolved in lower field clinical strength magnets.

Acknowledgements: These studies were performed at the *In vivo* NMR Lab, University of Manitoba. Thanks to Dr. Richard Buist for assistance and expertise in MR imaging.

middle area in Fig 5.2d). Small muscle precursors and inflammatory cells can be viewed invading the area. The fibrotic region which seems to separate the histological section in the top middle part of the photo is faintly observed in the image. Bar = 200μm.

FIGURE 5.4: A result of one spectroscopic imaging trial.

a) The crushed area is indicated by the arrow. This image is inverted compared to Figures 5.1 and 5.2.

b) The left top panel shows the muscle divided into small voxels from which spectra were acquired. The spectrum at the bottom is the best result and is from the encircled voxel in the upper left panel. A broad lipid signal is present between 0 and 2 ppm, while another broad signal is present at around 3 ppm. This is the area where the taurine and creatine peaks appeared in *ex vivo* and extract muscle spectra. These peaks cannot be assigned in this spectrum.

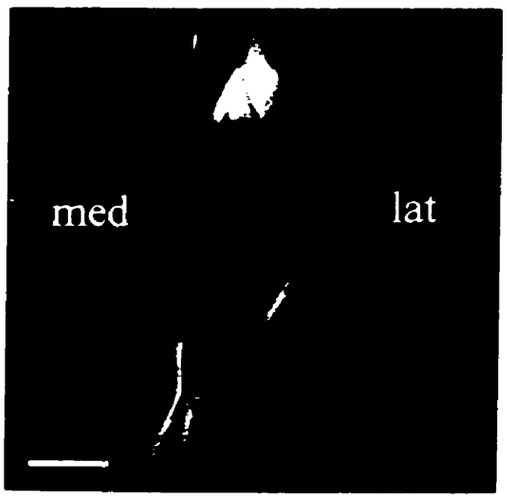

a) control

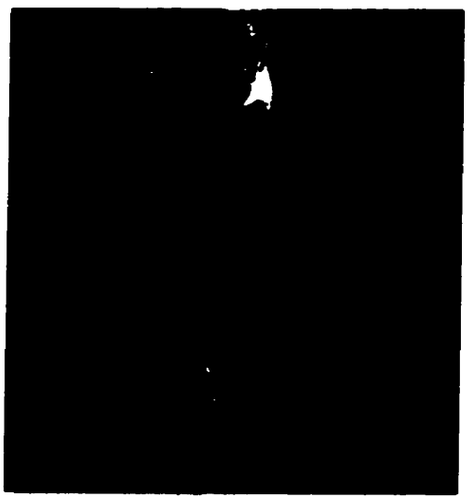

b) mdx

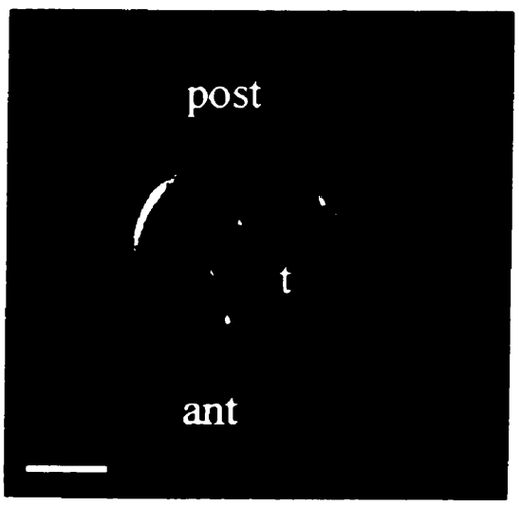

c) control

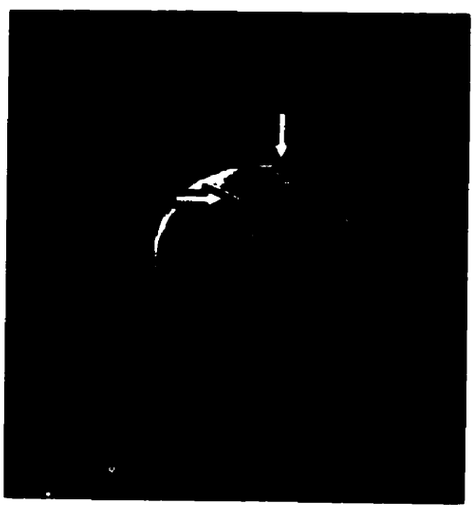

d) mdx

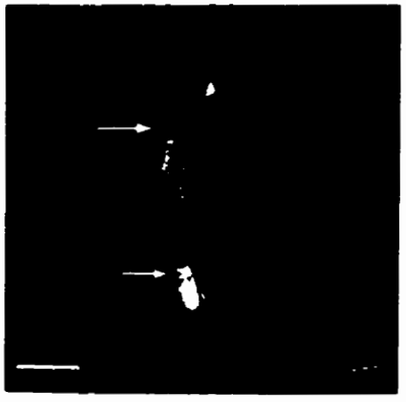

a) 1d recovery

b) 2d recovery

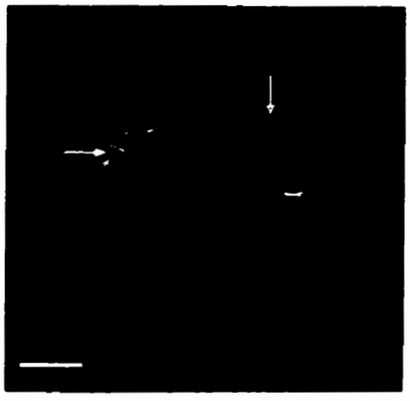

c) 1d recovery

d) 2d recovery

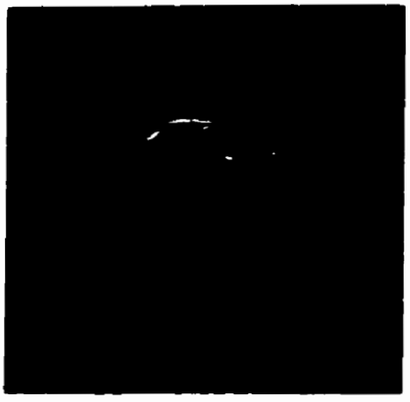

d) 3d recovery

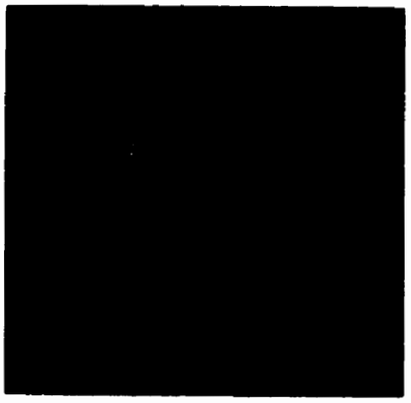

e) 21d recovery

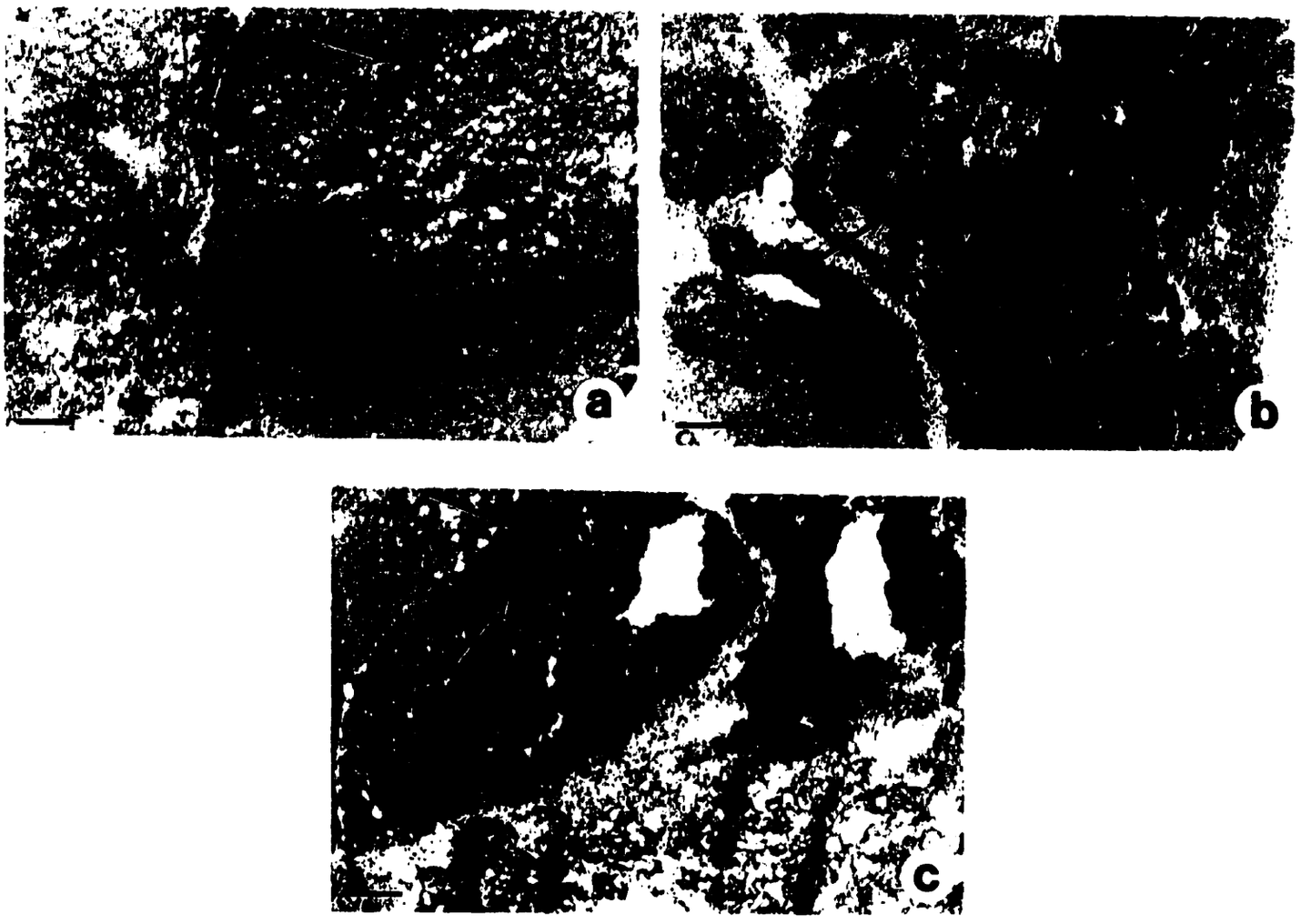
a
b
c

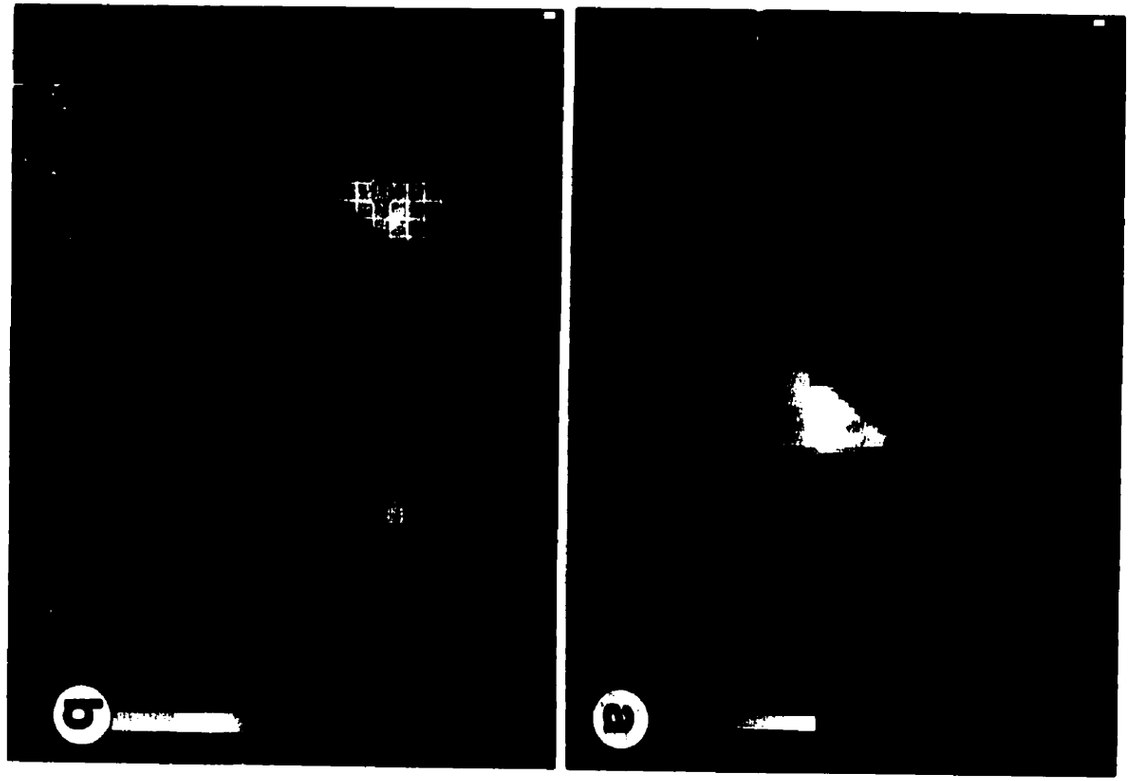
a
b

CHAPTER 6

GENERAL DISCUSSION

1. SUMMARY

This work provides strong indication of the potential of 1-H NMR spectroscopy for characterizing and monitoring disease states. Together, *ex vivo* (Chapters 2 and 3), *in vitro* (Chapter 4), and *in vivo* (Chapter 5) approaches of NMR helped to elucidate the metabolism of living normal control and dystrophic *mdx* muscle tissue. Each approach gives different and unique information that, when integrated, provide a unique view of the disease of muscular dystrophy. The studies reported in each chapter lay crucial groundwork for *in vivo* spectroscopy of dystrophic tissue.

The data reported in Chapter 2 provide a 1-H NMR profile of normal and *mdx* muscle during growth and dystrophy. It was concluded that *ex vivo* 1-H NMR differentially discriminates: 1) normal control and *mdx* dystrophic muscle, 2) developmental stages in normal growth, 3) the three stages of *mdx* dystrophy, and 4) mild and severe dystrophic muscle phenotypes. Of particular interest was the finding that the *mdx* phenotype was identified before the onset of histologically evident dystrophic necrosis. Spectral features which contributed to the discrimination of *mdx* muscle were correlated to the phenotype of the muscle by histological measures of accumulated muscle repair. Information obtained from this study allowed standardization of a typical dystrophic spectrum against the expected normal population at that age, and a number of possible peaks were suggested for further examination (see Chapter 2; Table 2.1). These included peaks due to proton resonances of the free intracellular amino acid taurine.

The data reported in Chapter 3 indicate that treatments in dystrophic muscle can be

2. METHOD OF SPECTRAL ANALYSIS

2.1. Peak height and area measurements

Ex vivo studies were not concerned with detailed assignments of metabolites, but rather on detecting any spectral characteristics which could mark growth, the progression of dystrophy, and regeneration (including treatment effects) (Chapters 2 & 3). A reliable and reproducible method of quantification was established (see Chapter 2). Area measurements from *ex vivo* 1-H NMR spectra were semi-quantitative, since the spectral dispersion and resolution of separate peaks were quite low, and quantification of individual metabolites was difficult. The "area of signal groups" (A1, A2, etc) with contributions from more than one metabolite (corrected for amount of tissue and intensity of the reference; suggested by Kuesel et al., 1992) was measured in *ex vivo* spectra. Since all samples were obtained and handled in exactly the same manner in tissue studies, the clear differences found in area signals were real and were interpreted in terms of differences in cellular composition and metabolism. Peak heights were also measured in the *ex vivo* studies because the peaks of interest overlapped with adjacent peaks. Peak height is a valid alternative for quantifying isolated resonances, although it does not correlate to metabolite concentration. In conclusion, although the *ex vivo* data are semi-quantitative, they reliably characterized different treatment groups, stages of dystrophy, and strains (control vs. *mdx*), and were supported by data from 1-H NMR studies of extracts.

1-H NMR spectra of PCA extracts (Chapter 4) of control and *mdx* muscle allowed much more detailed assignments. In contrast with *ex vivo* spectra, signal intensity in extract

spectra varies directly with concentration (Nakajima et al., 1994). Therefore, after correcting for tissue mass, intensity of the reference solution and number of protons contributing to the peak, the area under the peak represents metabolite concentration. Peak areas are more sensitive to changes since they take into account the entire area of the peak (not an average of a doublet, for example, as in height measurements). Thus, it is felt that the changes observed in the extract studies were almost entirely due to changes in concentrations of isolated assigned peaks (i.e. taurine and carnitine). Animal strains and treatment groups were discriminated in this manner.

2.2. Linear discriminant analysis (LDA)

It is often difficult to extract relevant and important biological information from a complex spectrum; this results in only a fraction of available information being used in a given typical analysis. LDA of an entire spectrum decreases the emphasis on individual peak height and area analyses in interpretation and quantification, and may extract valuable information that is not obvious on visual inspection. LDA is therefore proposed as a faster and more reliable method for diagnostic applications (Shaw et al., 1995).

In these studies, LDA was successful in separating: 1) control from *mdx* tissue, 2) the phases of dystrophy, and 3) treatment groups in the dystrophic muscles (LTA), and to a lesser extent in the crushed muscle (RTA) and the diaphragm (DIA). In general, the conclusions from analyzing peak height and area measurements corresponded with LDA findings. In Chapter 3, we were able to determine the exact regions the algorithm used for discrimination. Interestingly, the taurine resonance was used in the LDA to discriminate

treatment effects in the DIA. Recall that peak height and area measurements were not successful in finding treatment effects in *ex vivo* DIA spectra. Therefore, the method of LDA appears to be more specific and sensitive than peak height/area measurements in distinguishing changes in the DIA with treatment.

However, it is not recommended that LDA be used in isolation. First, it is not yet known if slight variations in spectra monitored by LDA correlate to improved muscle function, although they do correlate to improved phenotype (Anderson et al., 1996b). This is important to determine, especially if the goal is to treat very young DMD patients, before they achieve the milestone of full mobility. Second, false positive results could easily be acquired by LDA due to ignorance of the investigator. Spectra must be aligned and phased in exactly the same manner, otherwise seemingly minute differences in processing can mask real information in spectra and dominate LDA classifications. Therefore, although time consuming, peak height and area measurements, including the determination of concentration values where possible, should be performed to gain insight on disease processes. In this way, specific metabolic and pharmaceutical interventions can be made in attempts to improve particular aspects of disease phenotype.

3. SPECIFICITY OF 1-H NMR IN MONITORING REPAIR CAPACITY

The results reported here focus on monitoring muscle repair. It is hypothesized that the significant peaks (especially taurine resonances) would be effective in monitoring muscle repair in any circumstance. The evidence suggests that the differences found

between control and *mdx* animals were due not only to the degeneration in dystrophy, but also to the regenerative process that continuously occurs in *mdx* animals. Further to this, effective accumulated repair was monitored after glucocorticoid treatment in *mdx* animals and following the imposed crush-injury in both control and *mdx* tissue.

Recent studies from the laboratory (Anderson et al., 1996a) show that *ex vivo* 1-H NMR monitors repair capacity in mice which lack the muscle regulatory factor MyoD (see Chapter 1, section 2.3 for a review of the MRFs), as well as in mice which lack both MyoD and dystrophin (mdx:MyoD-/-). In the double mutant animals, dystrophy is more severe and repair after a crush injury is less compared to *mdx* mice. However, repair is better in the double mutants than in MyoD-/- mice. Levels of taurine peaks again correspond with accumulated repair and increase with successful regeneration (myotube fusion) post-crush (i.e. taurine levels are ranked in order: *mdx*>double mutants>MyoD-/-). Other peaks decrease over the same range of groups.

Therefore, 1-H NMR monitors specific changes in the biochemistry of muscle regeneration which reflect phenotypic and genotypic alterations. Study of other neuromuscular disorders is necessary (with and without repair) to test the spectral specificity of markers for muscle regeneration in other disease states, or even general soft tissue repair.

4. RECOMMENDATIONS FOR FURTHER STUDIES

A set of peaks consistently showed statistical significance through different aspects

and experiments of the various 1-H NMR studies. These findings should prove valuable in possible monitoring of DMD by 1-H NMR. Changes in taurine resonances (heights and areas 2 and 3 in *ex vivo* studies and the concentration of taurine in 1-H NMR of extracts) were consistent markers for: 1) *mdx* muscle, 2) accumulated muscle repair over the course of *mdx* dystrophy, 3) positive treatment effects, 4) regenerating muscle, and 5) differential dystrophic phenotypes (limb vs. DIA). It is suggested that high taurine is an indicator of high levels of accumulated muscle repair, a very important factor for glucocorticoid-treatment. In addition, results indicate that taurine is decreased during proliferation and increases during myoblast fusion into myotubes. Therefore, it is suggested that the success of both long- and short-term repair can be monitored after treatment by careful analysis of taurine peaks over time. Since it is difficult to provide external references *in vivo*, the ratio of taurine to creatine (HT2/HT4 - Chapter 3; Fig 3.4) may also be a valuable measure of treatment effects. HT2/HT4 was consistently different across groups in all aspects of the studies.

The regulation of muscle metabolism and the relationship between metabolism and other cellular processes (i.e. regeneration) are very complex and cannot be duplicated *in vitro* or *ex vivo*. Therefore, in the future, it will be very important to characterize the taurine profile by 1-H NMR in *mdx* muscle *in vivo*. Once a more suitable coil is built for examining the limb of mice, spectroscopic imaging should prove invaluable for the chronological monitoring of regenerating control and *mdx* muscle (with and without treatments). At each time-point studied, dystrophic lesions and unaffected muscle could also be examined. Timely completion of these studies is an important goal.

5. RELEVANCE TO THE CLINICAL SETTING

Magnetic resonance spectroscopy of *ex vivo* samples and of extracts from animal models of disease can provide complementary information on metabolic processes which will aid in the interpretation of results of clinical studies *in vivo* (Sze & Jardetzky, 1994). However, high resolution NMR spectroscopy requires high field strengths in order to obtain good spectral resolution and sensitivity. Most clinical magnets are 1.5T (human volunteers have been placed in 4T experimental magnets), and the overlap of peaks in 1-H spectra is quite severe. Additionally, quantification of peaks *in vivo* poses a problem: most data is analyzed in the form of relative resonance ratios. Automated pattern recognition methods, such as LDA, may be the answer.

31-Phosphorus NMR is a well-established research tool for studying human muscle metabolism at low field strengths (Kent-Braun et al., 1994). However, only a handful of 1-H NMR studies of skeletal muscle have been performed *in vivo*, and focus on detecting changes in large lipid resonances due to disease (see Chapter 1, section 4.3). Proton NMR is the dominant spectroscopic modality for studying human brain, and at 2.1T, resolution of creatine, lactate, glutamate, glutamine, alanine, choline and taurine is possible (reviewed by Howe et al., 1993; Rothman, 1994). Therefore, further low-field studies of human skeletal muscle are warranted and feasible.

Mdx limb muscle exhibits very little adipose or fibrotic tissue (Dangain & Vrbova, 1984; Anderson et al., 1987). Therefore, these studies on *mdx* muscle are very relevant to DMD because it is important to begin treatment before the secondary effects of fibrosis or

adipose tissue deposition predominate. Very young children, in whom manual muscle strength testing is difficult, have the most to gain from glucocorticoid treatment. 1-H NMR spectroscopy is a promising tool by which to monitor any significant improvement. It is hoped that taurine peaks (and possibly HT2/HT4) will discriminate treatment effects in human patients.

Motion in the magnet distorts spectral acquisition, and small children would need to be sedated for spectroscopic evaluation. Sedation is routine for CT and MRI scans in children, with few side-effects (Vade et al., 1995). For examination of arms and legs, a magnet with a small bore (0.3 - 0.4 m in diameter) may suffice. This could also be used for the examination of human babies and smaller animals.

Of some concern in the clinical setting are negative health hazards of repeated exposure to magnetic fields, although, there are as yet no clearly documented ill-effects of low magnetic fields on humans (reviewed by Andrew, 1994). Minor episodes of nausea have been reported, possibly associated with motion of fluids in the inner ear in a magnetic field. Ferromagnetic objects, such as metallic implants, hemostatic clips, scissors and pens are dangerous, since they are easily attracted to the magnet and may move in position. Patients with pacemakers are not allowed in or near the magnet since the radiofrequency radiation may disturb the function. It is the practice to exclude women from MR testing during the first trimester of pregnancy, but there is no evidence that the embryo is sensitive (Evans et al., 1993). Despite some cautions, 1-H NMR offers a unique possibility for non-invasive evaluation of muscle biochemistry *in vivo*.

6. CONCLUSION

The present studies contribute valuable new information on the objective discriminating power of 1-H NMR to classify muscle repair status. These exciting results support the overall hypotheses that 1-H NMR spectroscopy is an alternative to conventional histology in monitoring the progression of *mdx* dystrophy and beneficial treatments on *mdx* dystrophy. Until now, muscle strength testing and biopsies were the only methods for clinically evaluating treatment. It is anticipated that the present findings will be significant factors in establishing a niche for 1-H NMR spectroscopy in monitoring DMD and treatment effects in the context of successful muscle repair.

REFERENCES

Acsadi G, Dickson G, Love DR, Jani A, Walsh FS, Gurusinghe A, Wolff JA, Davies KE: Human dystrophin expression in *mdx* mice after intramuscular injection of DNA constructs. *Nature*, 352: 815-818, 1991.

Acsadi F, Lochmuller H, Jani A, Huard J, Massie B, Prescott S, Simoneau M, Petrof B, Karpati G: Dystrophin expression in muscles of *mdx* mice after adenovirus-mediated *in vivo* gene transfer. *Hum Gene Ther*, 7: 129-140, 1996.

Airaksinen EM, Paljärvi L, Partanen J, Collan Y, Laakso R, Pentikäinen T: Taurine in normal and diseased human skeletal muscle. *Acta Neurol Scand*, 81: 1-7, 1990.

Alger JR: Spatial localization for *in vivo* magnetic resonance spectroscopy: Concepts and commentary in NMR in Physiology and Biomedicine (RJ Gillies, ed). Academic Press, Toronto, pp 151-167, 1994.

Allen RE, Rankin LL: Regulation of satellite cells during skeletal muscle growth and development. *Proc Soc Exp Biol Med*, 194: 81-86, 1990.

Anderson JE, Ovalle WK, Bressler BH: Electron microscopic and autoradiographic characterization of hindlimb muscle regeneration in the *mdx* mouse. *Anat Rec*, 219: 243-257, 1987.

Anderson JE, Bressler BH, Ovalle WK: Functional regeneration in the hindlimb skeletal muscle of the *mdx* mouse. *J Mus Res Cell Motil*, 9: 499-516, 1988.

Anderson JE: Myotube phospholipid synthesis and sarcolemmal ATPase activity in dystrophic *mdx* mouse muscle. *Biochem Cell Biol*, 69: 835-841, 1991.

Anderson JE, Liu L, Kardami E: Distinctive patterns of basic fibroblast growth factor (bFGF) distribution in degenerating and regenerating areas of dystrophic (*mdx*) striated muscles. *Dev Biol*, 147: 96-109, 1991.

Anderson JE, Kakulas BA, Jacobsen PF, Johnsen RD, Kornegay JN, Grounds MD: Comparison of basic fibroblast growth factor in X-linked dystrophin-deficient myopathies of human, dog and mouse. *Growth Factors*, 9: 107-121, 1993.

Anderson JE, Mcintosh LM, Garrett K, Megeney L, Rudnicki M: The absence of MyoD increases *mdx* mouse dystrophy and reduces muscle repair - in situ hybridization (ISH) and magnetic resonance spectroscopy studies (MRS). *Mol Biol Cell*, 7(S): 468, 1996a.

Anderson JE, McIntosh LM, Poettcker R: Deflazacort but not prednisone improves both muscle repair and fiber growth in diaphragm and limb muscle *in vivo* in the *mdx* dystrophic mouse. *Muscle Nerve*, 19: 1576-1585, 1996b.

Andrew ER: Introduction to NMR in NMR in Physiology and Biomedicine (RJ Gillies, ed). Academic Press, Toronto, pp 1-23, 1994.

Angelini C, Pegoraro E, Turella E, Intino MT, Pini A, Costa C: Deflazacort in Duchenne dystrophy: Study of long-term effect. *Muscle Nerve*, 17: 386-391, 1994.

Argov A, Bank WJ: Phosphorus magnetic resonance spectroscopy (31-P MRS) in neuromuscular disorders. *Ann Neurol*, 30: 90-97, 1991.

Arús C, Bárány M, Westler WM, Markley JL: ^{1}H NMR of intact muscle at 11T. *FEBS*, 165: 231-237, 1984a.

Arús C, Bárány M, Westler WM, Markley JL: Proton nuclear magnetic resonance of human muscle extracts. *Clin Physiol Biochem*, 2: 49-55, 1984b.

Arús C, Bárány M: Application of high-field ^{1}H-NMR spectroscopy for the study of perifused amphibian and excised mammalian muscles. *Biochim Biophys Acta*, 886: 411-424, 1986.

Bárány M, Venkatasubramanian PN, Mok E, Siegel IM, Abraham E, Wycliffe ND, Mafee NF: Quantitative and qualitative fat analysis in human leg muscle of neuromuscular diseases by ^{1}H MR spectroscopy *in vivo*. *Magn Reson Med*, 10: 210-226, 1989.

Baskin SI, Dagirmanjian R: Possible involvement of taurine in the genesis of muscular dystrophy. *Nature*, 245: 464-465, 1973.

Beilharz MW, Lareu RR, Garrett KL, Grounds MD, Fletcher S: Quantitation of muscle precursor cell activity in skeletal muscle by northern analysis of MyoD and myogenin expression: Application to dystrophic (*mdx*) mouse muscle. *Mol Cell Neurosci*, 3: 326-331, 1992.

Bell JD, Preece NE, Parkes HG: NMR studies of body fluids and tissue extracts in NMR in Physiology and Biomedicine (RJ Gillies, ed). Academic Press, Toronto, pp 221-236, 1994.

Berthillier G, Eichenberger D, Carrier HN, Guibaud P, Got R: Carnitine metabolism in early stages of DMD. *Clin Chim Acta*, 122: 369-375, 1982.

Bhagwati S, Ghatpande A, Shafiq SA, Leung B: In situ hybridization analysis for expression of myogenic regulatory factors in regenerating muscle of *mdx* mouse. *J Neuropathol Exp*

Neurol, 55: 509-514, 1996.

Bieber FR, Hoffman EP: Duchenne and Becker muscular dystrophies: Genetics, prenatal diagnosis, and future prospects. *Clin Perinatol*, 17: 845-865, 1990.

Bloch G, Jouvensal L, Carlier PG: ^{1}H NMR determination of lactate ^{13}C-enrichment in skeletal muscle: Using a double quantum filter for the simultaneous editing of ^{13}C-coupled and ^{13}C-uncoupled methyl protons resonance. *Magn Reson Med*, 34: 353-358, 1995.

Bober E, Lyons GE, Braun T, Cossu G, Buckingham M, Arnold HH: The muscle regulatory gene, Myf-6, has a biphasic pattern of expression during early mouse development. *J Cell Biol*, 113: 1255-1265, 1991.

Bongers H, Schick F, Skalej M, Jung WI, Stevens A: Localized *in vivo* ^{1}H spectroscopy of human skeletal muscle: normal and pathological findings. *Magn Reson Imaging*, 10: 957-964, 1992.

Braun T, Rudnicki MA, Arnold HH, Jaenisch R: Targeted inactivation of the muscle regulatory gene Myf-5 results in abnormal rib development and perinatal death. *Cell*, 71: 369-382, 1992.

Brière KM, Kuesel AC, Bird RP, Smith ICP: ^{1}H MR visible lipids in colon tissue from normal and carcinogen-treated rats. *NMR Biomed*, 8: 33-40, 1995.

Brooke MH, Fenichel GM, Griggs RC, Mendell JR, Moxley R, Florence J, King WM, Pandya S, Robison J, Schierbecker J, Signore L, Miller JP, Gilder BF, Kaiser KK, Mandel S, Arfken C: Duchenne muscular dystrophy: Patterns of clinical progression and effects of supportive therapy. *Neurol*, 39: 475-481, 1989.

Bulfield G, Siller W, Wight P, Moore K: X-chromosome linked muscular dystrophy (*mdx*) in the mouse. *Proc Natl Acad Sci USA*, 81: 1189-1192, 1984.

Burt CT, Koutcher J, Roberts JT, London RE, Chance B: Magnetic resonance spectroscopy of the musculoskeletal system. *Radiol Clinics North America*, 24: 321-331, 1986.

Callies R, Sri-Pathmanathan RM, Ferguson DYP, Brindle KM: The appearance of neutral lipid signals in the ^{1}H NMR spectra of a myeloma cell line correlates with the induced formation of cytoplasmic lipid droplets. *Magn Reson Med*, 29: 546-550, 1993.

Camiña F, Novo-Rodriguez MI, Rodriguez-Segade S, Castro-Gago M: Purine and carnitine metabolism in muscle of patients with Duchenne muscular dystrophy. *Clin Chim Acta*, 243: 151-164, 1995.

Carlson BM, Faulkner JA: The regeneration of skeletal muscle fibers following injury: a review. *Med Sci Sports Exerc*, 15: 187-198, 1983.

Carnwath JW, Shotton DM: Muscular dystrophy in the *mdx* mouse: histopathology of the soleus and extensor digitorum longus muscles. *J Neurol Sci*, 80: 39-54, 1987.

Carroll JE, Villadrego A, Brooke MH: Increased long-chain acyl CoA in Duchenne muscular dystrophy. *Neurol*, 33: 1507-1510, 1983.

Cazzaniga S, Schold SC, Sostman HD, Charles HC: Effects of therapy on the ^{1}H NMR spectrum of a human glioma line. *Magn Reson Imag*, 12: 945-950, 1994.

Chesney RW: Taurine: Its biological role and clinical implications. *Adv Pediat*, 32: 1-42, 1985.

Chinet AE, Even PC, Decrouy A: Dystrophin-dependent efficiency of metabolic pathways in mouse skeletal muscles. *Experientia*, 50: 602-605, 1994.

Czyzewski K, Stern LZ, Sadeh M, Bahl JJ: Changes in muscle carnitine during regeneration. *Ann Neurol*, 14: 126, 1983.

Dangain J, Vrbova G: Muscle development in mdx mutant mice. *Muscle Nerve*, 7: 700-704, 1984.

Davis HL, Jasmin BJ: Direct gene transfer into mouse diaphragm. *FEBS*, 333: 146-150, 1993.

Decrouy A, Even PC, Chinet A: Decreased rates of Ca^{2+}-dependent heat production in slow- and fast-twitch muscles from dystrophic (*mdx*) mouse. *Experientia*, 49: 843-849, 1993.

Dekhuijzen PNR, Gayan-Ramirez GG, deBoch V, Dom R, Decramer M: Triamcinolone and prednisolone affect contractile properties and histopathology of rat diaphragm differently. *J Clin Invest*, 92: 1534-1542, 1993.

Dekhuijzen PNR, Gayan-Ramirez GG, Bisschop A, deBock V, Dom R, Bouillon R, Decramer M: Rat diaphragm contractility and histopathology are affected differentially by low dose treatment with methylprednisolone and deflazacort. *Eur Respir J*, 8: 824-830, 1995.

DeLuca A, Camerino DC, Failli P, Franconi F, Giotti A: Effects of taurine on mammalian skeletal muscle fibers during development. *Prog Clin Biol Res*, 351: 163-173, 1990.

Derome AE: Modern NMR Techniques for Chemistry Research. Pergamon Press, Toronto, chapters 1-3, 1987.

Dhoot GK, Pearce GW: Transformation of fibre types in muscular dystrophies. *J Neurol Sci*, 65: 17-28, 1984.

DiMario J, Buffinger N, Yamada S, Strohman RC: Fibroblast growth factor in the extracellular matrix of dystrophic (*mdx*) mouse muscle. *Science*, 244: 688-690, 1989.

Dunckley MG, Wells DJ, Walsh FS, Dickson G: Direct retroviral-mediated transfer of dystrophin minigene into *mdx* mouse muscle *in vivo*. *Hum Mol Genet*, 2: 717-723, 1993.

Dunn JF, Frostick S, Brown G, Radda GK: Energy status of cells lacking dystrophin: an *in vivo - in vitro* study of *mdx* mouse skeletal muscle. *Biochim Biophys Acta*, 106: 115-120, 1991.

Dunn JF, Radda GK: Total ion content of skeletal and cardiac muscle in the *mdx* mouse dystrophy: Ca^{2+} is elevated at all ages. *J Neurol Sci*, 103: 226-231, 1991.

Dunn JF, Tracey I, Radda GK: A ^{31}P-NMR study of muscle exercise metabolism in *mdx* mice: evidence for abnormal pH regulation. *J Neurol Sci*, 113: 108-113, 1992.

Dunn JF, Tracey I, Radda GK: Exercise metabolism in Duchenne muscular dystrophy: a biochemical and ^{31}P-nuclear magnetic resonance study of *mdx* mice. *Proc R Soc Lond B*, 251: 200-206, 1993.

Dupont-Versteegden EE, McCarter RJ: Differential expression of muscular dystrophy in diaphragm versus hindlimb muscles of *mdx* mice. *Muscle Nerve*, 15: 1105-1110, 1992.

Durelli L, Matani R, Fassio F: The treatment of myotonia: evaluation of chronic oral taurine therapy. *Neurol*, 33: 559-603, 1983.

Edwards RHT, Dawson MJ, Wilkie DR, Gordon RE, Shaw D: Clinical use of nuclear magnetic resonance in the investigation of myopathy. *Lancet*, 1(i): 725-731, 1982.

Engel AG, Banker BQ, Eiben RM: Carnitine deficiency: clinical, morphological, and biochemical observations in a fatal case. *J Neurol Neurosurg Psychiatry*, 40: 313-322, 1977.

Evans JA, Savitz DA, Kanal E, Gillen J: Infertility and pregnancy outcome among magnetic resonance imaging workers. *JOM*, 35: 1191-1195, 1993.

Even PC, Decrouy A, Chinet A: Defective regulation of energy metabolism in *mdx*-mouse

skeletal muscle. *Biochem J*, 304: 649-654, 1994.

Fenichel GM, Florence JM, Pestronk A, Mendell JR, Moxley RT, Griggs RD, Brooke MH, Miller JP, Robison J, Wing W, Signore L, Pandya S, Schierbecker J, Wilson B: Long-term benefits from prednisone therapy in Duchenne muscular dystrophy. *Neurol*, 41: 1874-1877, 1991.

Garlick PB, Maisey MN: Magnetic resonance spectroscopy. *Br J Hosp Med*, 47: 330-335, 1992.

Garrett KL, Anderson JE: Colocalization of bFGF and the myogenic regulatory gene myogenin in dystrophic *mdx* muscle precursors and young myotubes *in vivo*. *Dev Biol*, 169: 596-606, 1995.

Gillet B, Doan BT, Verré-Sébrié C, Barbere B, Berenger G, Morin S, Koenig J, Peres M, Sébille A, Beloeil JC: *In vivo* 2D ^{1}H-NMR of *mdx* mouse muscle and myoblast cells during fusion: evidence for a characteristic signal of long chain fatty acids. *Neuromusc Disord*, 3: 433-438, 1993.

Gillet B, Verré-Sébrié C, Lefaucheur JP, Sébille A, Beloeil JC: Time course of muscular regeneration assessed by 1H 2D NMR. *Proc Soc Magn Reson*, 3: 1870, 1995.

Grauman R, Oppelt A, Stetter E: Multiple spin-echo imaging with a 2D Fourier method. *Magn Reson Med*, 3: 707-721, 1986.

Greenberg CR, Jacobs HK, Halliday W, Wrogemann K: Three years' experience with neonatal screening for Duchenne/Becker muscular dystrophy: Gene analysis, gene expression, and phenotype prediction. *Am J Med Genet*, 39: 68-75, 1991.

Griffiths RD, Cady EB, Edwards RHT, Wilkie DR: Muscle energy metabolism in Duchenne dystrophy studied by 31-P NMR: Controlled trials show no effect of allopurinol or ribose. *Muscle Nerve*, 8: 760-767, 1985.

Griggs RC, Moxley RT, Mendell JR, Fenichel GM, Brooke MH, Pestronk A, Miller JP, and the Clinical Investigation of Duchenne Dystrophy Group: Prednisone in Duchenne dystrophy: A randomized, controlled trial defining the time course and dose response. *Arch Neurol*, 48: 383-388, 1991.

Grounds MD: Towards understanding skeletal muscle regeneration. *Path Res Prac*, 187: 1-22, 1991.

Grounds MD, McGeachie JK: Skeletal muscle regeneration after crush injury in dystrophic

mdx mice: An autoradiographic study. *Muscle Nerve*, 15: 580-586, 1992.

Grounds MD, Yablonka-Reuveni Z: Molecular and cellular biology of muscle regeneration in Molecular and cellular biology of muscular dystrophy (T. Partridge, ed). Chapman and Hall, London, UK, pp 210-256, 1993.

Gussoni E, Pavlath GK, Lanctot AM, Sharma KR, Miller RG, Steinman L, Blau HM: Normal dystrophin transcripts detected in Duchenne muscular dystrophy after myoblast transplantation. *Nature*, 356: 435-438, 1992.

Hannon K, Smith CK, Bales KR, Santerre RF: Temporal and quantitative analysis of myogenic regulatory and growth factor gene expression in the developing mouse embryo. *Dev Biol*, 151: 137-144, 1992.

Hardiman O, Brown RH, Beggs AH, Specht L, Sklar RM: Differential glucocorticoid effects on the fusion of Duchenne/Becker and control muscle cultures: Pharmacologic detection of accelerated aging in dystrophic muscle. *Neurol*, 42: 1085-1091, 1992.

Hauser MA, Chamberlain JS: Progress towards gene therapy for Duchenne muscular dystrophy. *J Endocrinol*, 149: 373-378, 1996.

Heinriksen O: MR spectroscopy in clinical research. *Acta Radiol*, 35: 96-116, 1994.

Hiatt WR, Regensteiner JG, Wolfel EE, Ruff L, Brass EP: Carnitine and acylcarnitine metabolism during exercise in humans. *J Clin Invest*, 84: 1167-1173, 1989.

Hoffman EP, Brown RH, Kunkel LM: Dystrophin: The protein product of the Duchenne muscular dystrophy locus. *Cell*, 51: 919-928, 1987.

Howe FA, Maxwell RJ, Saunders DE, Brown MM, Griffiths JR: Proton spectroscopy *in vivo*. *Magn Reson Quar*, 9: 31-59, 1993.

Huang Y, Majumdar S, Genant HK, Chan WP, Sharma KR, Yu P, Mynhier M, Miller RG: Quantitative MR relaxometry study of muscle compostition and function in Duchenne muscular dystrophy. *J Magn Reson Imaging*, 4: 59-64, 1994.

Huard J, Bouchard JP, Roy R, Malquin F, Dansereau G, Labrecque C, Albert N, Richard CL, Lemieux B, Tremblay JP: Human myoblast transplantation: Preliminary results of 4 cases. *Muscle Nerve*, 15: 550-560, 1992.

Hudecki MS, Pollina CM, Granchelli JA, Daly MK, Byrnes R, Wang JC, Hsiao JC: Strength and endurance in the therapeutic evaluation of prednisolone-treated *mdx* mice. *Res Comm*

Chem Pathol Pharmacol, 79: 45-60, 1993.

Hurme R, Kalimo H, Lehto M, Jarvinen M: Healing of skeletal muscle injury: an ultrastructural and immunhistochemical study. *Med Sci Sports Exerc*, 23: 801-810, 1991.

Huxtable RJ: Physiological actions of taurine. *Physiol Rev*, 72: 101-163, 1992.

Karczmar G: Imaging, diffusion, perfusion and flow in NMR in Physiology and Biomedicine (RJ Gillies, ed). Academic Press, Toronto, pp 25-42, 1994.

Karpati G, Carpenter S, Prescott S: Small-caliber skeletal muscle fibers do not suffer necrosis in *mdx* mouse dystrophy. *Muscle Nerve*, 11: 795-803, 1988.

Karpati G, Ascadi G: The potential for gene therapy in Duchenne muscular dystrophy and other genetic muscle diseases. *Muscle Nerve*, 16: 1141-1153, 1993.

Kelly FJ, McGrath JA, Goldspink DF, Cullen MJ: A morphological/biochemical study on the actions of corticosteroids on rat skeletal muscle. *Muscle Nerve*, 9: 1-10, 1986.

Kemp GJ, Taylor DJ, Dunn JF, Frostick SP, Radda GK: Cellular energetics of dystrophic muscle. *J Neurol Sci*, 116: 201-206, 1993.

Kent-Braun JA, Miller RG, Weiner MW: Magnetic resonance spectroscopy studies of human muscle. *Radiol Clin North Am*, 32: 313-335, 1994.

Khan MA: Corticosteroid therapy in Duchenne muscular dystrophy. *J Neurol Sci*, 120: 8-14, 1993.

Kissel JT, Burrow KL, Rammohan KW, Mendell JR, and the CIDD Study Group: Mononuclear cell analysis of muscle biopsies in prednisone-treated and untreated Duchenne muscular dystrophy. *Neurol*, 41: 667-672, 1991.

Kissel JT, Lynn DJ, Rammohan KW, Klein JP, Griggs RC, Moxley RT, Cwik VA, Brooke MH, Mendell JR: Mononuclear cell analysis of muscle biopsies in prednisone- and azathioprine-treated Duchenne muscular dystrophy. *Neurol*, 43: 532-536, 1993.

Kuesel AC, Kroft T, Saunders JK, Préfontaine M, Mikhael N, Smith ICP: A simple procedure for obtaining high-quality NMR spectra of semiquantitative value from small tissue specimens: Cervical biopsies. *Magn Reson Med*, 27: 349-355, 1992.

Kuesel AC, Donnelly SM, Halliday W, Sutherland GR, Smith ICP: Mobile lipids and metabolic heterogeneity of brain tumours as detectable by *ex vivo* ^{1}H MR spectroscopy.

NMR Biomed, 7: 172-180, 1994.

Lamminen AE: Magnetic resonance imaging of primary skeletal muscle diseases: Patterns of distribution and severity of involvement. *Br J Radiol*, 63: 946-950, 1990.

Lefaucheur JP, Pastoret C, Sebille A: Phenotype of dystrophinopathy in old *mdx* mice. *Anat Rec*, 242: 70-76, 1995.

LeRumeur E, LeTallec N, Lewa CJ, Ravalec X, deCertaines JD: *In vivo* evidence of abnormal mechanical and oxidative functions in the exercised muscle of dystrophic hamsters by 31-P NMR. *J Neurol Sci*, 133: 16-23, 1995.

Liu GC, Jong YJ, Chiang CH, Jaw TS: Duchenne muscular dystrophy: MR grading with functional correlation. *Radiol*, 186: 475-480, 1993.

Liu M, Chino N, Ishihara T: Muscle damage progression in Duchenne muscular dystrophy evaluated by a new quantitative computed tomography method. *Arch Phys Med Rehabil*, 74: 507-514, 1993.

Louboutin JP, Fichter-Gagnepain V, Thaon E, Fardeau M: Morpometric analysis of *mdx* diaphragm muscle fibres. Comparison with hindlimb muscles. *Neuromusc Disord*, 3: 463-469, 1993.

Louboutin JP, Fichter-Gagnepain V, Pastoret C, Thaon E, Noireaud J, Sebille A, Fardeau M: Morphological and functional study of extensor digitorum longus muscle regeneration after iterative crush lesions in *mdx* mouse. *Neuromusc Disord*, 5: 489-500, 1995.

Lundberg P, Harmsen E, Ho C, Vogel HJ: Nuclear magnetic resonance studies of cellular metabolism. *Analytical Biochem*, 191: 193-222, 1990.

Marshall D, Hailey D, Menon D: Magnetic field strength issues in magnetic resonance imaging. *Can Assoc Radiol J*, 45: 180-184, 1994.

Matsumura K, Nakano I, Fukuda N, Ikehira H, Tateno Y, Aoki Y: Proton spin-lattice relaxation time of Duchenne dystrophy skeletal muscle by magnetic resonance imaging. *Muscle Nerve*, 11: 97-102, 1988.

Matsumura K, Campbell KP: Dystrophin-glycoprotein complex: its role in the molecular pathogenesis of muscular dystrophies. *Muscle Nerve*, 17: 2-15, 1994.

May GL, Wright LC, Holmes KT, Williams PG, Smith ICP, Wright PE, Fox RM, Mountford CE: Assignment of methylene proton resonances in NMR spectra of embryonic and

333: 832-838, 1995.

Mesa LE, Dubrovsky AL, Corderi J, Marco P, Flores D: Steroids in Duchenne muscular dystrophy - Deflazacort trial. *Neuromusc Disord*, 1: 261-266, 1991.

Metzinger L, Passaquin AC, Warter JM, Poindron P: α-Methylprednisolone promotes skeletal myogenesis in dystrophin-deficient and control mouse cultures. *Neurosci Lett*, 155: 171-174, 1993.

Metzinger L, Passaquin AC, Leijendekker WJ, Poindron P, Ruegg UT: Modulation by prednisolone of calcium handling in skeletal muscle cells. *Br J Pharmacol*, 116: 2811-2816, 1995.

Mitchell CA, McGeachie JK, Grounds MD: Cellular differences in the regeneration of murine skeletal muscle: a quantitative histological study in SJL/J and BALB/c mice. *Cell Tiss Res*, 269: 159-166, 1992.

Mizuno Y, Yoshida M, Nonaka I, Hirai S, Ozawa E: Expression of utrophin (dystrophin-related protein) and dystrophin-associated glycoproteins in muscles from patients with Duchenne muscular dystrophy. *Muscle Nerve*, 17: 206-216, 1994.

Mokhtarian A, Even PC: Effect of intraperitoneal injection of glucose on glucose oxidation and energy expenditure in the *mdx* mouse model of Duchenne muscular dystrophy. *Pflügers Arch*, 432: 379-385, 1996.

Moreno A, Rey M, Montane JM, Alonso J, Arús C: ^{1}H NMR spectroscopy of colon tumours and normal mucosal biopsies; Elevated taurine levels and reduced polyethyleneglycol absorption in tumours may have diagnostic significance. *NMR Biomed*, 6: 111-118, 1993.

Moreno A, Arús C: Quantitative and qualitative characterization of 1-H NMR spectra of colon tumours, normal mucosa and their perchloric acid extracts: Decreased levels of myo-inositol in tumours can be detected in intact biopsies. *NMR Biomed*, 8: 33-45, 1996.

Moss FP, Leblond CP: Satellite cells as the source of nuclei in muscles of growing rats. *Anat Rec*, 170: 421-436, 1971.

Mountford CE, Saunders JK, May GL, Holmes KT, Williams PG, Fox RM, Tattersall MHN, Barr JR, Russell P, Smith ICP: Classification of human tumours by high-resolution magnetic resonance spectroscopy. *Lancet*, 651-653, 1986.

Mountford CE, Wright LC: Organization of lipids in the plasma membranes of malignant and stimulated cells: a new model. *TIBS*, 13: 172-177, 1988.

Mountford CE, Delikatny EJ, Dyne M, Holmes KT, Mackinnon WB, Ford R, Hunter JC, Truskett ID, Russell P: Uterine cervical punch biopsy specimens can be analyzed by ^{1}H MRS. *Magn Reson Med*, 13: 324-331, 1990.

Muntoni F, Mateddu A, Marchei F, Clerk A, Serra G: Muscular weakness in the *mdx* mouse. *J Neurol Sci*, 120: 71-77, 1993.

Murphy WA, Totty WG, Carroll JE: MRI of normal and pathologic skeletal muscle. *Am J Roentgenol*, 146: 565-574, 1986.

Nakajima H, Sugie H, Tsurui S, Ito M: Application of 1-H NMR spectroscopy for qualitative measurement of muscle carnitine levels. *Clin Chim Acta*, 224: 81-88, 1994.

Nikulin A, Brière KM, Friesen L, Smith ICP, Somorjai RL: Genetic algorithm-guided optimal attribute selection: a novel preprocessor for classifying magnetic resonance spectra. *Proc Soc Magn Reson*, 3: 1940, 1995.

Ohlendieck K, Campbell KP: Dystrophin-associated proteins are greatly reduced in skeletal muscle from *mdx* mice. *J Cell Biol*, 115: 1685-1694, 1991.

Olson EN: MyoD family: a paradigm for development? *Gene Dev*, 4: 1454-1461, 1990.

Partridge TA: Pathophysiology of muscular dystrophy. *Br J Hosp Med*, 49: 26-36, 1993.

Passaquin AC, Metzinger L, Léger JJ, Warter JM, Poindron P: Prednisolone enhances myogenesis and dystrophin-related protein in skeletal muscle cell cultures from *mdx* mouse. *J Neurosci Res*, 35: 363-372, 1993.

Pastoret C, Sebille A: Time course study of the isometric contractile properties of *mdx* mouse striated muscles. *J Mus Res Cell Motil*, 14: 423-431, 1993.

Pastoret C, Sebille A: Age-related differences in regeneration of dystrophic (*mdx*) and normal muscle in the mouse. *Muscle Nerve*, 18: 1147-1154, 1995.

Peeling J, Sutherland G: High-resolution ^{1}H-NMR spectroscopy studies of extracts of human cerebral neoplasms. *Magn Reson Med*, 24: 123-136, 1992.

Peeling J, Sutherland G: 1-H magnetic resonance spectroscopy of extracts of human epileptic neocortex and hippocampus. *Neurol*, 43: 589-594, 1993.

Penner KAH: An EM study of immonogold-labelled basic FGF in dystrophic *mdx* and normal mouse diaphragm. A Master's thesis, Univerisity of Manitoba, 1993.

Pernitsky AP, Anderson JE: Differential effects of 3,5,3'-triiodothyronine on control and *mdx* myoblasts and fibroblasts: Anaylsis by flow cytometry. *Exp Cell Res*, 227: 214-222, 1996.

Pernitsky AP, McIntosh LM, Anderson JE: Hyperthyroidism impairs early repair in normal but not dystrophic *mdx* mouse tibialis anterior muscle. An *in vivo* study. *Biochem Cell Biol*, 74: 315-324, 1996.

Petersen SB, Muller RN, Rinck PA: The magnetic resonance phenomenon in An Introduction to Biomedical Nuclear Magnetic Resonance (SB Petersen, RN Muller and PA Rinck, eds). Thieme Inc, New York, pp 1-9, 1985.

Petrof BJ, Shrager JB, Stedman HH, Kelly AM, Sweeney HL: Dytrophin protects the sarcolemma from stresses developed during muscle contraction. *Proc Natl Acad Sci*, 90: 3710-3714, 1993a.

Petrof BJ, Stedman HH, Shrager JB, Eby J, Sweeney HL, Kelly AM: Adaptive alterations in myosin heavy chain expression and contractile function in the dystrophic (*mdx*) mouse diaphragm. *Am J Physiol*, 265: C834-C841, 1993b.

Petroff OAC: Biological ^{1}H NMR spectroscopy. *Comp Biochem Physiol*, 90B: 249-260, 1988.

Phoenix J, Betal D, Roberts N, Helliwell TR, Edwards RHT: Objective quantification of muscle and fat in human dystrophic muscle by magnetic resonance imaging analysis. *Muscle Nerve*, 19: 302-310, 1996.

Ragot T, Vincent N, Chafey P, Vigne E, Gilgenkrantz H, Couton D, Caraud J, Briand P, Kaplan JC, Perricaudet M, Kahn A: Efficient adenovirus-mediated transfer of a human minidystrophin gene to skeletal muscle of *mdx* mice. *Nature*, 361: 647-650, 1993.

Rebouche CJ, Engel AG: Kinetic compartmental analysis of carnitine metabolism in the human carnitine deficiency syndromes: Evidence for alterations in tissue carnitine transport. *J Clin Invest*, 73: 857-867, 1984.

Rennie MJ, Ahmed A, Khogali SEO, Low SY, Hundal HS, Taylor PM: Glutamine metabolism and transport in skeletal muscle and heart and their clinical relevance. *J Nutr*, 126: 1142S-1149S, 1996.

Rifai Z, Welle S, Moxley RT, Lorenson M, Griggs RC: Mechanism of action of prednisone in Duchenne dystrophy. *Neurol*, 42: 1428, 1992.

Robertson TA, Maley MAL, Grounds MD, Papadimitriou JM: The role of macrophages in skeletal muscle regeneration with particular reference to chemotaxis. *Exp Cell Res*, 207:

321-331, 1993a.

Robertson TA, Papadimitriou JM, Grounds MD: Fusion of myogenic cells to the newly sealed region of damaged myofibers in skeletal muscle regeneration. *Neuropathol Appl Neurobiol*, 19: 350-358, 1993b.

Rothman DL, Arias-Mendoza F, Shulman GI, Shulman RG: A pulse sequence for simplifying hydrogen NMR spectra of biological tissues. *J Magn Reson*, 60: 430-436, 1984.

Rothman DL: 1-H NMR studies of human brain metabolism and physiology in NMR in Physiology and Biomedicine (RJ Gillies, ed). Academic Press, Toronto, pp 353-372, 1994.

Rudnicki MA, Braun T, Hinuma S, Jaenisch R: Inactivation of MyoD in mice leads to upregulation of the myogenic HLH gene Myf-5 and results in apparently normal muscle development. *Cell*, 71: 383-390, 1992.

Rudnicki MA, Schnegelsberg PNJ, Stead RH, Braun T, Arnold HH, Jaenisch R: MyoD or myf-5 is required for the formation of skeletal muscle. *Cell*, 75: 1351-1359, 1993.

Rudnicki MA, Jaenisch R: The MyoD family of transcription factors and skeletal myogenesis. *Bioessays*, 17: 203-209, 1995.

Rutter A, Hugenholtz H, Saunders J, Smith ICP: Classification of brain tumours by ex vivo ^{1}H NMR spectroscopy. *J Neurochem*, 64: 1655-1661, 1995.

Schick F, Eismann B, Jung WI, Bongers H, Bunse M, Lutz O: Comparison of localized proton NMR signals of skeletal muscle and fat tissue *in vivo*: Two lipid compartments in muscle tissue. *Magn Reson Med*, 29: 158-167, 1993.

Schmalbruch H: The morphology of regeneration of skeletal muscle in the rat. *Tissue Cell*, 8: 673-692, 1976.

Schultz E, Albright DJ, Jaryszak DL, David TL: Survival of satellite cells in whole muscle transplants. *Anat Rec*, 222: 12-17, 1988.

Shaw RA, Kotowich S, Eysel HH, Jackson M, Thomson GTD, Mantsch HH: Arthritis diagnosis based upon the near infrared spectrum of synovial fluid. *Rheumatol Int*, 15: 159-165, 1995.

Shaw RA, Mantsch HH, Anderson JE: Infrared spectroscopy of dystrophic *mdx* mouse muscle tissue distinguishes among treatment groups. *J Appl Physiol*, 81: 2328-2335, 1996.

Shen D, Gregory CD, Dawson MJ: Observation and quantitation of lactate in oxidative and glycolytic fibers of skeletal muscles. *Magn Reson Med*, 36: 30-38, 1996.

Sicinski P, Geng Y, Ryder-Cook AS, Barnard EA, Darlinson MG, Barnard PJ: The molecular basis of muscular dystrophy in the *mdx* mouse: A point mutation. *Science*, 244: 1578-1580, 1989.

Sklar RM, Brown RH: Methylprednisolone increases dystrophin levels by inhibiting myotube death during myogenesis of normal human muscle in vitro. *J Neurol Sci*, 101: 73-81, 1991.

Sklar RM, Hudson A, Brown RH: Glucocorticoids increase myoblast proliferation rates by inhibiting death of cycling cells. *In Vitro Cell Dev Biol*, 27A: 433-434, 1991.

Snow MH: Satellite cell distribution within the soleus muscle of adult mouse. *Anat Rec*, 201: 463-469, 1981.

Stedman HH, Sweeney HL, Shrager JB, Maguire HC, Panettieri RA, Petrof B, Narusawa M, Leferovich JM, Sladky JT, Kelly AM: The *mdx* mouse diaphragm reproduces the degenerative changes of Duchenne muscular dystrophy, *Nature*, 352: 536-538, 1991.

Styles P, Dixon RM, Radda GK: Unexpected heterogeneity in the 1H creatine signal from human skeletal muscle. *Proc Soc Magn Reson*, 3: 1890, 1995.

Suput D, Zupan A, Sepe A, Demsar F: Magnetic resonance imaging of muscular dystrophies and neuropathies. *BAM*, 2: 285-290, 1992.

Sze DY, Jardetzky O: Determination of metabolite and nucleotide concentrations in proliferating lymphocytes by ^{1}H-NMR of acid extracts. *Biochim Biophys Acta*, 1054: 181-197, 1990.

Sze DY, Jardetzky O: High-resolution proton NMR studies of lymphocyte extracts. *Immunomethods*, 4: 113-126, 1994.

Tanabe Y, Esaki K, Nomura T: Skeletal muscle pathology in X chromosome-linked muscular dystrophy (*mdx*) mouse. *Acta Neuropathol Berl*, 69: 91-95, 1986.

Tanguy O, Bielicki G, Zanca M, Renou JP: A possible way to detect proteolysis in muscular dystrophy by ^{1}H NMR proton. 11th meeting of the European Society of Magnetic Resonance in Biology and Medicine. April 20-24, p 158, 1994.

Tapscott SJ, Davies RL, Thayer MJ, Cheng PF, Weintraub H, Lassar AB: MyoD1: A nuclear phosphoprotein requiring a *myc* homology region to convert fibroblasts to myoblasts.

Science, 242: 405-411, 1988.

Thomson WHS, Smith I: X-linked recessive (Duchenne) muscular dystrophy (DMD) and purine metabolism: Effects of oral allopurinol and adenlyate. *Metabolism*, 27: 151-163, 1978.

Trivedi RA, Dickson G: Liposome-mediated gene transfer into normal and dystrophin-deficient mouse myoblasts. *J Neurochem*, 64: 2230-2238, 1995.

Turner O, Phoenix J, Wray S: Developmental and gestational changes of phospho-ethanolamine and taurine in rat brain, striated and smooth muscle. *Exp Physiol*, 79: 681-689, 1994.

Turner PR, Fong P, Denetclaw WF, Steinhardt RA: Increased calcium influx in dystrophic muscle. *J Cell Biol*, 115: 1701-1712, 1991.

Vade A, Sukhani R, Dolenga H, Habisohn-Schuck C: Chloral hydrate sedation of children undergoing CT and MR imaging: Safety as judged by American Academy of Pediatrics guidelines. *Am J Roentol*, 165: 905-909, 1995.

Venkatasubramanian PN, Arús C, Bárány M: Two-dimensional proton magnetic resonance of human muscle extracts. *Clin Physiol Biochem*, 4: 285-292, 1986.

Venuti JM, Morris JH, Vivian JL, Olson EN, Klein WH: Myogenin is required for late but not early aspects of myogenesis during mouse development. *J Cell Biol*, 128: 563-576, 1995.

Vincent N, Ragot T, Gilgenkrantz H, Couton D, Chafey P, Gregoire A, Briand P, Kaplan JC, Kahn A, Perricaudet M: Long-term correction of mouse dystrophic degeneration by adenovirus-mediated transfer of a minidystrophin gene. *Nat Genet*, 5: 130-134, 1993.

Webster G, Silberstein L, Hays AP, Blau HM: Fast muscle fibers are preferentially affected in DMD. *Cell*, 52: 503-513, 1988.

Weintraub H: The MyoD family and myogenesis: Redundancy, networks and thresholds. *Cell*, 75: 1241-1244, 1993.

Weller B, Massa R, Karpati G, Carpenter S: Glucocorticoids and immunosuppressants do not change the prevalence of necrosis and regeneration in *mdx* skeletal muscles. *Muscle Nerve*, 14: 771-774, 1991.

Williams SR, Gadian DG, Proctor E, Sprague DB, Talbott DF, Young IR, Brown FF: Proton NMR studies of muscle metabolites *in vivo*. *J Magn Reson*, 63: 406-412, 1985.

Worton R: Muscular dystrophies: Diseases of the dystropin-glycoprotein complex. *Science*, 270: 755-756, 1995.

Wright CE, Tallan HH, Yong YL: Taurine: biological update. *Ann Rev Biochem*, 55: 427-453, 1986.

Yablonka-Reuveni Z, Rivera AJ: Temporal expression of regulatory and structural muscle proteins during myogenesis of satellite cells on isolated adult rat fibers. *Dev Biol*, 164: 588-603, 1994.

Yoshizaki K, Seo Y, Nishikawa H: High-resolution proton magnetic resonance spectra of muscle. *Biochim Biophys Acta*, 678: 283-291, 1981.

Younkin DP, Berman P, Sladky J, Chee C, Bank W, Chance B: ^{31}P-NMR studies in Duchenne muscular dystrophy: Age related metabolic changes. *Neurol*, 37: 165-169, 1987.

Zacharias JM, Anderson JE: Muscle regeneration after imposed injury is better in younger than older *mdx* dystrophic mice. *J Neurol Sci*, 104: 190-196, 1991.

Zhang W, Behringer RR, Olson EN: Inactivation of the myogenic bHLH gene MRF4 results in upregulation of myogenin and rib anomalies. *Gene Dev*, 9: 1388-1399, 1995.

APPENDIX A: STRUCTURAL FORMUALE OF IMPORTANT 1-H NMR METABOLITES

NAME	STRUCTURAL FORMULA
Valine	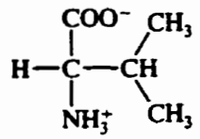
Lactate	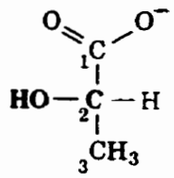
Alanine	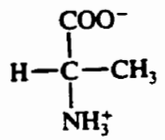
Glutamate	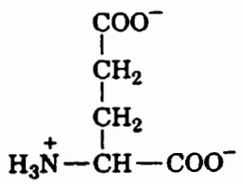
Succinate	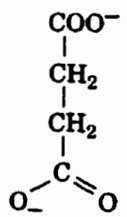
Glutamine	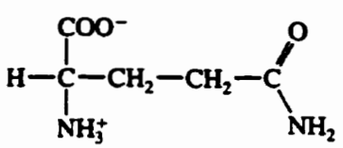

NAME	STRUCTURAL FORMULA
Carnitine	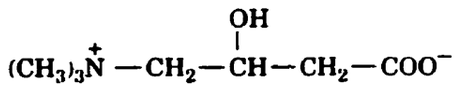
Taurine	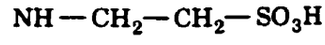
Glycine	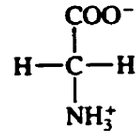
Glucose